ARCTIC TECHNOLOGY CENTRE

DTU Danmarks Tekniske Universitet

Master Thesis - June 2018

Recycling fishing nets into concrete

Student: Edurne Suárez Lejardi - s180271
Supervisors: Lisbeth M. Ottosen
Ida Maria Gieysztor Bertelsen

Technical University of Denmark
Department of Civil Engineering DTU-Byg
June 2018

Abstract

Annually, it is estimated that 12,7 million tons of plastic waste enters our oceans. Nowadays, particularly, the fishing industry is on the top of marine waste product generation. Over 30,000 nets are estimated to be lost in selected European fisheries annually due to bad weather conditions, gear conflict, ocean currents, and by action of fishermen. Furthermore, the plastic waste going into the ocean is not only a specific problem for the marine ecosystem, but for humans too. The microplastics created because of the degradation of waste products in the ocean are ingested by animals entering later the human food chain.

Following the objective of minimizing marine waste and as part of the research for the Circular Ocean Interreg Project in the Northern Peninsula Area Region, this master thesis investigates the use of fibers from waste fishing nets thrown into the ocean as fiber reinforcement in cement mortar samples. Fiber-reinforced cement-based specimens are already widely used in the construction sector, with different kinds of fibers, from steel to natural fibers. In this project, two types of fibers were used: commercial fibrillated polypropylene (PP), already used in cement-based specimens and recycled polyethylene (PE) fibers from discarded fishing nets.

The thesis is divided into two main parts. The first part is focused on reporting the environmental impact of the discarded fishing nets. The degradation of the nets was tested with a small-scale ocean water experiment simulation, in which microplastics were quickly visualized. Moreover, a characterization of the impurities as sand, seaweeds, salt and microplastics coming together with the fibers was carried out. The purpose of the analysis was to get an overview of the impurities presence in the fibers mix to have a better understanding about the need to carry out a washing process before the casting.

The second part of the thesis investigates the recycled fibers in cement mortar samples in terms of mechanical properties as compressive strength, flexural strength, flexural toughness and the interface bonding between the fibers and the cement-based material matrix. Finally, concerning the plastic shrinkage prevention, the digital image correlation (DIC) method was used to measure the specimens' microstrain and compare the values with the results achieved with the manual Linear Variable Differential Transformer (LVDT) test to prove the reliability of both test.

Promising results regarding the mechanical properties were achieved for the recycled PE reinforced mortar samples, showing a similar workability comparing with the commercial PP reinforced mortar samples. This means that the commercial PP fibers, fabricated only with the concrete reinforcement purpose, could be substituted with the PE recycled fibers. In addition to a positive environment impact, minimizing the discarded fishing nets quantity, the use of PE recycled fibers could lead also to an economical benefit to the Scandinavian construction companies along with a transition to a more sustainable production.

Preface

This project represents the Master Thesis carried out by Edurne Suárez Lejardi, at the department of Civil Engineering, Technical University of Denmark, DTU.

The Master Thesis constitutes to the work of 30 ECTS and was conducted and written in the period from the 29th of January 2017 to the 15th of June 2018.

The project was conducted with the assistance and guidance of Professor Lisbeth M. Ottosen and PhD student Ida Maria Gieysztor Bertelsen.

Acknowledgements

The author of the thesis would like to thank Professor Lisbeth M. Ottosen for her help, her guidance and her ideas throughout the project period and to Phd student Ida Maria Gieysztor Bertelsen for her help, motivation, availability and teaching from 7500 km of distance.

The author would also like to thank Klaus Bræmer, for the great assistance and kindness in the concrete laboratory and Ebba Schnell for the laboratory work at DTU Byg.

Finally, the author would like to thank her friends and office mates, Lenka, Lorena and Xurxo for being awesome, positive, motivated, funny, kind and helpful people. My stay here would not have been the same without you.

_____

Signature

Edurne Suárez Lejardi

Technical University of Denmark

15 June 2018

Contents

CONTENTS

List of figures

LIST OF FIGURES

List of tables

LIST OF TABLES

List of Symbols

Abbreviation	Elaboration
b	Side length of square section of prism mortar sample
f_{cr}	Crack strength
F_{cm}	Compressive load applied to mortar samples of area 40x40 mm
F_f	Load applied to the middle of the prism at fracture
I_5	Toughness index for 2 times initial crack deflection
I_{10}	Toughness index for 3 times initial crack deflection
l	Distance between supports for testing flexural strength of mortar
FEF	Fiber efficiency factor
P	Load
P_0	Stress where the fibers start working
P_{cr}	Critical load of mortar sample
P_{pb}	Maximum post-break load of mortar sample
R_c	Compression strength of mortar sample
R_f	Flexural strength of mortar sample
T	Toughness
$T_{\delta cr}$	Toughness at initial crack deflection
$T_{2\delta cr}$	Toughness at 2 times initial crack deflection
$T_{3\delta cr}$	Toughness at 3 times initial crack deflection
w/c	Water/cement ratio
$R_{5,10}$	Residual strength factor
μ_ϵ	Microstrain
L_0	Reference's length for the LVDT test
ΔL	Length's difference measured in the LVDT test
δ_{cr}	Initial crack load
R_{pb}	Maximum post-break strength

List of Abbreviations

Abbreviation	Elaboration
DIC	Digital Image Correlation
FRM	Fiber Reinforced Mortar
LVDT	Linear Variable Differential Transformer
PA6	Polyamide 6 (Nylon 6)
PE	Polyethylene
PP	Polypropylene
Ref-	Reference mortar sample
Ref PE	Reference ‘yellow’ PE recycled fiber mortar samples
Ref PE2	Reference ‘green’ PE recycled fiber mortar samples
Ref PP	Reference PP commercial fiber mortar samples
SD	Standard deviation
SEM	Scanning Electromagnetic Microscope
UV	Ultraviolet
HSM	High Speed Movement

1. Introduction

Annually, it is estimated that 12,7 million tons of plastic waste enters our oceans. This grievous incident can be attributed to many causes as the lack of social awareness, education and information, but especially due to the lack of efficient management practices. Nowadays, particularly, the fishing industry is on the top of marine waste production, and fishing-related gears are the main threat to the marine ecosystem. Over 30,000 nets are estimated to be lost by European fisheries annually due to bad weather conditions, gear conflicts, ocean currents, or in purpose by the action of fishermen, under the criterion that is cheaper acquire a new net instead of fix a broken net. Furthermore, it has been demonstrated that the plastic waste going into the ocean is not only a specific problem for the marine ecosystem, but for humans too. Microplastics created because of the degradation of waste products in the ocean are ingested by animals that later enter the human food chain with unknown effects for health. Several experiments have been carried out to analyze the content of microplastics in tap water around the world, and the results has shown a high level of water pollution, creating a big concern over the population.

It is of interest to minimize marine waste and more social awareness and hard laws could be part of the solution, but it is important to find new applications to recycle or reuse the marine waste and avoid them to end into the ocean or in the incineration plant. Some European companies as Plastix in Denmark and Nofir in Norway are already collecting discarded fishing nets and transforming them into plastic raw material. Following this approach, and as part of the research for the Interreg Programme in the Northern Periphery and Arctic region, within the project Circular Ocean, the focus of this Master thesis consists in the possible way to reuse waste fishing nets into reinforced cement-based materials. The reuse of waste products in the construction sector has increased recently due to the economic, technical, social and environmental benefits of the term known as *upcycling*. However, there are still some challenges that must be overcome to boost the use of waste materials in construction as: production, material characteristics, functionality and durability.

Figure 1.1. Circular Ocean Project Logo. Source: Circular Ocean website

Figure 1.2. Discarded fishing nets floating in the ocean. Source: coastmonkey.ie

Nowadays, the use of fibers in the construction industry is not a new concept. Several studies with different type of fibers have been accomplished, from glass and steel fibers to natural and plastic recycled fibers. This project is focused on plastic recycled fibers. Plastic fibers are being already used in the construction industry as reinforcement because it has been proved that their use leads to a decrease in shrinkage cracking in concrete. The most popular commercial plastics fibers used in the construction industry are made of polypropylene (PP), polyethylene terephthalate (PET) and high-density polyethylene (HDPE). Hereby, the new insight under investigation is to test recycled fibers from discarded fishing nets, and compare their mechanical and physical properties with current commercial fibers used in the sector as reinforcement, mostly made of polypropylene.

In this project polyethylene (PE) fibers will be used for the experimentation, which is one of the main materials used for fabricate the fishing nets collected in the Arctic region. Several tests will be carried out with different reinforced mortar mixtures, such as flexural and compression strength tests and microstrain measurement to analyze the effect of the PE fibers in the mortar mixture, and compare the workability with the results achieved with the commercial PP reinforced mortar samples, as well as with the plain mortar results. Through this process, it is intended to gain knowledge and consolidate the use of PE recycled fibers from discarded fishing nets as the first option.

1.1. Problem statement

The problem statement of this project is the use of fibers from discarded fishing nets as mortar reinforcement.

Firstly, the project is focus on the demonstration, quantification and measurement of the microplastics release during the degradation of the fishing nets thrown into the ocean. The project analyses the impurities coming together with the recycled PE fibers that could influence the mechanical properties of the mortar samples.

Secondly, it is pretended to analyze and compare the mechanical and physical properties of PE recycled fibers with commercial PP fibers used currently in the construction industry as concrete reinforcement. Furthermore, the project presents an analysis of the free drying shrinkage in different mortar samples, using a digital image correlation (DIC) method, to finally compare the accuracy and reliability of the method with the manual Linear Variable Displacement Transducer (LVDT) test.

1.2. Previous studies

This section presents an overview of the most relevant studies that precede this Master thesis. The studies presented on Table 1.1. are focus on wasted fishing nets used as fiber reinforcement or in the comparison of different methods to quantify the shrinkage cracking of concrete samples.

Table 1.1. Relevant studies and projects used for the theory.

Studies using waste plastics from fishing nets as fiber reinforcement	
Reference	**Research**
S. J. Svensson. Methodology and Testing of Waste Fishing Net as Fiber Reinforcement in Mortar. 2016.	The project examines the use of polyamide fibers from waste fishing nets as fiber reinforcement in cement mortar samples. The first part is focused on compare the fibers' mechanical properties, alkali resistance and thermal properties, comparing them with commercial PP fibers. The second part of the project is focused on carrying out the compressive strength test, flexural strength test and flexural toughness calculation, and compares the results with commercial PP reinforced mortar samples.
G. Cardinaud. Reuse of waste plastic fibers from discarded fishing nets in cement-based specimens. 2017.	The project investigates the potential use of PE fibers from discarded fishing nets in plastic shrinkage prevention of cement-based specimens. The project also investigates a new method of shrinkage crack characterization that was developed based on the strain pattern over the surface.
C. Marquar Larsen. Plastic shrinkage cracking of cement based materials reinforced with waste fibers. 2017.	The project investigates the potential of using digital image correlation (DIC) to quantify the plastic shrinkage cracking of cement based materials reinforced with recycled PE fibers from used fishing nets. Some properties as compressive strength, secant elastic modulus, setting time and free shrinkage of mortar reinforced with PE fibers are tested.
S. Spadea et al. (2015)	The study investigates engineering applications of recycled fibers obtained from waste fishing nets, but in this case the material used is nylon. The study focuses on the use of these fibers as tensile reinforcement of cementitious mortars. Firstly, the study begins with a characterization of the nylon fibers to assess the resistance to chemical attacks and their workability. The second part contains the results and conclusions achieved in compression and bending tests carried out to cementitious samples.
Studies using devices based on digital image correlation (DIC) to study drying shrinkage	

T. Mauroux et al. (2012)	The study investigates a new device based on digital image correlation (DIC) to measure 2D displacement fields on mortars and substrates at early age in drying conditions and compare it with intrusive methods, validating it with measurements of drying shrinkage using LVDT. Furthermore, a post-processing tool is proposed to determine the evolution of the cracking patterns, enabling the quantification of the widths and the depths of cracks.
F. Lagier et al. (2011)	The study investigates the ability of two different models (using either smeared or discrete cracks description) to describe the experimental behavior observed at the microscopic scale of cement paste and aggregate on cementitious materials. Both experimental and numerical studies are presented dealing with the separation, identification and quantification of drying shrinkage incompatibilities effect.

1.3. Introduction to the report

The structure of the report is outlined below with a short description of each chapter.

Structure
The project has been divided into two main parts; Part 1- Microplastics in the Arctic and Part 2- Recycled fibers as mortar reinforcement.

In the first part, the project is focus on the characterization of the microplastics release during the degradation of the PE fishing nets in a simulated ocean. The project also analyses the impurities coming together with the recycled PE fibers. In the second part, it is pretended to analyze the mechanical properties of recycled PE fibers with commercial PP fibers. Furthermore, the project presents an analysis of the dry shrinkage in which was used a digital image correlation (DIC) method, to finally compare the results with the manual Linear Variable Displacement Transducer (LVDT) test.

Theory
The Theory, Chapter 2, includes a brief introduction to the microplastics from marine waste and fishing gear, as well as the presentation of some environmental factors affecting the degradation of the fishing nets as the wearing resistance. Moreover, it is included a description of cement-based materials, with special emphasis on the fiber reinforced concrete and the effect of the fibers in the shrinkage, plastic or dry.

Objectives
Objectives, Chapter 3 and 8, corresponding one chapter to each part of the project, respectively. In these chapters the main objectives to obtain during the development of the project are explained.

Materials
Materials, Chapter 4 and 9, corresponding one chapter to each part of the project, respectively. Chapter 4 presents the PE fibers and PE nets used, with the corresponding dimensions. Chapter 9 describes deeply the waste PE fibers and the commercial PP fibers used in the second part of the project. A description of the mortar mixture in detail, the procedure followed during the casting process and the number of specimens casted is presented.

Methods
Methods, Chapter 5 and Chapter 10, corresponding one chapter to each part of the project, respectively. Chapter 5 describes the methodology followed to quantify the percentage of impurities in the fibers and to create the simulation of the ocean in small scale. Chapter 10 describe the methods used for the mortar samples, among the testing of the flexural and compressive strength and the SEM analysis of the fracture surface of the FRM samples as well as the plain mortar samples. Furthermore, Chapter 10 presents the methodology used during the LVDT test as well as during the DIC test.

Results
Results, Chapter 6 and Chapter 11, corresponding one chapter to each part of the project, respectively. The results from all the tests performed are presented. The results are discussed internally, but not compared to other studies.

Discussion
Discussion, Chapter 7 and Chapter 12, corresponding one chapter to each part of the project, respectively. These chapters compare the results with studies and research from the literature, in order to validate the results in this study.

Economic analysis and future solutions
Chapter 13 includes a brief economic analysis with real data provided by the suppliers of the different fibers used in the project. Some alternatives to minimize the amount of fishing nets discarded into the ocean and some ideas to boost the use of the waste fibers by construction companies are presented.

Conclusions
Chapter 14 includes the final conclusions as well as recommendation and improvements to future studies within the same field.

2. Theory

This chapter is focused on the theory behind ocean microplastic release, cement-based composites with a special emphasis in fiber- reinforced concrete, and finally on the shrinkage concrete.

2.1. Microplastics from maritime waste or fishing nets

Microplastics are defined as small particles or fragments of plastic measuring less than 5 mm in diameter. While 'Primary' microplastics are purposefully manufactured for industrial purposes as cosmetic and personal healthcare products, 'Secondary' microplastics are created by the weathering and fragmentation of larger plastic objects. Weathering and fragmentation is enhanced by exposure to UV irradiation, but the process becomes extremely slow once this is removed, as in much of the ocean. Plastics will tend to degrade and start to lose their initial properties over time, at a rate depending on the physical, chemical and biological conditions to which they are subjected. Weathering-related degradation results in a progression of changes: the loss in mechanical integrity, embrittlement, further degradation and fragmentation into 'Secondary' microplastics. In an ocean setting the principal weathering agent is UV irradiation followed by physical abrasion due to wave activity. (Dr. P.J. Kershaw, 2016)

Different types of polymers have a wide range of properties, and this influences their behavior in the environment. One of the most important parameters is the density relative to that of seawater. Densities of common plastics range from 0,90 to 1,39 (kg/m^3), while the density of seawater is approximately 1,027, depending on the temperature and salinity which vary geographically and with water depth. On this basis, only PE and PP would be expected to float in freshwater. However, the buoyancy of a plastic particle or object will be dependent on other factors such as entrapped air, water currents and turbulence. (Dr.P.J. Kershaw, 2016)

Marine plastics are distributed throughout the ocean, from the Arctic to the Antarctic due to the durability of plastics. This is also the reason why plastics persist in the ocean for many years after first being introduced. Sea-based sources of plastics appear to be dominated by the fisheries and shipping sectors, but rivers appear to act as conduits for significant but largely unquantified amounts of macro and microplastics. (Dr. P.J. Kershaw, 2016)

2.1.1. Wearing resistance

The durability of a net or a rope depends entirely on the wearing resistance of the material. The highest degree of wear appears to occur on board the vessel where the material rubs against rollers, pipes, hull etc. On stern trawlers a high degree of wear occurs when the bag is hauled up through the ramp. The wear occurring while the tool is being used for fishing is a problem in bottom trawling and seining. Sand, gravel and rocks

will result in a lot of wear, but in most cases many efforts have been made in the construction of the tool to avoid that the tool comes into contact with the sea bed. The highest degree of wear occurs in the knots of the net. Furthermore, on rope you often see wear produced by the fibers rubbing against each other. It is difficult to compare studies of the wearing resistance of different materials. However, it seems that the coarser the material, the higher the wear. Thus, staple fiber lines will wear faster than continuous fiber lines. Similarly, it seems that the higher the strength of the individual fibers, the higher the wear resistance (U. Oxvig and U.J. Hansen, 2007).

2.2. Cement-based materials

Cement-based material includes every material in which cement is the main ingredient, such as mortar and concrete. Mortar is a mixture of sand (fine aggregate), cement and water, and concrete includes the same materials plus coarse aggregate, which consists in granular materials as gravel and crushed stone, among others (P. Kumar, 2014).

The use of cement-based materials is much expanded in the construction industry for some reasons: its water resistance, the variety of shapes and sizes that can be formed, the low price and its ease. However, concrete is mostly considered more suitable for bearing compressive load than tensile and bending loads. In order to improve these mechanical properties, concrete is usually reinforced (P. Kumar, 2014).

2.2.1. Fiber-reinforced concrete

Although steel fibers remain as the number one material to reinforce cement-based materials, due to its high cost, other alternatives of reinforcement are being tried. Discrete fibers made of plastic, glass and natural materials in a variety of shapes and sizes are added to concrete in order to improve its mechanical properties. Disperse fibers offer a series of advantages over steel bars and wire mesh, as higher resistance to local crack formation and growth, less sensitivity to corrosion and a reduction in labor cost (P. Kumar, 2014).

In general, the use of fibers as reinforcement improves the concrete properties like tensile strength, chemical resistance, drying shrinkage and creep on short and long term basis. However, the workability and compressive strength are in general reduced due to partially replacement of sand by waste plastic flakes (A.K. Jassim, 2017). But the properties of fiber-reinforced concrete depend on the type, amount and dimensions of the fibers added, as well as the properties of the cement-based matrix and the fiber-to- matrix interface. Moreover, the spatial and orientation distribution of the fibers within the concrete affect the cracking performance and toughness. Depending on the application required, random or oriented distribution is preferred (P. Kumar, 2014).

2.3. Shrinkage

Shrinkage is caused by loss of water by evaporation or by hydration of cement and it is an important property with respect to potential cracking and bond failure (P.Kumar, 2014). Deformation due to shrinkage of concrete is one of the main reasons for occurrence of cracks, especially for concrete elements with large exposed surfaces. The presence of

plastic fibers reduces the appearance of cracks during shrinkage. By reducing the crack width, the penetration of aggressive substances from the environment is reduced, however, if there is no control, microcracks formed due to the drying shrinkage lead to the development of larger cracks (M. Serdar et al., 2015).

2.3.1. Plastic shrinkage

Plastic shrinkage is the volumetric contraction that undergoes the cement paste caused by the loss of water by evaporation from the surface of concrete or by suction by dry concrete below. The contraction induces tensile stress in the surface layers because they are restrained by the non-shrinking inner concrete, and, since the concrete is very weak in its plastic state, plastic cracking at the surface can readily occur.

Plastic shrinkage is greater the greater the rate of evaporation of water, which in turn depends on the air temperature, the concrete temperature, the relative humidity of the air and the wind speed (A.M. Neville, 2010).

2.3.2. Dry shrinkage

Withdrawal of water from hardened concrete stored in unsaturated air causes drying shrinkage, which is an irreversible phenomenon due to the deformation of additional physical and chemical bonds in the cement gel when absorbed water has been removed. The general pattern behavior is as follows. When concrete dries, first of all, there is the loss of free water, which induces internal relative humidity gradients within the cement paste structure. So that, with time, water molecules are transferred from the large surface area of the calcium silicate hydrates into the empty capillaries and then out of the concrete.

In consequence, the cement paste contracts but the reduction in volume is not equal to the volume of water removed because the initial loss of free water dos not causes a significant volumetric contraction of the paste. (A.M. Neville, 2010).

Part I – Microplastics in the Arctic

3. Objectives

The objective in the first part of the project is to analyze the microplastics release from discarded fishing nets thrown in the ocean, which, eventually, with the abrasive environmental conditions tend to break up in progressively smaller fragments. The experimentation is carried out in order to boost the ashore return or collection of discarded fishing nets to avoid the pollution of marine environment, which could cause the reduction of the marine fauna and the entrance of microplastics into the animal and human food chain. Moreover, the analysis of the different impurities coming along with the nets and waste fibers as salt, sand, clay and microplastics, is carried out in order to clarify the need of a washing process before the casting to no alter the mechanical properties of the FRM samples.

4. Materials

4.1. Preparation of fishing nets and fibers

For this part of the project, fishing nets collected from the North Sea are analyzed in order to prove and determinate the microplastics' release rate to the marine environment.

In the preparation of the experiment, two small scale squared pieces of PE nets collected at the Arctic Region were used, as well as the cut fibers obtained when they were processed.

On figure 4.1., it is shown the two different fishing nets used for the test, differentiating between 'green' PE and 'yellow' PE fishing nets.

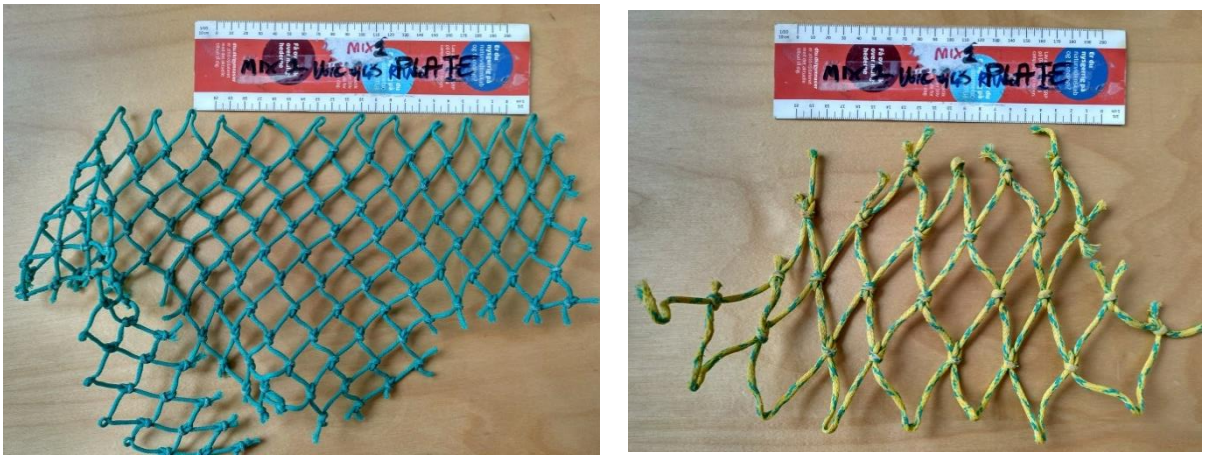

(a) Piece of discarded 'green' PE fishing net. **(b) Piece of discarded 'yellow' PE fishing nets.**

Figure 4.1. Pieces of discarded PE fishing nets.

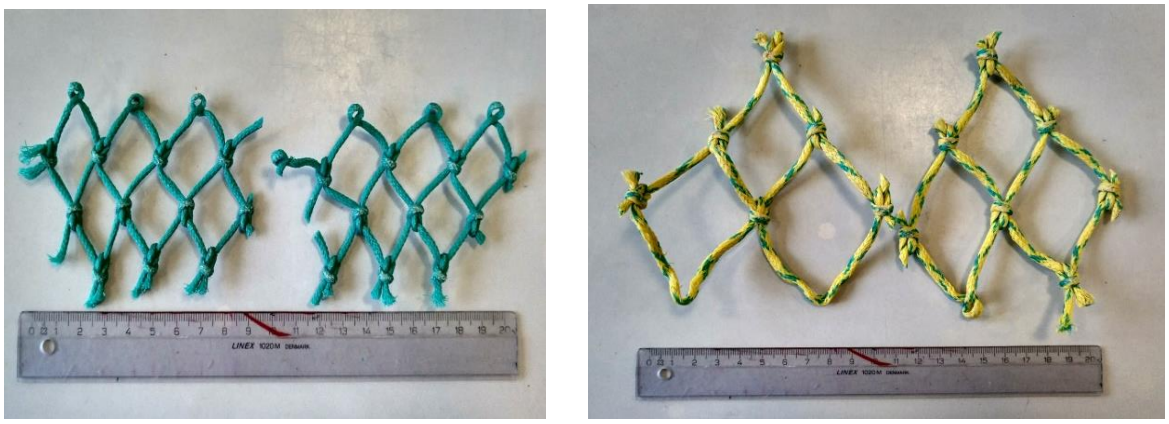

(a) Small scale 'green' PE fishing net. **(b) Small scale 'yellow' PE fishing nets.**

Figure 4.2. Small scale PE fishing nets.

The fishing nets were cut and measured for the small- scale experimentation as it is shown on figure 4.2. The small scale 'green' PE fishing nets were compound by six net meshes with an inside dimension of 30 mm and the small scale 'yellow' PE fishing nets were compound by three net meshes with an inside dimension of 75 mm.

Cut fibers from used fishing nets made of PE and collected by the Danish company Plastix were also measured and used in the experimentation, differentiating between 'green' and 'yellow' PE fibers. Before starting the experiment these fibers were cleaned and sieved to ensure that only the longer fibers were added to the samples to make easy to evaluate the microplastics release results at the end. More information about the fibers is provided in section 9.1.

(a) PE 'yellow' fibers from discarded nets. **(b) PE 'green' fibers from discarded nets.**

Figure 4.3. The PE fibers used in the test experimentation.

4.2. Environment

To simulate the environmental conditions, an internal method was set up in the laboratory. In order to improve the credibility of the experiment, substituted ocean water was prepared to simulate the degradation of the fishing nets and cut fibers.

As the degradation of fishing nets could endure a very long time, in order to simulate the marine environmental conditions, some of the tests were carried out with high UV exposure and high oxygen levels, which are known to increase the rate of degradation.

5. Methods

This section includes the different experimentation carried out for the analysis and characterization of the plastics and impurities delivered along with the discarded fishing nets fibers. Furthermore, it is presented the methodology used for evaluating the degradation of the fishing nets and the analysis of the microplastics released in the simulation samples.

5.1. Analysis of impurities

The uncleaned fibers delivered by the company Plastix, contain a small amount of impurities from the fishing operations, which included particles of salt, wood, metals, sand, silt, clay, microplastics and other materials. These impurities should be removed before the casting, so they can affect the mechanical and physical properties of the concrete mixtures when are added in big quantities during and after the curing period (S. Svensson, 2016).

A quantification test of impurities, according to their size, and a microscope analysis are performed to identify and measure some of these impurities before the washing process. An overview of the current marine pollution in the Artic zone, where fishing nets were collected, is presented. An analysis of the microplastics found in the samples is provided in order to characterize them and prove their origin and relation with the discarded fishing nets.

Set-up

In order to analyze and characterize the materials coming together with the fibers, the impurities were classified in three categories depending on the size: particles and fibers bigger than 1 mm, particles and microplastics smaller than 1 mm but bigger than 250 µm and particles and microplastics smaller than 250 µm. The separation was done mechanically, using sieves of 1 mm and 250 µm holes' length.

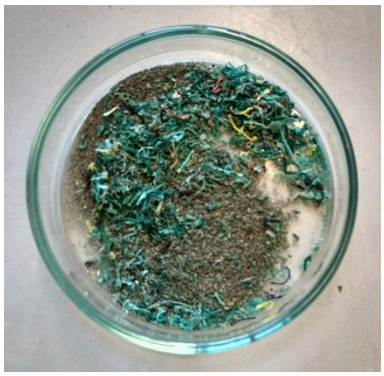

(a) Sample of 60 gr of 'green' PE fibers and impurities.

(b) Sieve of 1 mm hole size.

(c) Sieve of 250 µm hole size.

Figure 5.1. Sample and sieves used for impurities quantification test.

Six samples of 0, 60 gr containing uncleaned PE fibers were prepared to quantify the different average percentage of impurities according to their size. As it was exposed above, the variation of the weakness of the samples caused by the addition of impurities depends on the quantity.

After the quantification test, one sample of each size was analyzed in the microscope. Some microplastics and particles found in the samples were measured and characterize with the electronic microscope.

5.2. Analysis of microplastics release

The aim of the analysis is to determinate and quantify the degradation and the creation of microplastics from discarded fishing nets thrown in the North Sea.

Several tests simulating ocean water were carried out with fibers and small scale fishing nets, to measure how well the fishing nets resist the sea environmental conditions.

Fishing nets that spend a significantly amount of time exposed to sunlight becomes weaker (S. Thomas and C. Hridayanathan, 2006). In order to simulate different condition for the experiment, the discarded fishing nets thrown in the ocean were considered floating on the surface and floating several meters under the water. The wave movement and the possible friction on the fishing nets that can result in embrittlement and microcraking of the fishing nets were considered.

Sea water

Five liters of substitute ocean water were produced for the simulation of the degradation tests. The Standard Practice for the Preparation of Substitute Ocean water by Dr. Barr Harbor, The American Society for testing and materials, was followed to prepare the ocean water.

The preparation of substitute Ocean water is as follow. To prepare 5,0 L of substitute ocean water, dissolve 122,67 g of sodium chloride and 20,47 g of anhydrous sodium sulfate in 3 to 4 L of water. Add 100 mL of Stock Solution No. 1 (Table 5.1.) slowly with vigorous stirring and then 100 mL of Stock Solution No. 2 (Table 5.2.). Dilute to 5,0 L. Adjust the pH to 8,2 with 0,05 N sodium hydroxide solution. Only a few milliliters of NaOH solution should be required.

Table 5.1. Stock Solution No. 1 (Dr. B. Harbor,2013).

Stock Solution No. 1	
Salts	**Concentration [g/l]**
$MgCl_2.6H_2O$	555,6
$CaCl_2$ (anhydrous)	57,9
$SrCl_2.6H_2O$	2,1

Table 5.2. Stock Solution No. 2. (Dr. B. Harbor,2013).

Stock Solution No. 2	
Salts	**Concentration [g/l]**
KCl	69,5
$NaHCO_3$	20,1
KBr	10,0
H_3BO_3	2,7
NaF	0,3

On table 5.3., it is shown the chemical composition of substitute ocean water,

Table 5.3. Chemical composition of substitute ocean water. (Dr. B. Harbor,2013).

Salts	Concentration [g/l]
NaCl	24,530
$MgCl_2$	5,200
Na2SO4	4,090
$CaCl_2$	1,160
KCl	0,695
$NaHCO_3$	0,201
KBr	0,027
H_3BO_3	0,025
NaF	0,003

Set-up

In total, eight different small scale experiments were carried out. The experiment started to run the 15th of March 2018 at 10:20 h, and was running until the 14th of May 2018 at 12:00 h.

On table 5.4. it is shown the characteristics of each experiment sample.

Table 2.4. Characteristics considered for each microplastic release test.

Specimen	PE Fibers/Net	Initial weight [g]	Sun light exposure	Wave agitation	Simulation Comments
1	'green' Net	2,59	Yes	Yes	Surface
2	'green' Net	2,76	No	No	Under surface
3	'yellow' Net	5,18	Yes	Yes	Surface
4	'yellow' Net	4,80	No	No	Under surface
5	'green' Fibers	2,14	Yes	Yes	Surface
6	'green' Fibers	2,14	No	No	Under surface
7	'yellow' Fibers	2,14	Yes	Yes	Surface
8	'yellow' Fibers	2,14	No	No	Under surface

For each test, a 600 ml glass was used. To avoid sunlight exposition, aluminum paper was used to cover the samples considered under water surface, as it is shown on figure 5.2.

Figure 5.2. Preparation of the set-up for the microplastic release experimentation.

The fibers and nets were deposited freely within the glasses and covered with film to avoid water evaporation. Mixers were added to specimen's number 1, 3, 5 and 7, in which surface nets were simulated with sunlight exposure and wave agitation. On figure 5.3. it is shown the set-up for the experimentation. Specimen's number 2, 4, 6 and 8 were left totally covered during the whole period as it is shown on figure 5.4.

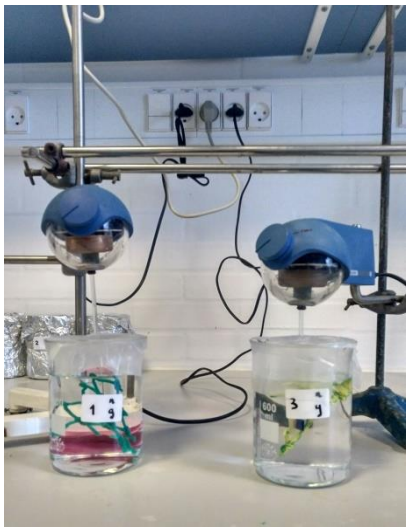

(a) Small-scale nets experimentation set-up. Number 1 and 3.

(b) Small-scale fibers experimentation set-up. Number 5 and 7.

Figure 5.3. Set-up for the microplastic release experimentation.

Figure 5.4. Specimens covered during the experimentation period.

The visualization of the degradation process could last many days. The experiment was running in the laboratory with the conditions described above during 2 months, when proves of microplastics release were assured. Each week the samples were visually examined in order to quantify the nets' degradation and to check the workability of the mixers.

Once the simulation was dissembled, the small scale PE fishing nets from experiment nº 1, 2, 3 and 4 were dried in the furnace at 50 ^{o}C during 2 days (Figure 5.6.), and then measured to quantify the loss of material of each sample. After that, the water was absorbed by a vacuum with a circular filter of Φ 45 mm and 0,45 µm of porosity (Figure 5.5.) The microplastics that remained in the filter were analyzed in the electronic microscope.

For test nº5, 6, 7 and 8 the thick layer of fibers in the top was removed, and then, the water was absorbed by the vacuum and the microplastics and impurities found in the filter were analyzed in the electronic microscope.

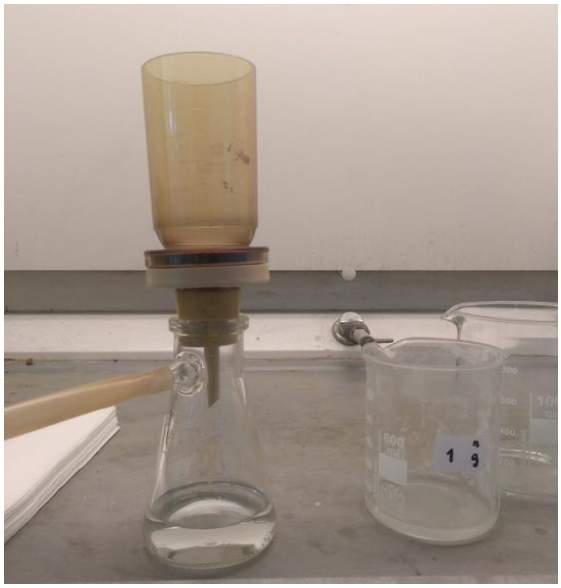

Figure 5.5. Vacuum system to filter the microplastics.

Figure 5.6. PE small scale fishing nets drying into the oven.

6. Results

This chapter includes the results from the tests conducted on Chapter 5: the analysis and characterization of the impurities coming with the PE fibers and the simulation test of microplastics release from discarded fishing nets into ocean water.

In this Chapter the results are commented on, but the discussion and comparison of the results are presented in Chapter 7.

6.1. Analysis of impurities

The aim of the analysis was to carry out the quantification of impurities coming with the PE fibers delivered by Plastix, classifying them depending on their size. As it was explained in section 5.1., two different sieves, with holes' length of 1 mm and 250 µm, were used to separate and weight different samples of fibers and impurities.

On table 6.1. it is presented the results from the impurities quantification test.

Table 3.1. Quantification of impurities delivered with the PE fibers by Plastix.

Reference	Sample weight [g]	Impurities >1 mm [g]	Impurities <1 mm and > 250 µm [g]	Impurities <250 µm [g]
Sample A	0,60	0,13	0,20	0,27
Sample B	0,60	0,11	0,19	0,30
Sample C	0,60	0,08	0,16	0,36
Sample D	0,60	0,22	0,19	0,19
Sample E	0,60	0,16	0,21	0,23
Sample F	0,60	0,16	0,22	0,22
Average [g]	**0,60**	**0,14**	**0,20**	**0,26**
Percentage [%]	**100**	**24**	**32**	**44**

The weight measurements can vary disproportionately depending on the sample because, usually, the clay and small particles of sand are disposed at the bottom of the plastic bag in which the fibers are delivered. However, this fact was taken into account for the test and all the samples were caught from the same part of the bag.

As can be seen on table 6.1., the percentage (average) of impurities coming with the fibers smaller than 250 µm is 44%. The percentage number is high for the impurities addition in the mortar or concrete mix , which means that the mechanical and physical properties of the concrete mixes using uncleaned PE fibers could be affected.

Microscope analysis

As it is presented from figure 6.1. to figure 6.3., one sample of each size was analyzed in the microscope and some impurities were characterized and measured.

On figure 6.1., it is presented the microscope image (scale 1000 µm) of the sample with fibers and impurities' size bigger than 1 mm.

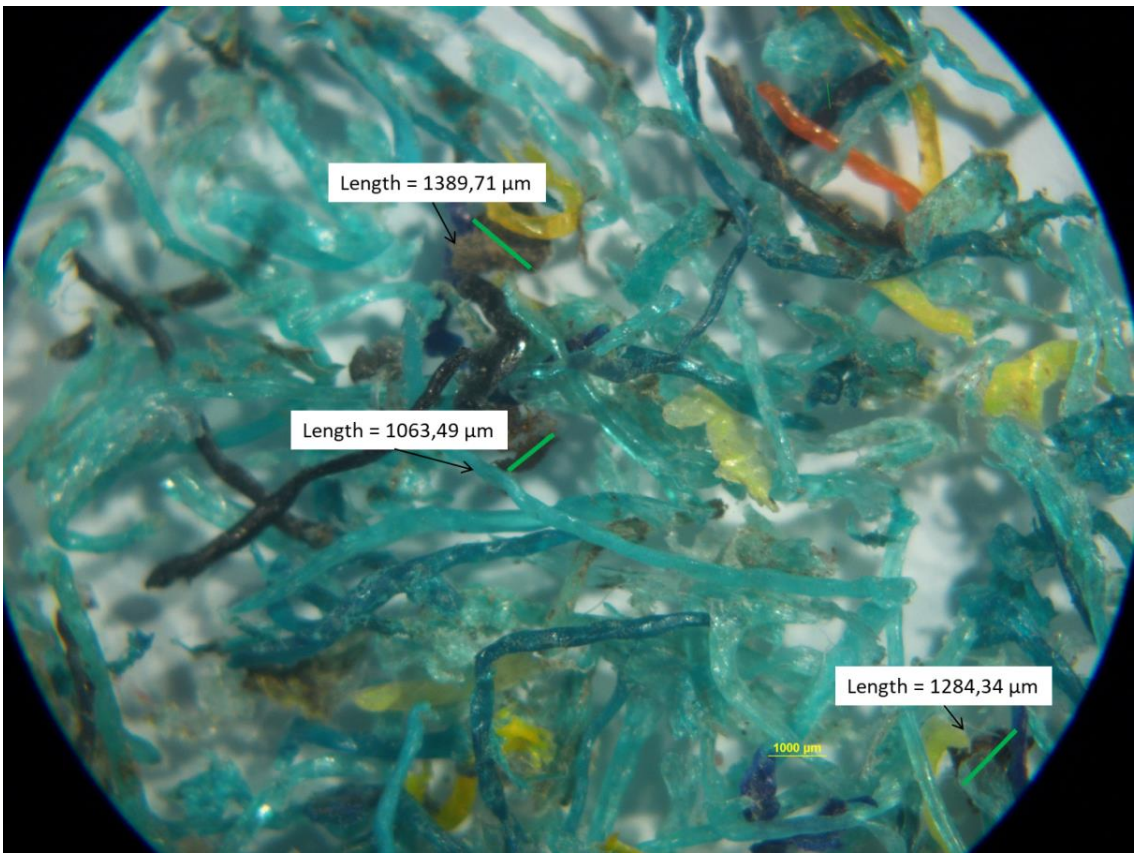

Figure 6.1. Fibers and impurities with size > 1 mm. Scale 1000µm.

As it is observed on figure 6.1., in the sample with fibers and impurities bigger than 1 mm, the main component are the PE fibers, in which the green color is predominating. Furthermore, some grains of sand and some particles of dried seaweed adhered to the fibers were found and measured in the sample.

On figure 6.2., it is presented the microscope image (scale 1000 µm) of the sample with fibers and impurities' size smaller than 1 mm and bigger than 250 µm.

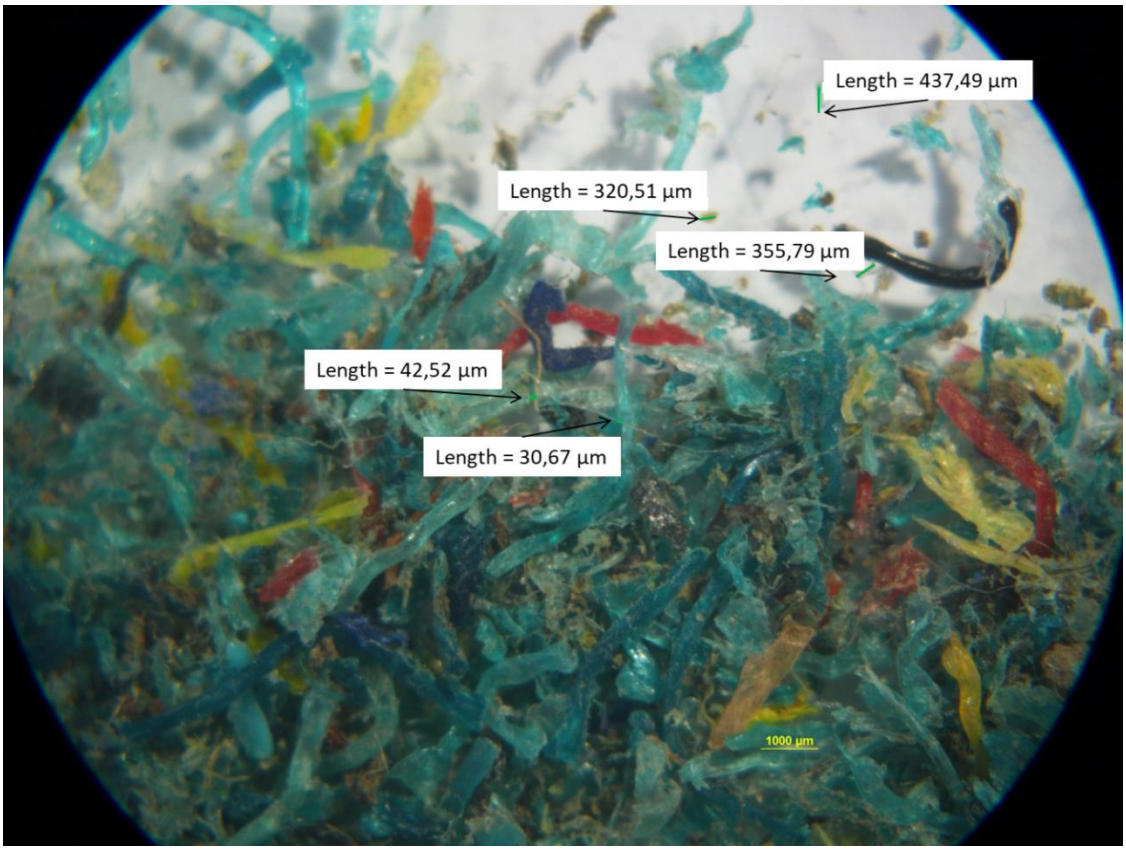

Figure 6.2. Microplastic fibers and impurities with size < 1 mm > 250µm. Scale 1000 µm.

As it is observed on figure 6.2., in the sample with fibers particles and impurities smaller than 1 mm but bigger than 250 µm, the PE fibers are more degraded comparing the fibers from figure 6.1. Fibers from figure 6.2. have a shorter length and a loss of the fiber shape and a loss of color brightness can be appreciated. The evolution of the nets degradation stages, releasing microplastic can be observed on the sample. Furthermore, several white and ocher plastic fibrillated fibers with a width in the range between 30-50 µm can be observed on the figure. The origin of these filaments is not clear, they could be formed after a long degradation of the PE nets, but the fibrillated shape could indicate they are made of a different type of plastic, as PP, due to their similarity to the white or transparent fibrillated commercial PP fibers used in this project. Moreover, some sand particles can be observed in the sample with indicated measures.

On figure 6.3., it is presented the microscope image (scale 1000 µm) of the sample with fibers and impurities' size smaller than 1 mm.

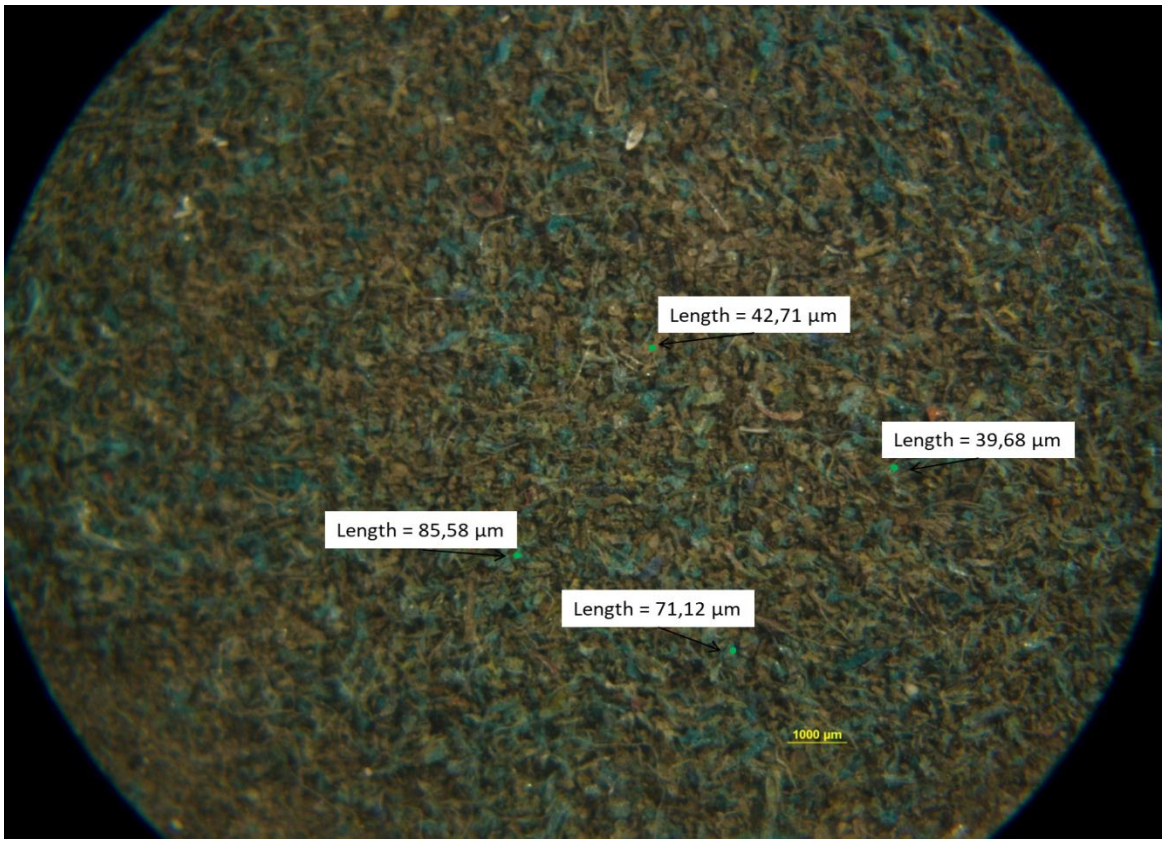

Figure 6.3. Impurities and fibers' microplastics with size < 250µm. Scale 1000µm.

As it is observed on figure 6.3., in the sample with impurities and microplastics smaller than 250 µm, several 'green' PE microplastic were found and measured as examples. The length of the microplastics differentiated and measured were within the range of 20-100µm. In a first visual inspection of the sample, clay and small particles of sand and salt seems to be the main component of the mix, but the analysis with the microscope shows that green 'PE' microplastic predominates in the impurities. The green color of these microplastics clearly indicates that the origin of the microplastics are the discarded fishing nets. The high quantity of 'green' microplastics found in the sample proved the degradation of the nets and consequently of the fibers. Apart from the clay and small particles of sand observed in the sample, the same fibrillated microplastics found in the sample on figure 6.2., but with a smaller length, were found.

6.2. Analysis of microplastics release

During the whole period in which the experiment was running, the degradation of fishing nets and the releasing of microplastics was checked each week to analyze the workability

and reliability of the experiment and quantify the days in which the microplastics release started of the nets for samples nº1 and nº3.
On table 6.2. is provided an overview of the visual examination during the whole period.

Tabla 6.2. Overview of the visual inspection of the different samples during the experimentation period.

Date	Comments
15-03-18	Starting of the experiment.
3-04-18	No microplastics observed in samples.
9-04-18	No microplastics observed in samples.
16-04-18	Microplastics and impurities observed in sample nº 3. Impurities in the bottom of the glass (sand, silt…) and microplastics observed floating in the surface.
23-04-18	Microplastics and impurities observed in sample nº 3. Impurities in the bottom of the glass (sand, silt…) and microplastics observed floating in the surface. No evolution from last day.
30-04-18	Experiment spoilt. Some microplastics found in the remaining water. More ocean water added.
7-05-18	Microplastics and impurities observed in sample nº 3. Impurities in the bottom of the glass (sand, silt…) and microplastics observed floating in the surface. No evolution from last day.
14-05-18	End of experimentation. Microplastics and impurities observed in sample nº 3 and nº1.

In a first visual analysis after two months of running the experiment, it was easy to recognize the degradation suffered by the nets as well as the fibers. Furthermore, although the nets and fibers were washed before the test, some impurities as small particles of sand and salt were visualized in the samples.

As was presented on table 6.2., the 'yellow' PE net was degraded quicker than the 'green' PE nets. The microplastics release during the experiment was visualized one month before than in the PE 'yellow' net sample. At the end of the experiment, a higher quantity of microplastics could be observed in sample nº3 comparing with sample nº1.

Although the material of the nets and the braided shape was the same, the size and the braiding compression of the nets was different and could have affected the process of degradation and release of microplastics. Furthermore, analyzing the nets after being exposed two months to ocean conditions, it was proved that the braided was less tight and, besides, it was appreciated the disentanglement of the fibers.

On figure 6.4. it is presented some pictures were microplastics can easily be recognized visually after the nets were removed. Although only the biggest microplastics found in the samples are indicated in red, smaller particles were also observed.

(a) 'yellow' PE microplastic in simple nº3 (b) 'green' PE microplastic in simple nº 1

Figure 6.4. Microplastics visually observed.

Concerning test nº 2 and nº4, with PE fibers, it was also observed in a first visual inspection that the fibers degraded during the experiment period, because several microplastics were found. As was exposed in section 5.2., before starting the experiment the fibers were cleaned and sieved to improve the evaluation of the results at the end, and recognize easily the microplastics released. The degradation observed visually resulted higher for the fibers samples than for the nets samples.

After two months, no microplastics were found in the samples nº2,4,6 and 8, which were not exposed to surface conditions as wave's friction and UV light. It can be concluded, that the simulation for nets in surface conditions affected harder the degradation and release of microplastic than the nets exposed to under surface conditions. Probably, to have found microplastics in the experiments were immersion of nets was simulated, the experiment should have been running much more time than 2 months. Some impurities were found in the bottom of the glasses although a washing process was done before starting the experiment

On table 6.3. it is presented an overview of the visual results achieved in the different tests.

Table 6.3. Overview of the results achieved after 2 months.

Test	PE Fibers/Net	Microplastic	Impurities	Comments
1	'green' Net	✓	✓	Microplastics generated after 2 months. Particles of sand and salt were observed

				in the bottom.
2	'green' Net			Neither microplastics or impurities found.
3	'yellow' Net	✓	✓	Microplastics generated after 1 month. More microplastics observed than in test nº1. Particles of sand and salt were observed in the bottom
4	'yellow' Net			Neither microplastics or impurities found.
5	'green' Fibers	✓	✓	Microplastics found in the sample. Fishing nets origin.
6	'green' Fibers		✓	No microplastics found. Some impurities found in the bottom of the glasses.
7	'yellow' Fibers	✓	✓	Microplastics found in the sample. Fishing nets origin.
8	'yellow' Fibers		✓	No microplastics found. Some impurities found in the bottom of the glasses.

Only the quantification for the nets tests is presented due to the difficulty of quantifying the microplastics released in tests in which fibers were used.

On table 6.4. it is presented the initial and final weight and material loss for the nets.

Table 6.4. Results generated in the experimentation.

Test	PE Fibers/Net	Initial weight [g]	Final weight [g]	Weight loss [g]	Weight loss [%]
1	'green' Net	2,69	2,66	0,03	1,112
2	'green' Net	2,76	2,75	0,01	0,362
3	'yellow' Net	5,18	5,16	0,02	0,386
4	'yellow' Net	4,91	4,90	0,01	0,204

As can be observed, the weight of the fishing nets decreased slightly due to their degradation and release of microplastic, which means loss of material. In samples nº2 and nº4, in which no microplastics or sings of degradation were found, the decrease of weight is less pronounced than in samples nº1 and nº3. The slight decrease of weight observed can be attributed to the separation of the impurities that were embedded in the fishing nets and were disposed in the bottom of the glass.

Visual analysis

Generally, as it is exposed by V.Hidalgo-Ruz et al. (2012), the plastic particles with a size range 1 nm to < 5 mm are considered microplastics. For the electronic microscope analysis and due to the size of the filter used, all the particles bigger than 0, 45 µm were analyzed. The filtering was made for all the samples to analyze and compare the microparticles found in each experiment.

From figure 6.5. to figure 6.6. it is presented a picture of the filter surface for each test, once the water was absorbed with the vacuum.

(a) Sample test nº1.

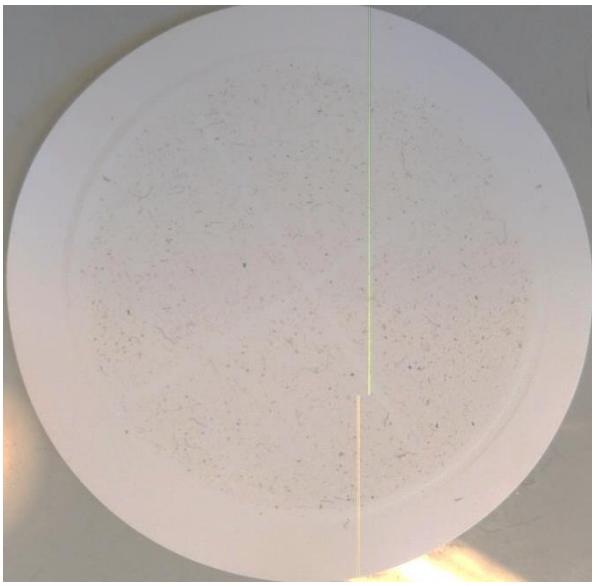

(b) Sample test nº2.

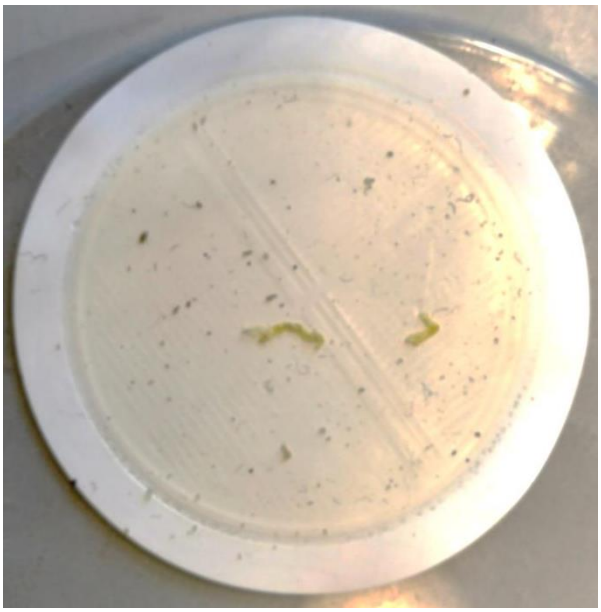

(c) Sample test nº3.

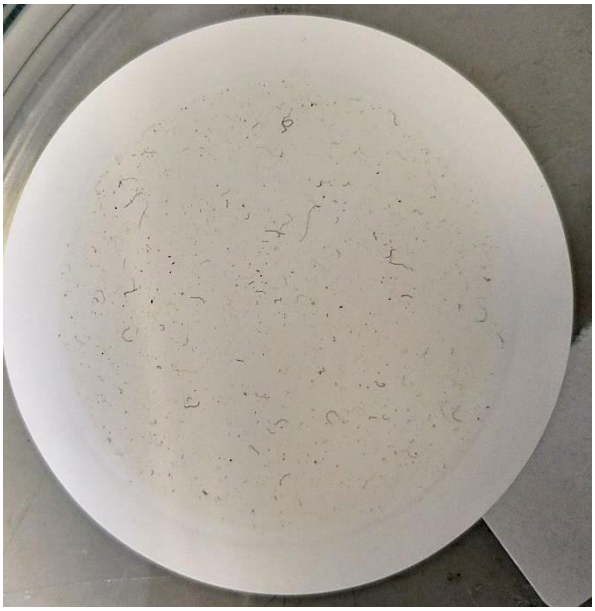

(d) Sample test nº4.

Figure 6.5. Filter surfaces of samples Nº 1,2,3 and 4, corresponding to the small scale fishing nets tests.

The differences among the nets that were exposed to the ocean conditions on the surface (Figure 6.5 (a) and (c)) and the nets that were not exposed to these conditions (Figure 6.5 (b) and (d)) can be appreciated simply taking a look to the figures. Moreover, it can be

observed easily the difference in the impurities attached to the filter between 'yellow' and 'green' PE nets exposed to waves' friction and UV light. The 'green' PE net (Figure 6.5. (a)) released a higher quantity of clay and sand particles than the yellow one (Figure 6.5. (c)).

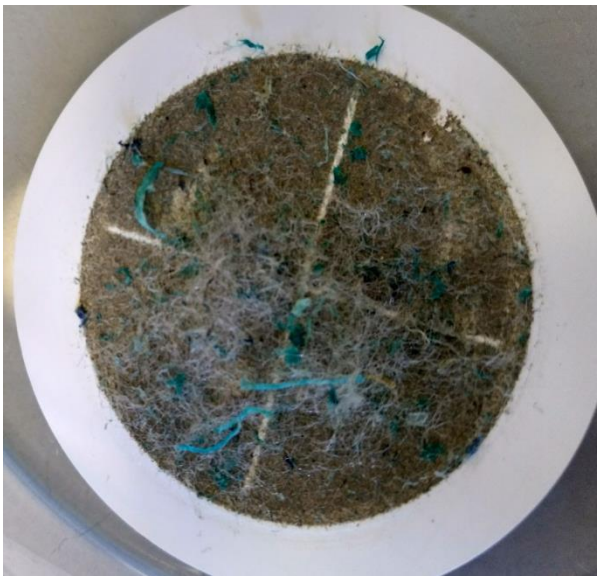

(a) Sample test nº5.

(b) Sample test nº6.

(c) Sample test nº7.

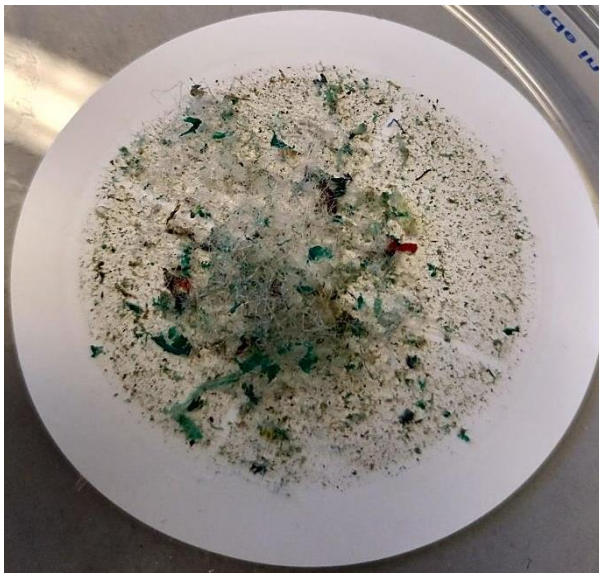

(d) Sample test nº8.

Figure 6.6. Filter surfaces of samples Nº 5,6,7 and 8, corresponding to the fibers' tests.

The same differences regarding the quantity of impurities found in each sample, comparing the 'green' and 'yellow' PE waste fibers (Figure 6.6 (a) and (c), Figure 6.6. (b) and (d), respectively) is recognized visually in test in which fibers were used. Although, several microplastics, not released during the two months experiment, were found in the samples nº 7 and nº8 (Figure 6.6 (c) and (d). Finally, it can be observed in sample nº 8 (Figure 6.6 (d), a ball of white plastic filaments, catching different microplastics inside.

Microscope analysis

From figure 6.7. to figure 6.14. it is presented a picture of the microscope analysis of each sample with the corresponding measurements indicated. In Appendix 2 more figures of the surface analysis are presented.

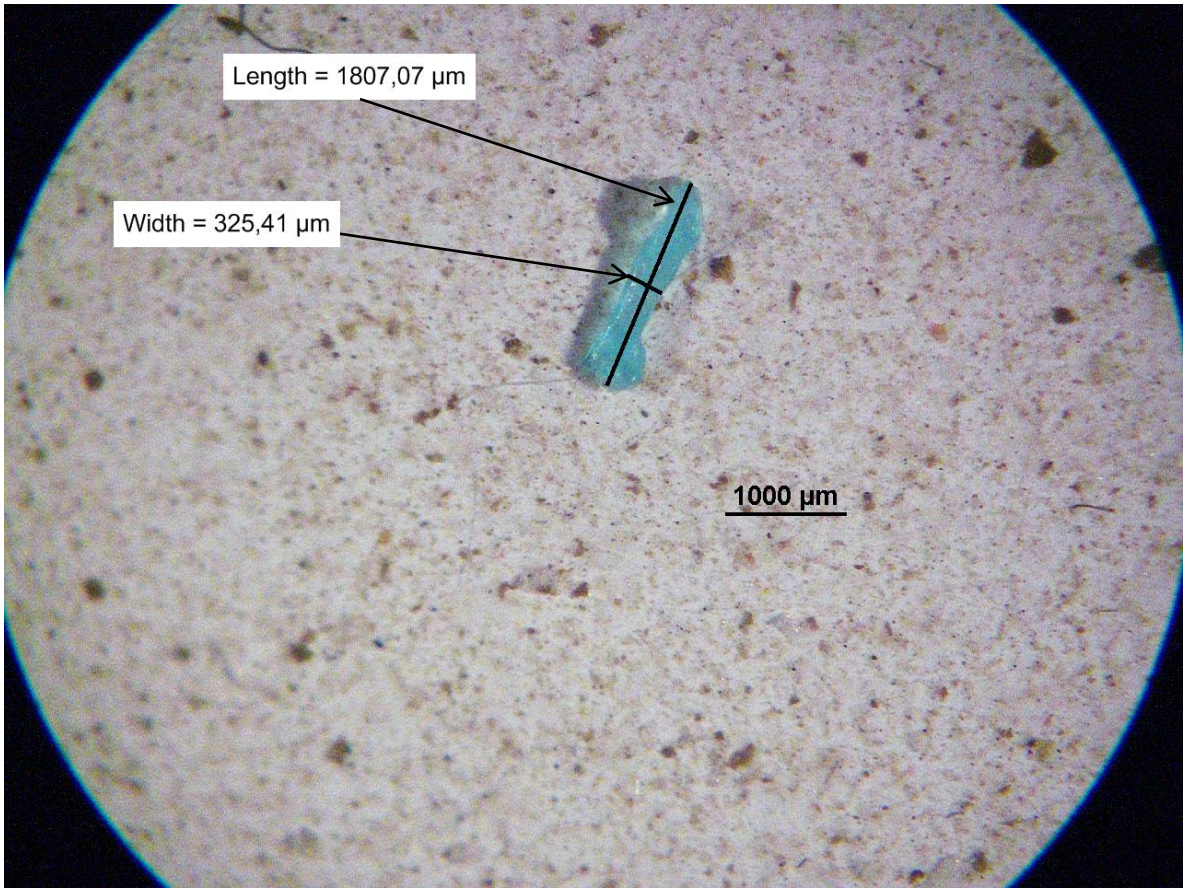

Figure 6.7. Microscope picture of sample nº1. 'green' PE microplastic measures. Scale 1000 µm.

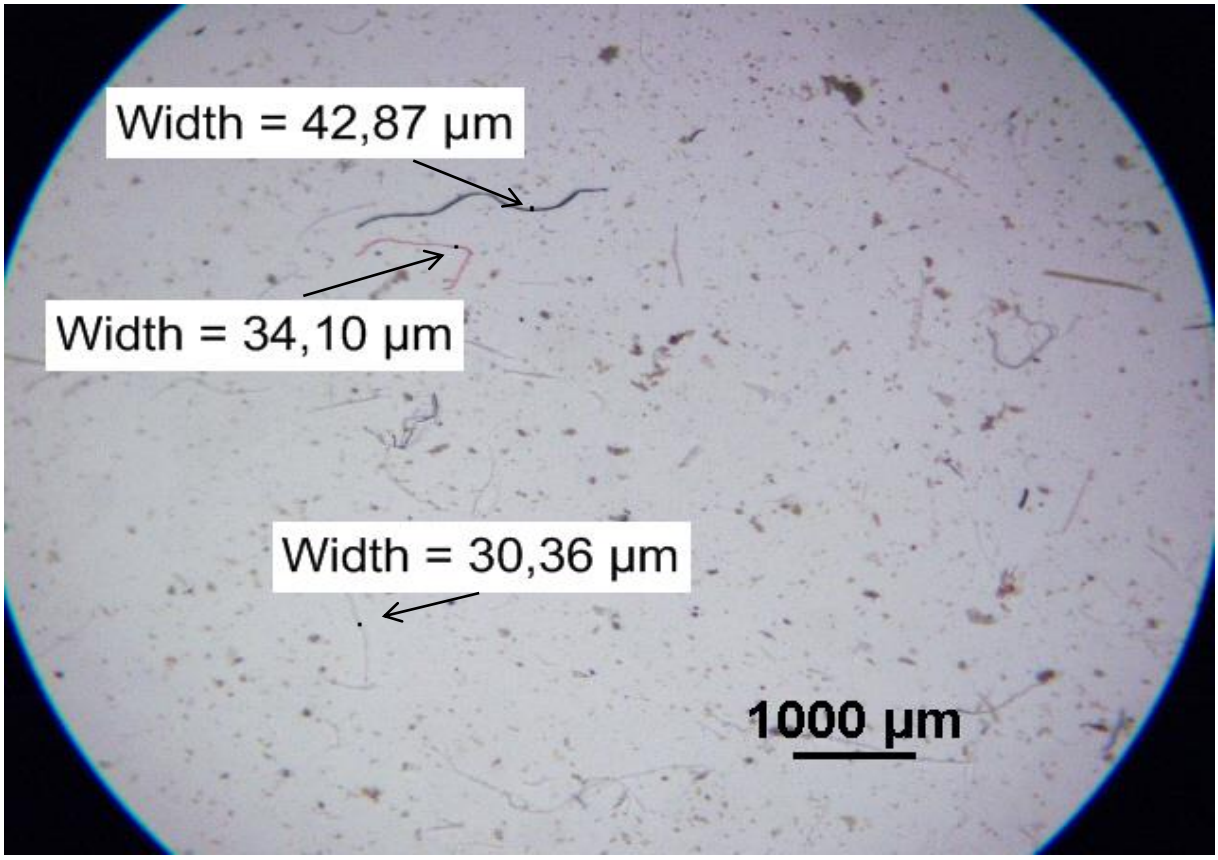

Figure 6.8. Microscope picture of sample nº2. Microplastic filaments measures. Scale 1000 µm.

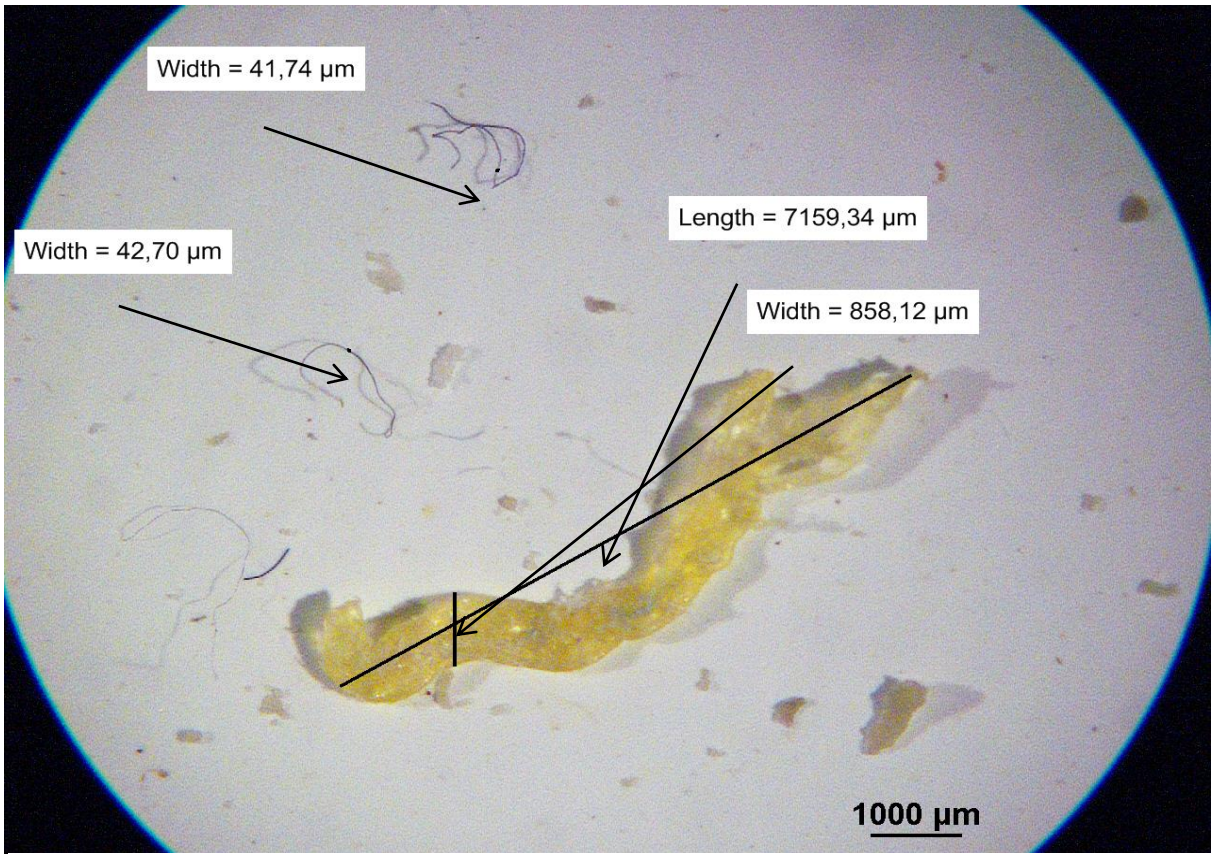

Figure 6.9. Microscope picture of sample nº3. 'yellow' PE and filaments microplastic measures. Scale 1000 µm.

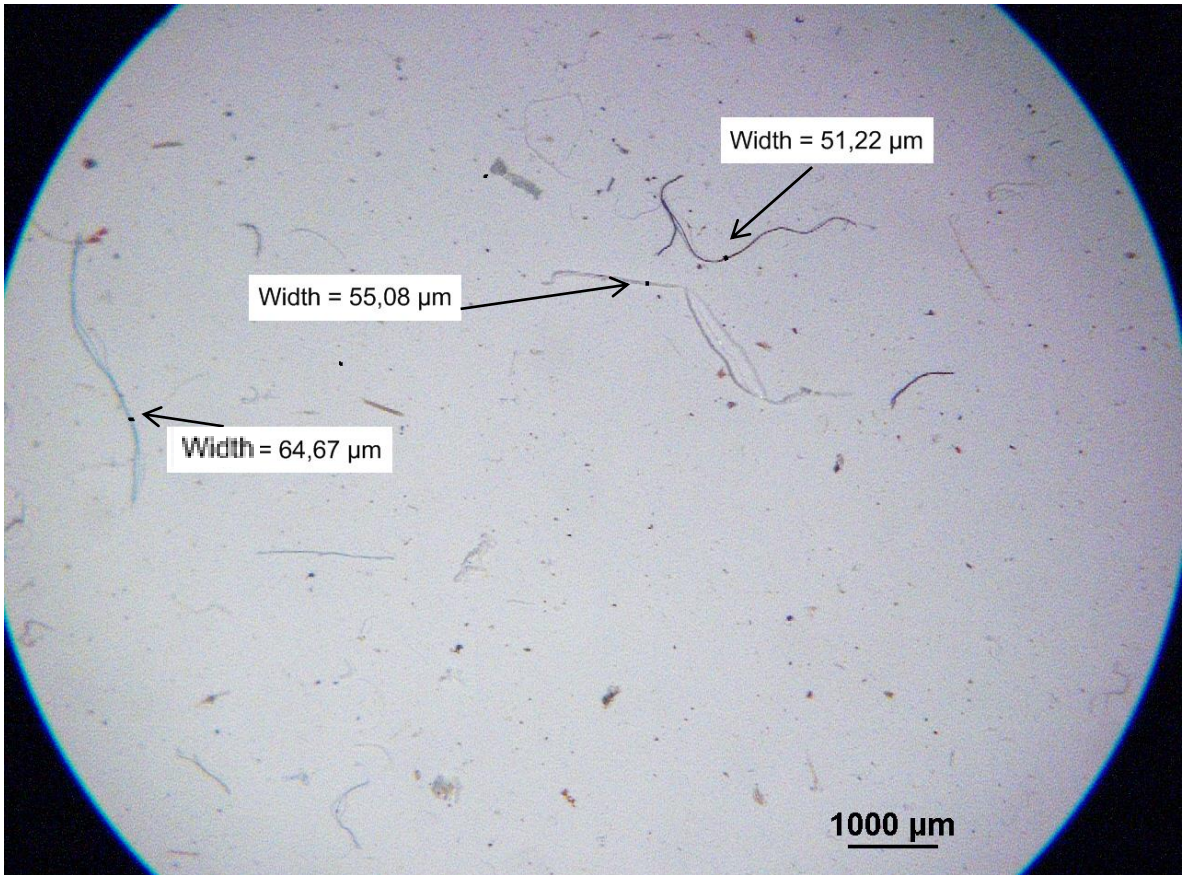

Figure 6.10. Microscope picture of sample nº4. Microplastic filaments measures. Scale 1000 µm.

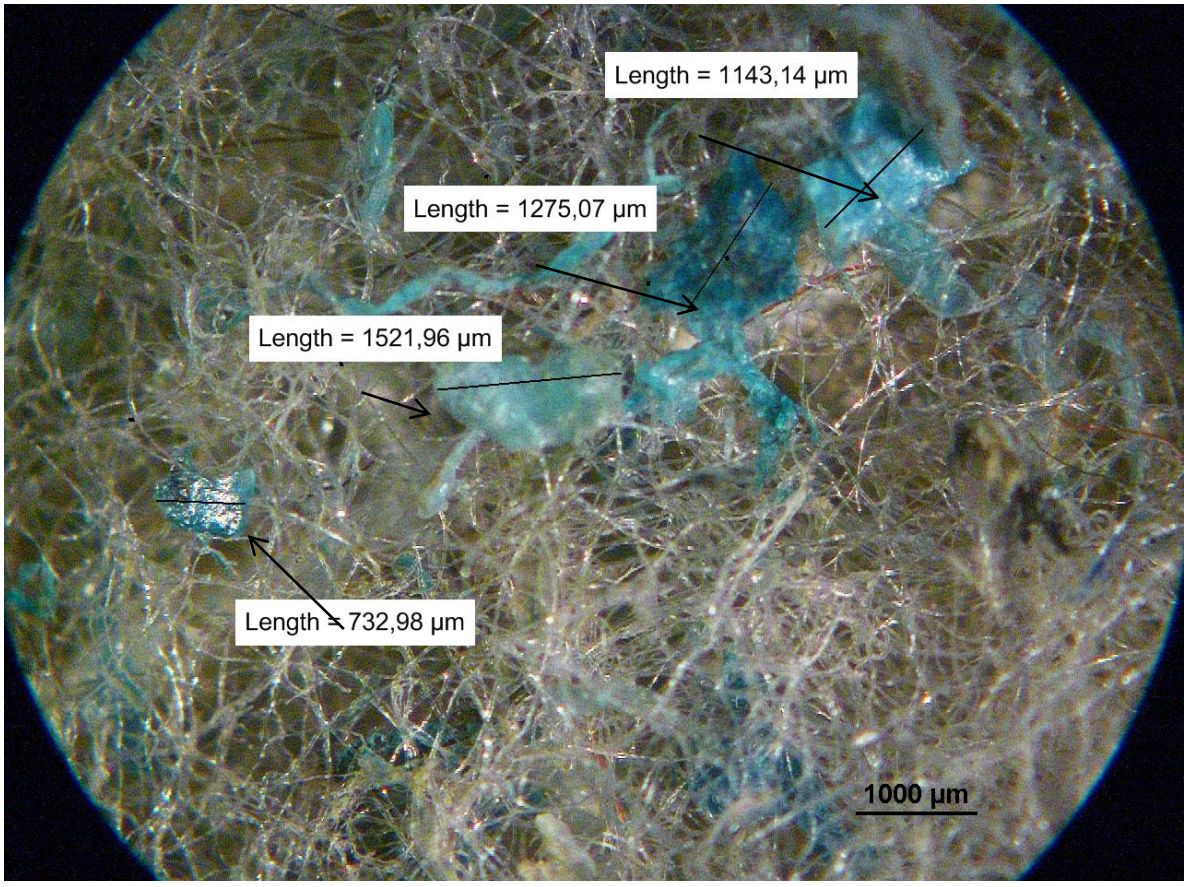

Figure 6.11. Microscope picture of sample nº5. Microplastic filaments measures . Scale 1000 µm.

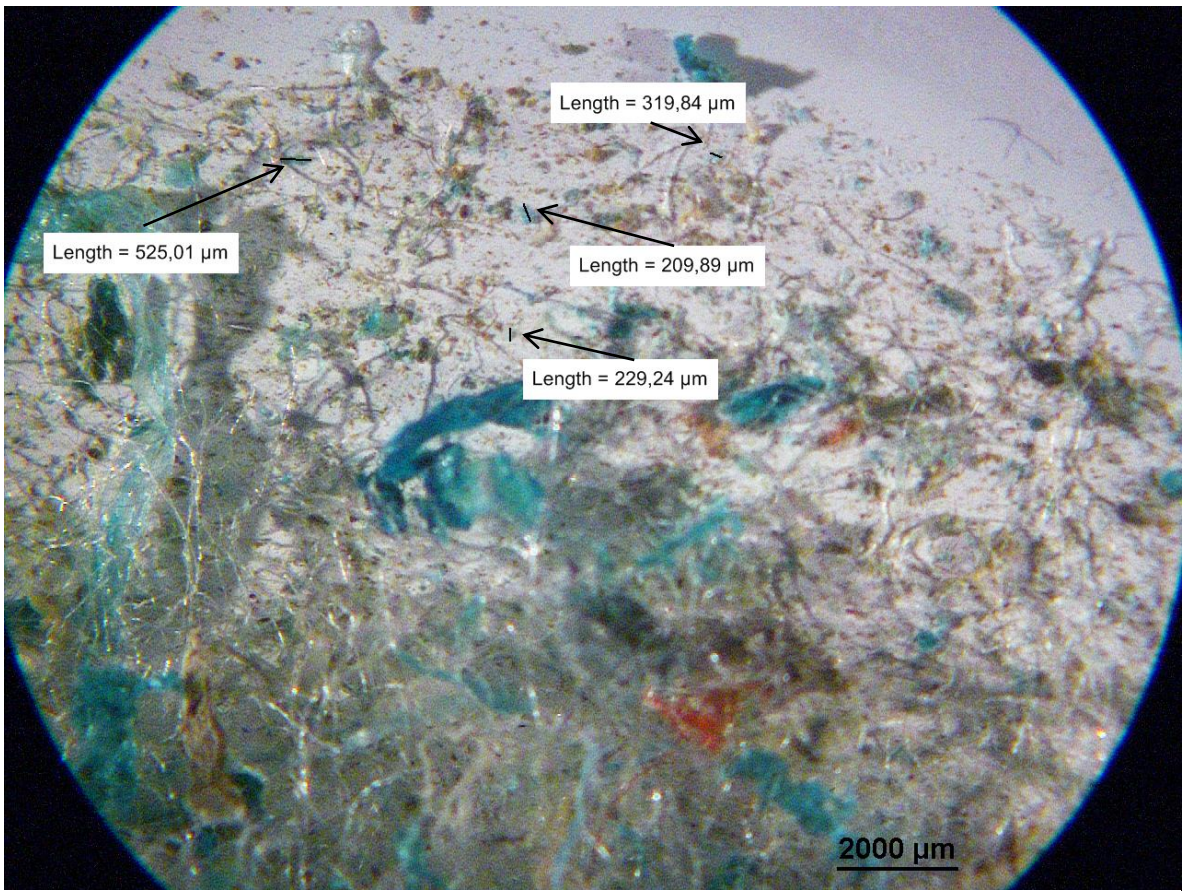

Figure 6.12. Microscope picture of sample nº6. Microplastic measures . Scale 2000 µm.

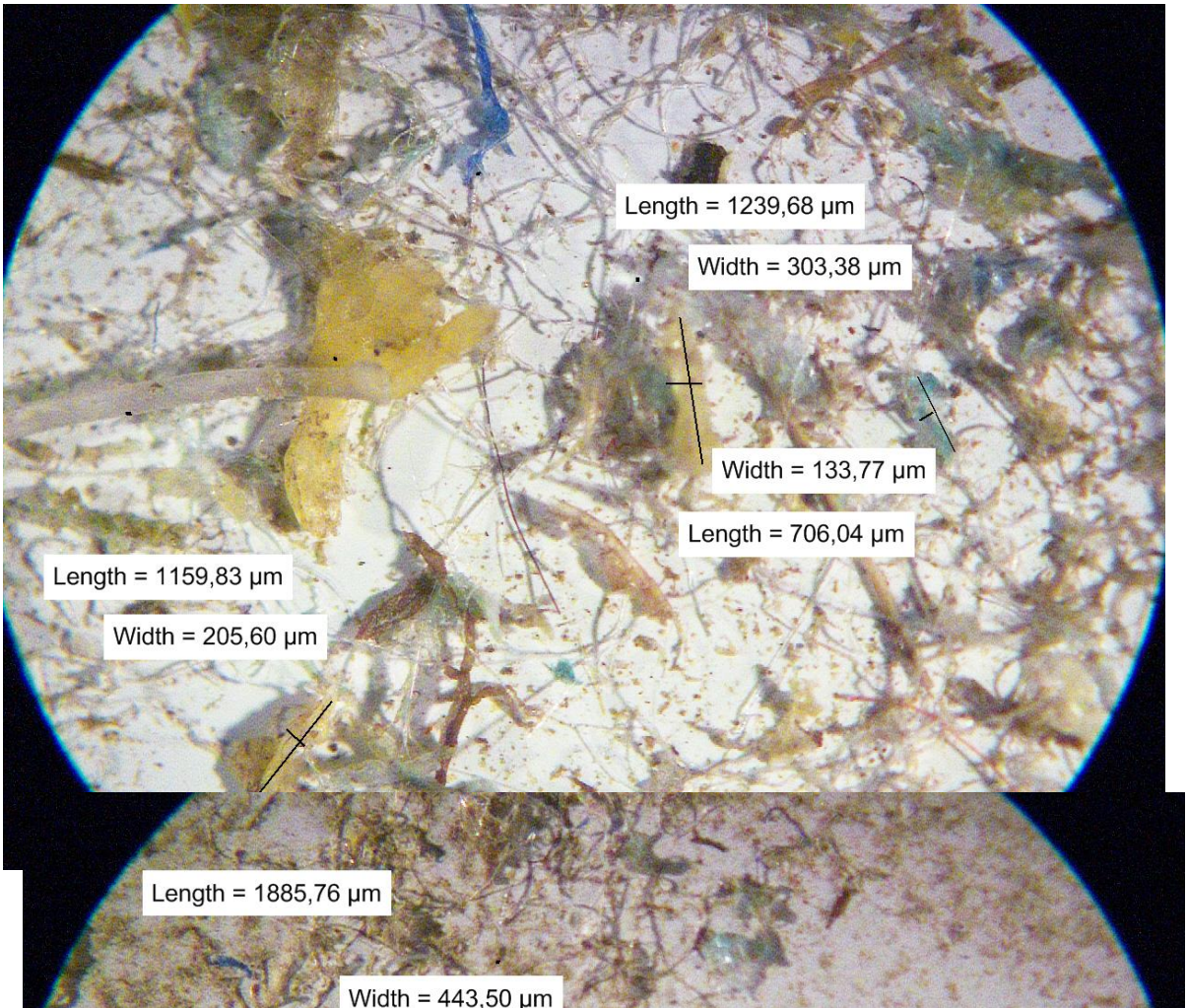

On figure 6.7. and 6.9., corresponding to test nº1 and nº3, some 'green' and 'yellow' PE microplastics, respectively, were found in the sample. Comparing to the tests in which different color fibers were used (test nº 5 and 7), the color of the microplastics released from the nets, was unitary, green for samples nº1 and light yellow for sample nº3. The length and width of these microplastics found can be seen indicated on the pictures. Larger particles had more elongate shapes and/or irregular surfaces, while progressively smaller particles were consistently more circular. Likely, if the experiment would endure more time, these particles would continue to fragment and degrade to ever smaller particles over time. Furthermore, in sample nº1, clay and small particles of sand were deposited covering all over the filter surface, whereas in sample nº3, only some small particles of sand were found scattered on the filter surface.

On figures 6.11. and 6.13., corresponding to test nº5 and test nº7, several microplastics were found. Owing to the difficulty to measure and quantify all the microplastics generated, only some examples of the microplastics found remaining in the water were presented and measured on the figures. It can be observed that on Figure 6.11., the main color of the microplastics found is green, whereas on figure 6.13. is yellow, corresponding to the main color of the fibers used for the experiment. Moreover, there is a big difference in the impurities found in the samples, especially the quantity of clay found in sample nº5 (Figure 6.11.), in which all the surface is covered by these particles. Whereas in the sample nº7 (Figure 6.12.), small particles of sand and clay are observed, but the quantity is much lower than in sample nº5.

On figures 6.8. and 6.10., corresponding to test nº2 and nº4, some fibrillated microplastics with different colors were observed in the samples, being white, the predominating color. As can be observed, some of these microplastics were indicated and measured. However, no round shape microplastics released from the PE nets were found in the sample. Furthermore, small particles of impurities as clay and sand were scattered in the surface homogeneously and in the same way in both samples.

Finally, on figures 6.12. and 6.14., corresponding to test nº6 and nº8, some microplastics were found in the filter surface. However, it can be easily proved that they were not released during the fibers degradation suffered during the two months experiment. Probably, these microplastics were added with the cut fibers at the beginning of the experiment due to an inaccurate washing process. As can be observed on figure 6.14, there is a bunch of white fibrillated microplastics, similar to the one observed on Figure 6.11., trapping other color microplastics inside.

7. Discussion

This chapter includes the discussion of the results from Chapter 6. The chapter includes more in-depth discussion of the results internally, as well as a perspective and a comparison to previous related studies and research.

7.1. Analysis of ocean plastic waste

The average percentage of impurities as microplastics and small particles of salt and sand smaller than 1 mm found in the samples of uncleaned PE fibers was 76%. Only a 24% of the sample mix can be considered as functional PE fibers without degradation effects. As was exposed in section 6.1, it should been taken into account that all the fibers were taken from the bottom part of the plastic bag, in which the fibers are delivered, and where clay and sand particles are accumulated.

As was seen on figure 6.2., there is a big quantity of PE fibers smaller than 1 mm but bigger than 250 µm. Probably, these fibers would not work as well as the fibers bigger than 1 mm due to the smaller contact surface to transmit the force. However, it is considered that these shorter fibers conserve an appropriate size and they preserve the fiber shape to work as reinforcement of the mortar samples, helping to improve the strength values during the post crack behavior. Conversely, the majority of clay and salt is found on the samples smaller than 250 µm, and as S. Svensson (2017) exposed, these materials should be removed to not be mixed during the casting and not damage or weaken the mortar samples. Furthermore, the 'green' PE microplastics smaller than 250 µm analyzed on section 6.1 have rounded or irregular shapes, they don not conserve a fiber shape; the contact area is even smaller. So, these microplastics coming from PE fibers would not work improving the strength during the post crack behavior of the mortar samples. The same effect produced on microplastic shape depending on their size and fragmentation process was proved by V.Hidalgo-Ruz et al. (2012). It can be concluded that a washing process is needed in order to no affect the mechanical properties of the samples. As PE microplastics found bigger than 250 µm but smaller than 1 mm could work as reinforcement, it is important to find a balance to make the washing process of the fibers efficient and not lose useful. After the analysis, it is concluded that sieves with 250 µm holes' length would be a suitable option for removing the impurities before the casting process.

Furthermore, as V.Hidalgo-Ruz et al. (2012) exposed, the samples from tests in which PE fibers were used can contain a wide variety of microplastics with multiples shapes, sizes and origins. It is also exposed that discolored yellow and clear-white-cream plastic

filaments, as the shown in figure 6.2., are one of the most common plastics found in debris samples taken from ocean surface. This fact could explain the filaments found in all the samples.

Finally, the results obtained from the analysis carried out in section 6.1 demonstrated the environmental problem represented by abandoned fishing gear because they microplastic release can enter directly in the marine food chain, as is concluded by A. Montarsolo et al. (2017).

7.2. Analysis of microplastics release

The premature results of the experimentation of the fishing nets degradation on ocean water showed a quicker fragmentation of the PE small scale fishing nets and PE fibers exposed to UV radiation and to abrasive waves simulation.

A wide difference in the quantity of microplastics generated can be observed among the different tests. In the tests were nets were used, the highest amount of microplastics was quantified in the 'yellow' PE net test nº3, followed by test nº1 with the 'green' PE net. The nets were simulated to be floating on the surface. As U. Oxvig and U.J. Hanse (2007) exposed, it can be concluded that the size, the braided type and the tightness of the nets are factors that have affected the microplastics release, because the same environment conditions were set for both tests. The 'yellow' PE net showed a quicker and higher degradation, and apart from a bigger inside dimension of the meshes, the braided of the fibers was less tight, so as was observed in the nets' analysis after two months of experimentation, it was easier to untwist the yellow net than the green one.

In the tests were fibers were used and surface conditions were simulated, a highest quantity of microplastics created was observed. Only longer and cleaned fibers were added to the samples at the beginning of the experiment to assure that all the microplastics observed at the end would come from the fibers degradation. Although the same speed in the mixes was used in all the experiments, fibers were exposed to stronger wave friction due to the small size of fibers and the higher centrifugal force, which increased the microplastics release during the test. However, the difference of microplastics released between 'yellow' and 'green' PE fibers tests was not quantify because of the difficulty.

According to the impurities, small particles of sand and salt were found in the samples. Although a washing process was done before the experiment, because of the centrifugal force applied and the untwisting process of the fishing nets, these particles were detached or released from the fibers and nets.

Furthermore, no microplastics or impurities were found in the samples simulating the immersion under the surface, with no wave friction and no UV light. To observe the degradation in these tests, much more time would have been needed. As N. Kalogerakis et al. (2017) presented in the results from sunlight exposure in seawater near the surface, the fragmentation of the PE film used for the study, resulted higher than under the surface. So, clearly, the exposition to UV light and wave's friction are proved factors affecting the speed of degradation of the PE nets. Similar results and conclusions are exposed by A. Montarsolo et al. (2017), in which fishing nets were also used.

Comparing the results with several studies, the degradation process in this project has been surprisingly fast, taken into account that in only one month, some PE microplastics were visualized in test nº 3, with 'yellow' fishing nets. To obtain a more pronounced degradation, easier to quantify, more time would be needed. As M. Sudhakar and M. Doble (2008), exposed, even after prolonged exposure, 10 to 32 years, the biodegradation of polyethylene was found to be very low.

Once the experiment was over, it was proved a slight loss of material in the nets, between 0,20 and 1,10 %, with the consequent decompression of the fiber braided. The loss of material and the braided decompression observed in the nets exposed to ocean surface conditions were higher. However, a slight decrease on weight was also measured in nets under immersion conditions, conditioned by the deposition of some impurities as sand and salt particles that were trapped in the nets since the beginning of the experiment.

Moreover, it should be highlighted that the simulation was done inside ocean water, where as it is confirmed by N.Kalogerakis et al. (2017), the microplastics fragmentation is much slower than onshore. N.Kalogerakis et al.(2017) study is focused on the degradation of PE film onshore and offshore, and the results presented showed that although onshore degradation is faster, the microplastics quickly return to the seawater with high waves or strong winds, where they much more difficult to collect.

As V.Hidalgo-Ruz et al. (2012) cited, the shape of plastic fragments depends on the fragmentation process as well as residence time in the environment. The microplastics analyzed in the project, presented more elongate shapes while progressively smaller particles were more rounded or circular. If the small-scale experiment had endured more time, the microplastics would continue to fragment and degrade to ever smaller particles over time. Moreover, the most common colors found in the microplastics in the samples were white, green or discolored yellow. In this case it is easy to conclude that the origin of these microplastics were the PE nets because all impurities were cleaned before starting the experimentation. However, usually these colors are attributed to the PE microplastics

found in the marine plastic pollution, as is presented in the study carried out by V.Hidalgo-Ruz et al. (2012).

As conclusion of the discussion, it should be highlighted that these results demonstrated the urgent need and the environmental problem represented by abandoned fishing gear in the ocean because of the proved microplastics release, that can enter directly the marine food chain, entering lately the human food chain with unknown effects for health.

Part II – Recycled fibers as mortar reinforcement

8. Objectives

The objectives in the second part of the project were to test several mechanical properties as flexural and compressive strength for different samples using waste PE fibers from discarded fishing nets as reinforcement, to compare the results with the commercial PP FRM samples used currently in the industry. Furthermore, an analysis was carried out in order to quantify the dry shrinkage in different mortar samples, using a digital image correlation (DIC) method to finally compare the microstrain results with the results obtained from the Linear Variable Displacement Transducer (LVDT) and demonstrate the workability of both methods.

9. Materials

This chapter includes the description of the materials used in the mortar mixture focused on their properties and the preparation before they were used. The casting of the different mortar samples, including the composition of the mix designs and the different types of specimens produced are also presented.

9.1. Fibers

For the experimentation in this project, three different types of fibers were used (Figure 9.1.). The main objective was to compare the effect of each type of fiber on the mortar samples with the experiments' results.

Commercial fibers

These fibers are polypropylene (PP) fibers used in the industry to reduce plastic shrinkage cracking. They are called Fibrin fiberflex and they are delivered by PP Nordica, a supplier company in the Scandinavian plastic fiber market. These fibers are 12 mm long and 18 µm wide and were added to the mortar mixture at volume percentage of 0,2%.

Recycled fibers

These fibers are waste fibers from discarded fishing nets made of polyethylene (PE) delivered by the Danish company Plastix, which is a cleantech company that collects discarded fishing nets and transforms them into new plastics materials. Within these PE fibers it has been differentiated between two different types of fibers due to the variety of nets processed. To differentiate these fibers along the project, they have been named according to their color, as 'yellow' fibers and 'green' fibers. All these PE fibers were of different length, thickness and color.

(a) Commercial PP fibers. (b) PE 'yellow' fibers from discarded nets. (c) PE 'green' fibers from discarded nets.

Figure 9.1. Different types of fibers used in the specimens.

The principal characteristics of these fibers are given on table 9.1.

Table 9.1. Characteristics of the different fibers used for the specimens.

	Polypropylene fibers (PP)	Polyethylene 'yellow' fibers (PE)	Polyethylene 'green' fibers (PE2)
Shape	Strand	Strand	Strand
Color	White	Yellow	Green
Diameter [μm]	18	348	348
Length [mm]	12	17,96	17,96
Density [g/cm3]	0,910	0,950	0,950

*Note: The data in the table is provided by the company Plastix and obtained from G. Carinaud (2017). The diameter and length data provided for the PE fibers is an average of the different measures taken in the G.Cardinaud (2017) project.

9.2. Casting- Mortar mixture

The mortar mixtures were made according to the standard DS/EN-196-1 (2005).

Mix design

In order to increase the possibility of cracking shrinkage production, it is important to include a low content of cement in the mortar mixture. For this reason, a ratio of water/cement (w/c) = 0.5 was used for all the experiments. During the project, four different mortar mixes were made, to assure the w/c ratio, the water content of the sand was measured each time to adjust the mix proportions before casting. A detailed experimental log of the water content measures can be obtained in Appendix 3.

Four types of mixtures are distinguished: reference or plain mortar (unreinforced), mortar with PP commercial fibers, mortar with 'yellow' PE fibers and mortar with 'green' PE fibers. All the mixtures used in the experiments of the project are shown on table 9.2.

Table 9.2. Mortar mixtures used in the experimentation with their respective references.

Nº	Reference	w/c [-]	PP fibers [v%]	PE 'yellow' fibers [v%]	PE 'green' fibers [v%]
1	Ref-	0.5	0	0	0
2	Ref PP	0.5	0.2	0	0
3	Ref PE	0.5	0	2.0	0
4	Ref PE2	0.5	0	0	2.0

The mix proportions used for each mortar mixture are shown from table 9.3 to table 9.6. with the date of casting:

Table 9.3. Mix design for plain mortar mixture, Ref –

Plain mortar [Ref-] 07/02/18	
Material	**Amount [g]**
Cement	3150 ± 2
Sand	4651 ± 5
Fibers	0
Water	1570 ± 1
Total	**9371** ± 8

Table 9.4. Mix design for fiber reinforced mortar mixture with commercial PP fibers, Ref PP

PP fibers mortar [REF PP] 12/02/18	
Material	**Amount [g]**
Cement	3500 ± 2
Sand	5176 ± 5
Fibers	9,1
Water	1736± 1
Total	**10421** ± 8

Table 9.5. Mix design for fiber reinforced mortar mixture with 'yellow' PE fibers, Ref PE

PE 'yellow' fibers mortar [REF PE] 14/02/18	
Material	**Amount [g]**
Cement	3500 ± 2
Sand	4912 ± 5
Fibers	95
Water	1740 ± 1
Total	10247± 8

Table 9.6. Mix design for fiber reinforced mortar mixture with 'green' PE fibers, Ref PE2

PE 'green' fibers mortar [REF PE2] 19/02/18	
Material	**Amount [g]**
Cement	3500 ± 2
Sand	4912 ± 5

Fibers	95
Water	1740 ± 1
Total	10247± 8

The cement used was Aalborg Portland Basis cement with a strength class of CEM II/A-LL 52.5 N (LA). The sand used in the mixture was wet sand with a grain size between 0- 4 mm, and the water was regular fresh tap water.

Specimens' dimensions

According to the tests carried out along the project, two types of samples were prepared in molds with different dimensions.

Prism Specimen

For each mixture, twelve samples were produced with a prism shape and a size of 40 x 40 x 160 mm. These mortar samples were tested after 1, 2, 7 and 28 days of curing. The table below shows an overview of all the samples produced during the study period.

Table 9.7. Number of prism specimens produced for each mortar mixture.

Reference	Fiber type	Fiber content [%]	Curing period [days]	Number of samples
REF -	-	0	1,2,7 and 28	12
REF PP	PP	0,2	1,2,7 and 28	12
REF PE	PE 'yellow'	2,0	1,2,7 and 28	12
REF PE2	PE 'green'	2,0	1,2,7 and 28	12

On figure 9.2., it is illustrated the mold used for prism samples and one prism specimen after the demolding process.

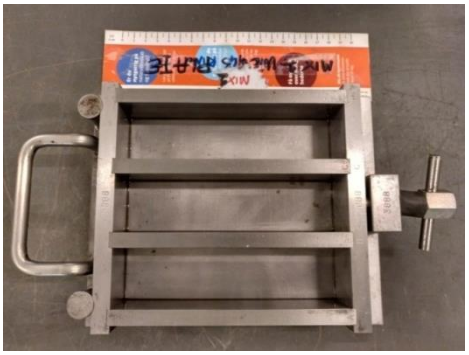

(a) Prism mold used in the casting.

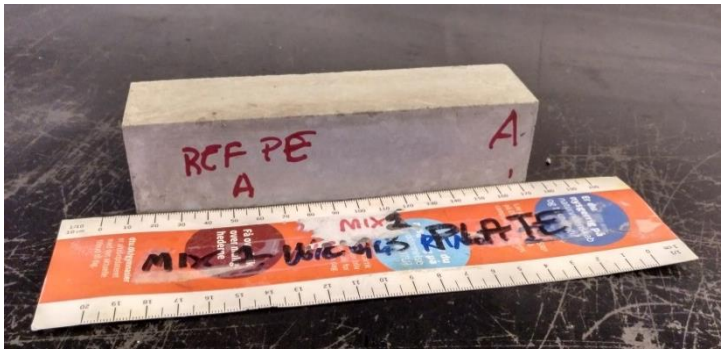

(b) Prism specimen REF PE A after demolding.

Figure 9.2. Prism mold and specimen with dimensions 160 x 40 x40 mm.

Bar Specimen

For each mixture, six samples were produced with a beam shape of size 2,5 x 2,5 x 28,5 mm for each mortar sample. In each mold, small screws are placed in order to use the bar on a micrometer. These mortar samples were drying freely during 28 days. The table 9.8., below, shows an overview of samples produced during the study period.

Table 9.8. Number of bar specimens produced for each mortar mixture.

Reference	Fiber type	Fiber content [%]	Testing period [days]	Number of samples
REF -	-	0	28	6
REF PP	PP	0,2	28	6
REF PE	PE 'yellow'	2,0	28	6
REF PE2	PE 'green'	2,0	28	6

On figure 9.3. is illustrated the mold used for bar samples and one bar specimen after the demolding.

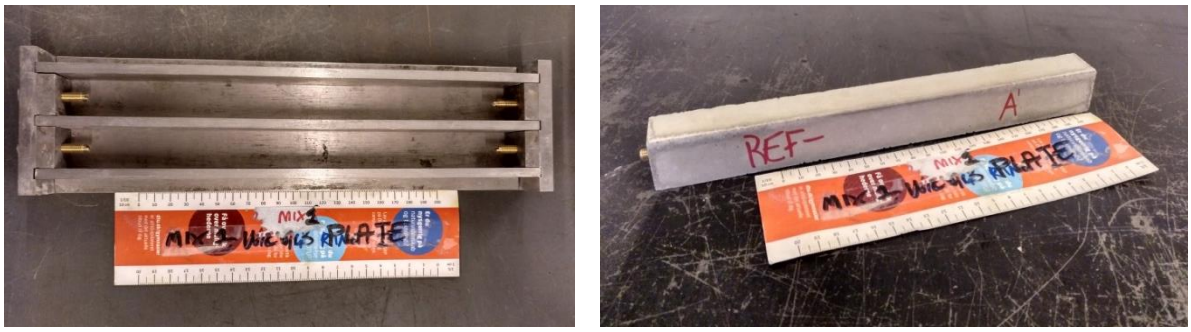

(a) Bar mold used in the casting.

(b) Bar specimen REF -A after demolding.

Figure 9.3. Bar mold and specimen with dimensions 285 x 25 x 25 mm.

Procedure

The mixing of the mortar mixture was performed on a Hobart Mixer, which has a volume capacity of 5 liters and a speed range from 0 to 3, being the fastest.

Figure 9.4. Hobart Mixer for high volume mixtures used for the experimentation.

The procedure for the mixing of the reference mortar samples was done according to DS/EN-196-1 (2005) and a step by step procedure for the casting process is shown in Table 9.9. The same procedure was following during all the castings made in the project.

Table 9.9. Casting step by step procedure in the Hobart Mixer for high volume.

Time [min]	Action	Period [s]	Mixing speed
0:00-2:00	Mix cement+ sand	120	1
↓			
2:00-2:30	Add water	30	1
↓			
2:30-5:00	Mixing	180	1
↓			
5:00-6:00	Break (add fibers)	60	-
↓			
6:00-11:00	Fast mix	300	2,5
↓			

The mixing period endured a total of 11 minutes. After the mixing, the mixture was cast into mortar molds completely clean and greased to facilitate the demolding with mold oil. A vibrator table was used, where the molds were filled a half and vibrated for 60 seconds at 60 Hz. This action was repeated again until the molds were completely filled, and the excessive mortar was scraped off during the second vibration to get an even surface. This was done as seen on Figure 9.5.

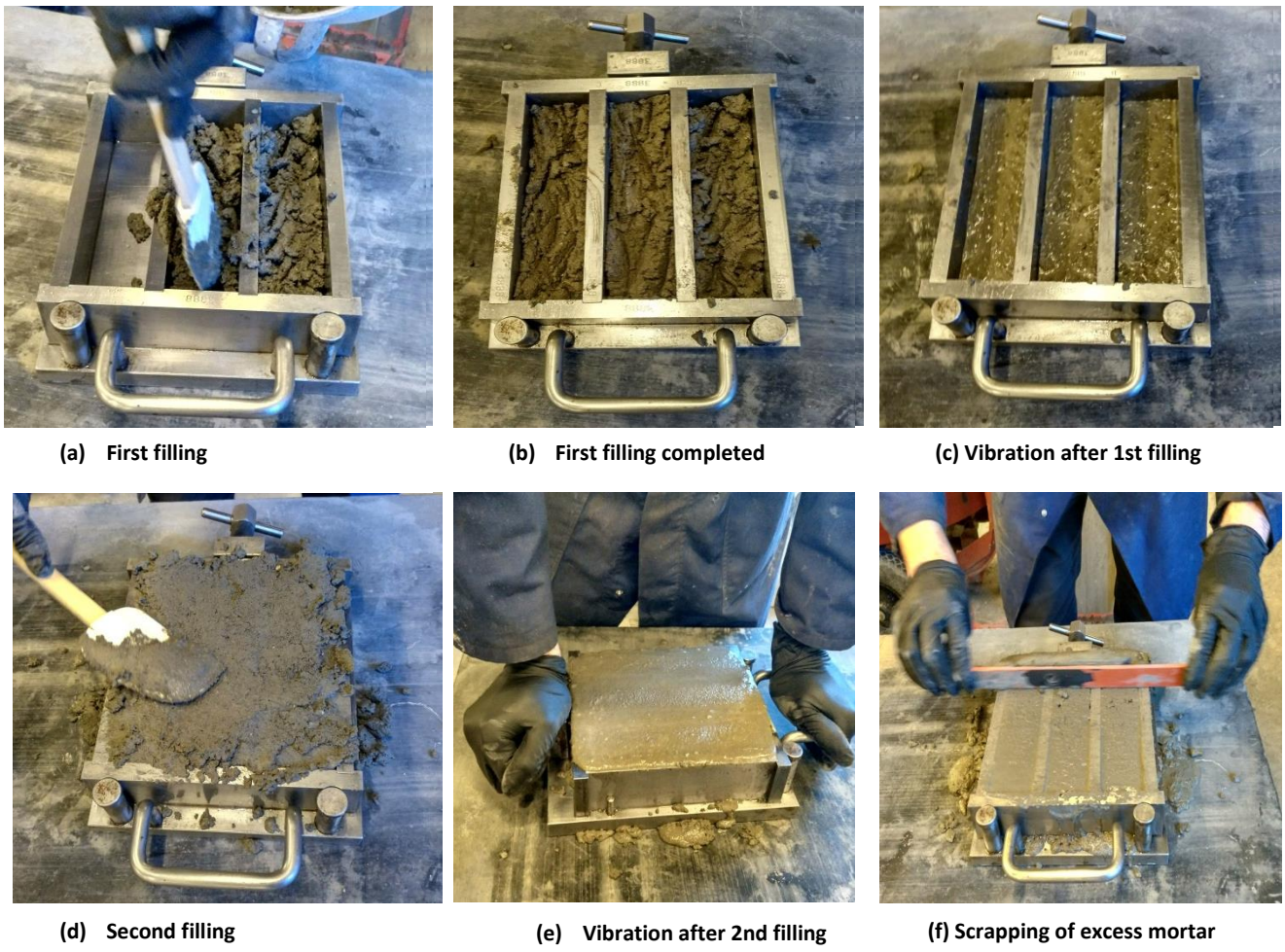

(a) First filling (b) First filling completed (c) Vibration after 1st filling

(d) Second filling (e) Vibration after 2nd filling (f) Scrapping of excess mortar

Figure 9.5. Step by step procedure in the casting of mortar samples.

The samples cured in the molds for 24 hours covered with a plastic to avoid the evaporation of water and maintain a moisture environment (Figure 9.6.). After 24 hours the samples were unmolded. The prism specimens were left to cure completely covered in water and the beams specimens were painted and left to dry free in the environment chamber.

Figure 9.6. Specimens after casting covered with plastic during 24 h.

Some failures were produced in the bending test machine during the experimentation, which caused the repetition of the casting for three prism specimens of each mix.

Due to the low volume needed for the second casting, the Hobar mix, up to 2 liters, on figure 9.7. was used.

Figure 9.7. Hobart Mixer for low volume mixtures used for the experimentation.

The step by step procedure for low volume casting is shown in Table 9.10.

Table 9.10. Casting step by step procedure in the Hobart Mixer for low volume.

Time [min]	Action	Period [s]	Mixing speed
0:00-0:30	Mix cement+ sand	30	1
↓			
0:30-1:00	Add water	30	1
↓			
1:00-3:00	Mixing	120	1
↓			
3:00-3:30	Break (add fibers)	60	-
↓			
3:30-4:30	Fast mix	300	2,5
↓			

The mix proportions for the casting repetition are presented on Appendix 3.

10. Methods

10.1. Methods I

This section includes the testing of some hardened mechanical properties of the mortar samples with a focus on bending strength, compressive strength and bonding between the fibers and the matrix. For each mortar mixture, after 1, 2, 7 and 28 days of curing, were calculated three results for the bending strength and three results for the compressive strength. The final strength for bending and compression was calculated with the average of these results separately. The bending toughness was calculated with the results obtained in the bending test. Finally, a SEM analysis of the different fiber surfaces was carried out and it is presented in the section.

Table 10.1. shows the experimental log for the mortar experiments. A more detailed experimental log can be obtained in Appendix 1.

Table 10.1. Experimental log for the mortar experiments.

Date	Experiment	Standard	Location
07-02-18	Casting of plain concrete samples (REF-)	DS/EN-196-1	DTU Concrete Lab
08-02-18	Bending and compression test 1 day prism samples (REF-)	DS/EN-196-1	DTU Byg
08-02-18	Starting of LVDT and DIC tests with bar samples (REF-)	-	DTU Concrete Lab
09-02-18	Bending and compression test 2 day prism samples (REF-)	DS/EN-196-1	DTU Byg
12-02-18	Casting of concrete with PP reinforced mortar samples (REF PP)	DS/EN-196-1	DTU Concrete Lab
13-02-18	Bending and compression test 1 day prism samples (REF PP)	DS/EN-196-1	DTU Byg
13-02-18	Starting of LVDT and DIC tests with bar samples (REF PP)	-	DTU Concrete Lab
14-02-18	Casting of concrete with PE 'yellow' reinforced mortar samples (REF PE)	DS/EN-196-1	DTU Concrete Lab
14-02-18	Bending and compression test 2 day prism samples (REF PP)	DS/EN-196-1	DTU Byg
14-02-18	Bending and compression test 7 day prism samples (REF-)	DS/EN-196-1	DTU Byg
15-02-18	Bending and compression test 1 day prism samples (REF PE)	DS/EN-196-1	DTU Byg
15-02-18	Starting of LVDT and DIC tests with bar samples (REF PE)	-	DTU Concrete Lab

16-02-18	Bending and compression test 2 day prism samples (REF PE)	DS/EN-196-1	DTU Byg
19-02-18	Casting of concrete with PE'green' reinforced mortar samples (REF PE2)	DS/EN-196-1	DTU Concrete Lab
19-02-18	Bending and compression test 7 day prism samples (REF PP)	DS/EN-196-1	DTU Byg
20-02-18	Bending and compression test 1 day prism samples (REF PE2)	DS/EN-196-1	DTU Byg
20-02-18	Starting of LVDT and DIC tests with bar samples (REF PE2)	-	DTU Concrete Lab
21-02-18	Bending and compression test 7 day prism samples (REF PE)	DS/EN-196-1	DTU Byg
21-02-18	Bending and compression test 2 day prism samples (REF PE2)	DS/EN-196-1	DTU Byg
26-02-18	Bending and compression test 7 day prism samples (REF PE2)	DS/EN-196-1	DTU Byg
7-03-18	Bending and compression test 28 day prism samples (REF -)	DS/EN-196-1	DTU Byg
7-03-18	End of LVDT and DIC tests with bar samples (REF -)	-	DTU Concrete Lab
12-03-18	Bending and compression test 28 day prism samples (REF PP)	DS/EN-196-1	DTU Byg
12-03-18	End of LVDT and DIC tests with bar samples (REF PP)	-	DTU Concrete Lab
14-03-18	Bending and compression test 28 day prism samples (REF PE)	DS/EN-196-1	DTU Byg
14-03-18	End of LVDT and DIC tests with bar samples (REF PE)	-	DTU Concrete Lab
19-03-18	Bending and compression test 28 day prism samples (REF PE2)	DS/EN-196-1	DTU Byg
19-03-18	End of LVDT and DIC tests with bar samples (REF PE2)	-	DTU Concrete Lab
05-04-18	Preparation of samples for the SEM analysis	-	DTU Byg
10-04-18	SEM Analysis of PE and PP fiber mortar samples	-	DTU Byg with help from Ebba Cederberg
01-05-18	SEM Analysis of PE and PP fiber mortar samples and electronic microscope analysis of4 impurities coming with the PE fibers		DTU Byg with help from Ebba Cederberg

10.1.1. Bending

Set-up

To test the bending strength of the prism mortar samples, a three point bending set-up was established.

The test was performed on a hydraulic testing machine, Instron 6022, which recorded the working curve for each testing. The testing was done according to standard DS/EN-196-1 (2005), where load was applied at the middle of the mortar prism until fracture for the reference samples or post-break strength starting to decrease significantly for the FRM samples.

The load tempo was set to 1 mm/min downward deflection. The set-up is illustrated on figure 10.1 (a) and the actual experiment set up on figure 10.1 (b).

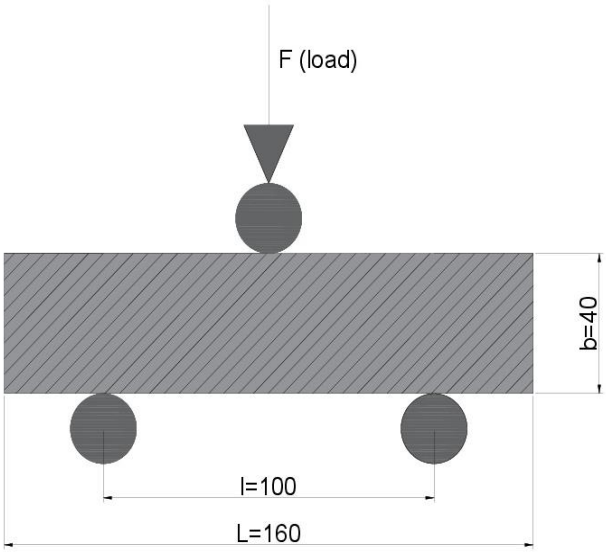

(a) Sketch set-up.

(b) Set-up in pressure machine Istron 10 kN.

Figure 10.1. Bending of mortar sample.

Theory

To calculate the bending strength of the mortar in Mpa, Rf , the following equation is used

$$Rf = \frac{1.5 \cdot F_f . l}{b^3} \qquad (10.1)$$

,F_f is the load applied to the middle of the prism at fracture [N], l was the distance between the supports [mm], and b was the side of the square section of the prism [mm].

As it is shown in the figure xxx, if the mortar was not reinforced with fibers, the load barring capacity would reach zero after the initial crack (point A), meaning the samples would break in two. However, the fiber reinforced mortar (FRM) samples would have a significantly load barring capacity after the initial crack with a maximum load (point B) and maximum post-break load (point C). The area under the graph in figure 10.2. is defined as the flexural toughness (blue area), and as it is shown the FRM will have a significantly higher toughness (light blue) that of the reference samples without fibers (dark blue).

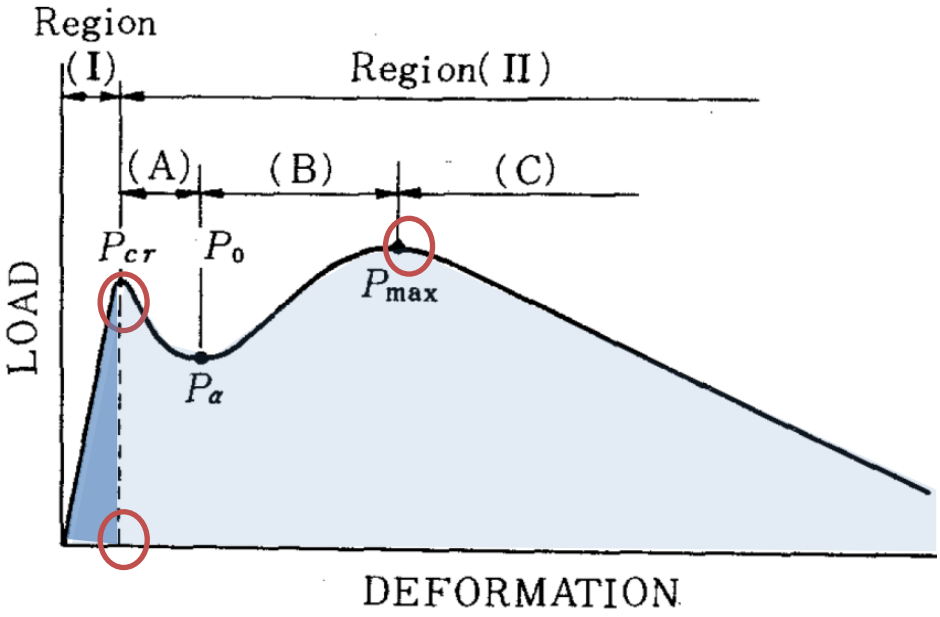

Figure 10.2. Schematic working curve for plain concrete and FRM. K. Kobayashi and R.Cho (1981)

Finally, to evaluate the workability of the fibers during the flexural test, the fiber efficiency factor (FEF) is calculated using the following equation,

$$FEF = \frac{P_0}{P_{cr}} \qquad (10.2)$$

,P_0 is the stress where the fibers start working [N] and P_{cr} is the material's flexural strength.

10.1.2. Toughness

Calculation's theory

To calculate the flexural toughness the normative ASTM C1018-02 (1998) was followed. The flexural toughness can be calculated as the area under the load-deflection curve up to a target value of deflection, δ. Three toughness indexes are determined for three specific values of deflection. The following equations were used. The first equation was used to calculate the toughness for the critical deflection $T_{\delta cr}$.; the second equation was used, to calculate the toughness value for two times the critical deflection; and the third equation was used to calculate the toughness value for three times the critical deflection.

$$T_{\delta cr} = \int_0^{\delta cr} P\delta d\delta \qquad (10.3)$$

$$T_{2\delta cr} = \int_0^{2\delta cr} P\delta d\delta \qquad (10.4)$$

$$T_{3\delta cr} = \int_0^{3\delta cr} P\delta d\delta \qquad (10.5)$$

Two toughness indices I_5 and I_{10} were determined to compare the flexural toughness values before and after the initial crack. The indices provide the improvement in flexural toughness compared with the flexural toughness obtained when the first crack appears.

$$I_5 = \frac{T_{2\delta cr}}{T_{\delta cr}} \qquad (10.6)$$

$$I_{10} = \frac{T_{3\delta cr}}{T_{\delta cr}} \qquad (10.7)$$

The residual strength factor, $R_{5,10}$, is calculated as

$$R_{5,10} = 20 \cdot (I_{10} - I_5) \qquad (10.8)$$

10.1.3. Compression

Set-up

The test was performed on a pressure machine 'Toni 300', in which is recorded the maximum load at fracture in kN for each testing. To test the compression strength of the prism mortar samples, the standard of DS/EN 196-1 was followed.
The load is applied on a 40 x 40 mm surface of the prism until fracture. The sketch set-up is illustrated on figure 10.3.

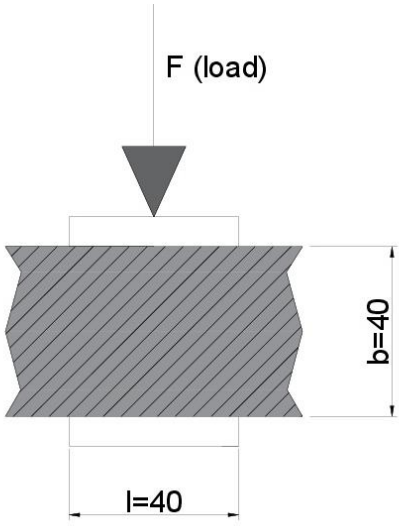

(a) Sketch set-up.

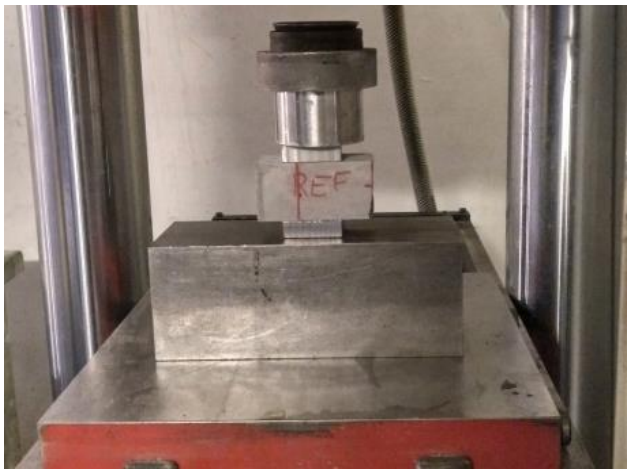

(b) Set-up in pressure machine Tony 300.

Figure 10.3. Compression of mortar sample.

Theory

Additionally the compression strength of the mortar in Mpa, Rc, was calculated by equation (10.9).

$$Rc = \frac{F_{cm}}{b.b} \qquad (10.9)$$

Where F_{cm} is the load applied to an area of 40 x 40 mm of the prism at fracture [N] and b is the side of the square section of the prism [mm].

As it is shown on figure 10.4., in general, the incorporation of plastic as aggregate decreased the compressive strength of the resulting concrete/mortar, having plain concrete the highest compressive strength. The factor responsible for this decrease in compressive strength can be attributed to the low bond strength between the surface of the plastic waste and the cement paste.

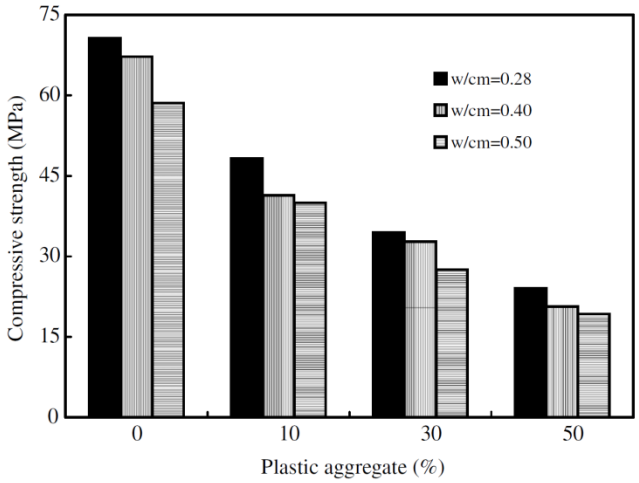

Figure 10.4. Compressive strength versus plastic fiber reinforcement percentage. A.A.Al-Manaseer (1997)

10.1.4. Interface bonding- SEM Analysis

The objective of carrying out the SEM analysis of the fracture surfaces after the bending test was to study the different interface bonding generated by shear deformation between the fibers and the cement-based material matrix. Fiber bonding is an important and effective parameter on fiber reinforced cement, as debonding is known as the primary form of failure in adhesively bonded structures. (H.R. Pakravan et al., 2009)

Mechanical bonding in fiber-cement interface has as important role to enhance the mechanical performance of cement composite materials. PP and PE fibers have low modulus of elasticity and hydrophobic characteristics, which develop a low bonding between fibers and cement matrix. However, these fibers are still attractive for concrete reinforcement, mainly because of their high resistance to alkaline environments and their low cost. (H.R. Pakravan et al., 2009)

The interface fiber-to-matrix debonding was determined using Scanning Electron Microscope (SEM).

Set-up

All the samples were cut with a radial saw and left to dry inside the environmental chamber (Figure 10.6) until the day before of the SEM analysis.

The fracture surfaces of the prisms were analyzed by a FEI-Quanta 200 machine, a scanning electron microscope fitted with a field emission gun electron source to provide high imaging resolution when information is required at the nano-meter scale. A low-vacuum mode was used during the analysis to avoid ignition to damage the sample. The samples used for the SEM analysis were the 28 days of curing samples for all the mixes.

Theory

A typical load-deflection curve for fiber-reinforced concrete in flexure is shown on figure 10.5. The segment AB represents the region where there is continuous cracking of the matrix and some debonding and pulling-out of the fibers. It should be noted that during this part of the debonding and pulling out process, the fiber stress is generally substantially less than the yield stress of the fibers, so yielding of the fibers does not occur. In the declining portion of the curve, BC, matrix cracking and fiber pull-out continue. If the fibers are long enough to maintain their bond, they may eventually fail by yielding or fracture in this region of the curve. (V. S. Parameswaran, 1991)

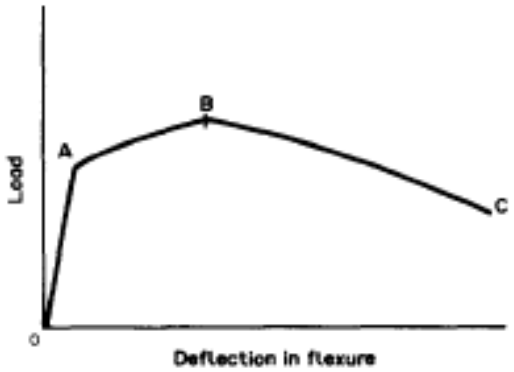

Figure 10.5. Typical load-deflection curve for fiber-reinforced concrete. Source: V. S. Parameswaran, 1991

10.2. Methods II

This section is focused on the analysis of a durability-related property as it is the shrinkage. Two different tests were carried out in this section to characterize the free drying shrinkage of the bar mortar samples: the Linear Variable Displacement Transducer Test (LVDT), which is done manually with a micrometer, and the Digital Image Correlation Test (DIC). Five bar samples were used for the DIC test, whereas one sample was used for the LVDT test.

10.2.1. Free shrinkage characterization

Environmental chamber

Both tests took place inside the environment chamber at the Concrete Lab with specific controlled temperature between 28-30 ºC and humidity rate between 25-30%. These conditions are required because at high temperature and low humidity the possibility of shrinkage cracking is enhanced. To maintain these conditions steady, the room was equipped with a dehumidifier. All bar samples were maintained at the same conditions during the 28 days.

On figure 10.6. below, the evolution of the temperature and the rate of humidity during the 28 days experiments' period are shown.

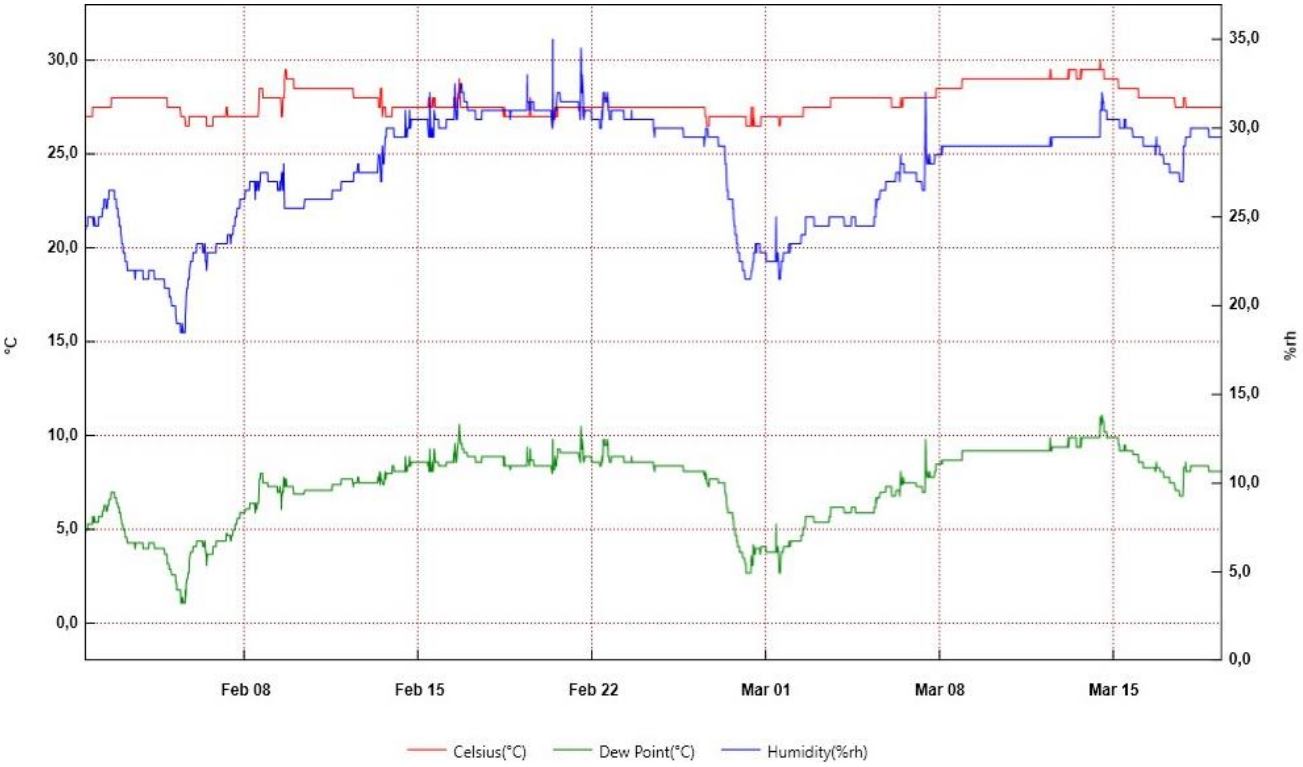

Figure 10.6 Temperature and humidity evolution during the experimentation period.

However, at it is observed, these parameters were not steady during the experiment. On table 10.2. are presented some statistics measured from the data.

Table 10.2. Statistics from temperature and humidity data evolution.

	Max	Min	Average	SD
Temperature (℃)	30	26,5	27,8	0,7
Dew Point (℃)	11,1	1,1	7,4	1,9
Humidity (% rh)	35	18,5	27,6	3

After the 28 days experiment period the results from both tests were contrasted to analyze the workability, accuracy and reliability of the DIC test to measure the shrinkage.

10.2.1.1. Linear Variable Displacement Transducer Test (LVDT)

The aim of this test was to measure the length variation of the bars samples, for at least 28 days with an absolute linear displacement transducer, which is an electrical transformer used for measuring linear displacement (position) converting the linear displacement from the zero or reference into a proportional electrical signal .

Set-up

The test was carried out in a micrometer placed in the environmental chamber. The zero of the micrometer is set with a reference bar whose length is 297, 5 mm. For each measurement, the micrometer gives the difference between the reference and the tested bar in mm.

Between 24 and 48 hours after the casting, measurements were taken every hour, between 48 and 120 hours measurements were taken every 3 hour and after 120 hours (5 days after the casting) one measurement was taken every day. For each bar, 5 measurements were taken at the same time and then the average was calculated. Temperature and humidity in the room were also recorded at each measurement.

(a) Micrometer with reference bar. (b) Micrometer with bar specimen.

Figure 10.7. Micrometer used for LVDT test.

Theory

The microstrain was determined thanks to the length's difference between the specimen and the reference. It was calculated with the formula 10.10.

$$\mu\epsilon = 1000\ x\ \frac{\Delta L}{L_0} \qquad (10.10)$$

, ΔL represents the length's difference in mm measured by the micrometer and L_0 the reference's length in mm.

10.2.1.2. Digital Image Correlation (DIC)

The idea of the free drying shrinkage experiment is to find the microstrain pattern over the bar's mortar surface of the different samples using the software GOM Correlate and compare the results with the data obtained with the LVDT test.

For this part, a Digital Image Correlation (DIC) method was used. The DIC method is a method which allows the measurement of 3D- coordinates without any contact and then allows finding the material's deformation by keeping the specimen intact. This method can provide quantitative and qualitative information on the surface's specimen. In the experiments of this project the method was only used for surface parameters' measurement, so only 2-D coordinates were measured (G. Cardinaud, 2017).

The DIC method is used along with the software GOM Correlate, which works with a picture analysis of a painted surface. Indeed, to analyze the surface, the software needs to build a mesh and this is possible only with a black and white painted surface.

Set-up

Before starting the DIC test in the environmental chamber, the bar samples of each mixture were painted with firstly, a layer of white paint, and secondly, black dots on top, so the gray level distribution remains easy to detect. Chalk paints must be used for the analysis and must be applied before the plastic shrinkage cracks appear, quite early after the casting.

On figure 10.8. it is shown the painting procedure.

(a) Mortar surfaces with a layer of white paint. **(b) Example of a bar's painted surface with black dots.** **(c) Chalk Paint Spray.**

Figure 10.8. Painting procedure for the DIC test.

On figure 10.9. it is shown the instrumentation used for the DIC test. Several bar samples of each mortar mix could be placed in both sides of the case at the same time. Each side of the case was divided in the half for the different types of mixtures. Two cameras with the same setups were capturing a picture of each mold every hour during the 28 days.

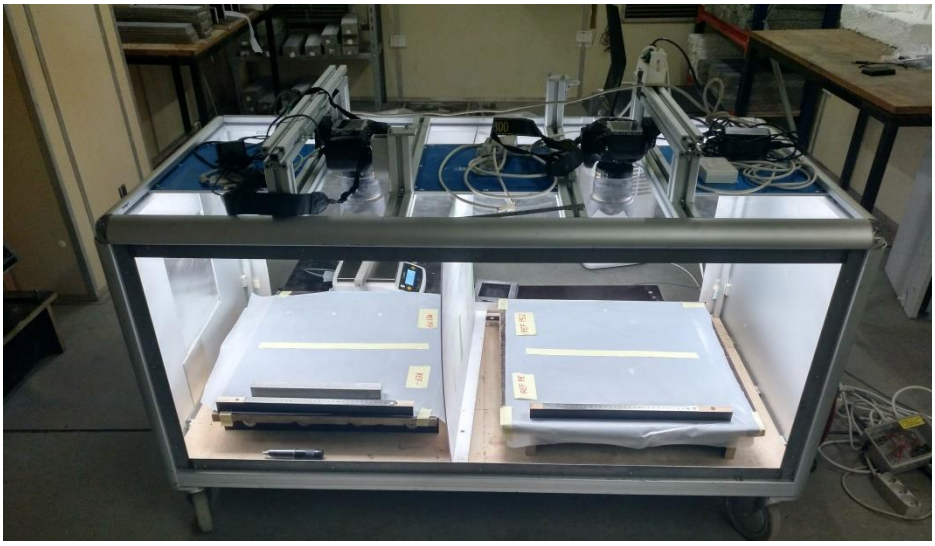

Figure 10.9. Camera setup inside the environmental chamber for DIC test.

Analysis

After 28 days of being the specimens in the environmental chamber, the pictures were analyzed with the software GOM Correlate. In this software, the mesh is created thanks to the paint and with the help of two different parameters: the facet's size and the point's distance. During the creation of the mesh and the surface component to analyze, GOM Correlate finds square facets in the pictures. With the help of the pattern structure on the pictures, the facets are identified. To be built, a facet needs to contain at least three pattern points. As a consequence, the closer the black dots are with each other, the more facets the software will create and the more accurate the results will be (C.M. Larsen, 2017).

For the microstrain analysis with GOM Correlate, 4 surface areas from each mix were analyzed. The displacements in Y-direction were measured and compare among the specimens.

The data obtained was loaded into Matlab to plot the surface microstrain evolution of the bars along the experiment period to compare it with the LVDT results.

11. Results

This chapter includes the results from the tests conducted on the different mortars samples as described in chapter 9. The chapter is divided in three sections containing: firstly, Casting – Mortar Mixture; secondly, the hardening properties tests as the bending strength, flexural toughness and the compressive strength tests, as well as the SEM analysis of the bonding between the fibers and matrix in the fracture surfaces; and finally, durability-related property tests are presented as the free drying shrinkage analysis, carried out comparing the DIC method with the LVDT test, included in Methods II.

In this Chapter the results are commented on, but the discussion and comparison of the results are presented in Chapter 12. The raw data for the results can be obtained from Appendix 4 to Appendix 8.

11.1. Casting – Mortar mixture

This section includes the analysis of the distribution of PE fibers in the mixture and the specimens' weights and dimensions measured after the demolding process.

11.1.1. Distribution of PE fibers in mixture

This section is focused on the analysis of the distribution of recycled PE fibers in the mortar samples and the comparison with the commercial PP fibers. Due to the small width of the fibers used in the experimentation, the importance of the study of the sample's transverse cross-section is more relevant than the longitudinal cross-section.

All the mortar samples were, firstly, tested for bending strength, which made possible to separate the prism sample into two halves, to later study the distribution of fibers along the cross-section.

On figure 11.1. is shown the transverse cross-section of Ref – samples, Ref PP samples (0, 2% PP fibers), Ref PE samples (2, 0% PE 'yellow' fibers) and Ref PE2 samples (2, 0% 'green fibers).

(a) Reference sample (Plain mortar), Ref- .

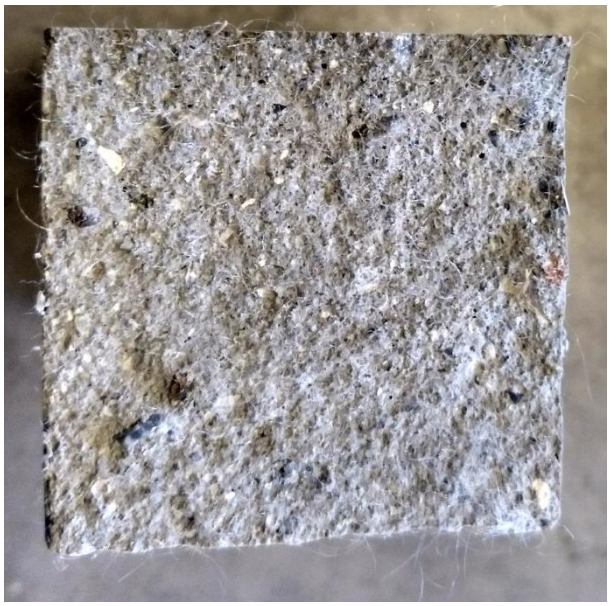

(b)PP commercial fibers, Ref PP.

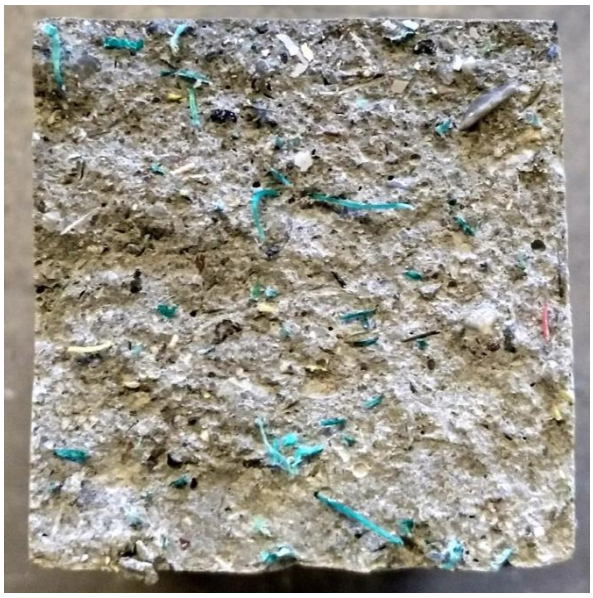

(d) 'green' PE fibers, Ref PE2.

(c) 'yellow' PE fibers, Ref PE.

Figure11.1.Transverse cross-section of mortar samples.

As can be seen on figure 11.1., the distribution of PE fibers is very homogeneous for 'yellow' PE fibers as well as for 'green' PE fibers, resulting in similar distribution patterns for both types. In the PE fiber surfaces analyzed there were not bundles formation observed. However, in the PP reinforced mortar samples, the distribution resulted more homogeneous (Figure 11.1 (b)), comparing it with the PE samples. Some fiber groups appeared as consequence of the small size and the preparation of these fibers, which are delivered in bundles. All the samples from the 1, 2, 7 and 28 days of curing were analyzed, and the same results were verified. One sample was analyzed for each curing day.

On table 11.1. it is shown the number of PE fibers in the different cross-sections analyzed in order to get an overview of the fibers in the mortar samples. Due to the small size of commercial PP fibers, it is not possible to quantify the number of fibers in the cross-section.

Table 11.1. Number of longitudinal and transverse fibers in the mortar specimens analyzed.

Sample Reference	Ref PE	Ref PE	Ref PE	Ref PE	Ref PE2	Ref PE2	Ref PE2	Ref PE2
Curing days	**1**	**2**	**7**	**28**	**1**	**2**	**7**	**28**
Longitudinal fibers [ud]	73	97	61	84	56	53	59	48
Transverse fibers[ud]	9	8	5	13	16	18	17	10
Percentage of longitudinal fibers [%]	89,02	92,38	92,42	86,60	77,78	74,65	77,63	82,76

As the results shown, there is a big difference between the amount of longitudinal and transverse fibers in all the surfaces analyzed. The percentage of longitudinal fibers over the total is around 78-92%, which means that without intention the majority of fibers are orientated in a convenient position to stand better the tensile strength, flexural strength (first crack strength and post-cracking behavior) and compressive strength. The longitudinal orientation preference for the majority of fibers could be related with the mold position during the curing period, allowing fibers to move when the mix is still viscous.

A characteristic aspect of the FRM samples is the predisposition of the fibers to protrude from the different samples, especially on the edges as can be seen on figure 11.2., which is associated with the procedure of the filling of the molds. This problem can cause difficulties to get an even surface on the samples.

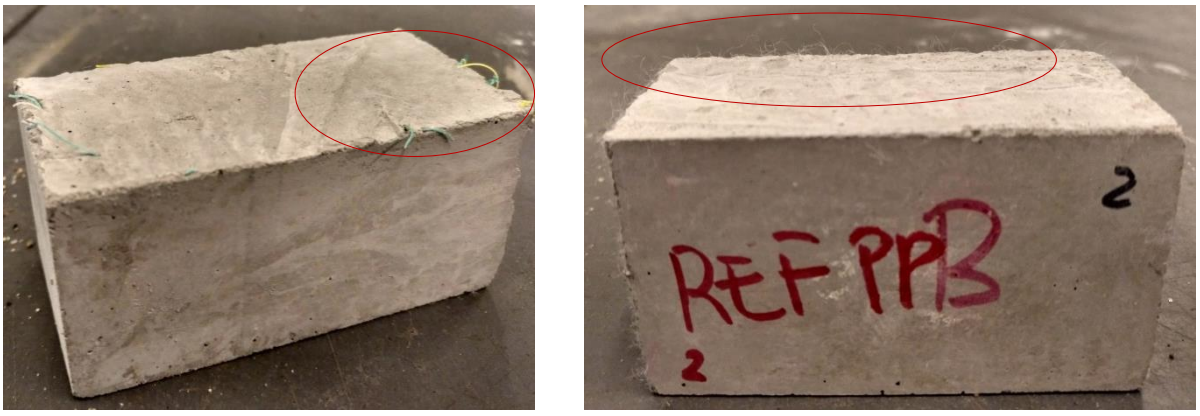

(a) PE fibers protruding from the edges. (b) PP fibers protruding from the edges.

Figure 11.2. Fibers protruding from the edge of the sample.

Other characteristic aspect of the fracture surfaces (Figure 11.1 (c) and (d)) is that many micro holes are observed in the fracture surface of PE reinforced mortar samples which indicates that fibers have been pulled-out of the cement-based matrix during the three-point bending test.

11.1.2. Specimens' weights and dimensions

In order to characterize the specimens, the measurements of the dimensions (height and breadth) and the weight have been measured immediately after the demolding, 24 hours after the casting.

In total, three prism specimens of each different mortar mixture were used for the measurement test. On tables 11.2. and 11.3. are presented the results of the measurements and the comparison with the theoretical dimensions and weights.

The theoretical weights are calculated with a density for the plain mortar equivalent to 2300 kg/m^3, and to determinate the theoretical weight for the fiber reinforced mortar specimens, the amount of fibers added for each mix is considered (mix-design).

On Appendix 4 it is shown the data used for the calculation of the density and theoretical weight for fiber reinforced mortar specimens.

Table 11.2. Height and breadth measures of each mixture prism specimens.

Dimensions [mm]	Plain concrete	PP fibers	PE 'yellow' fibers	PE 'green' fibers
Average height	16,01	16,00	16,01	16,02
Average breadth	3,99	4,02	4,03	4,04
Theoretical height	16,00	16,00	16,00	16,00
Theoretical breadth	4,00	4,00	4,00	4,00
Height error [%]	0,17	0,00	0,06	0,12
Breadth error [%]	0,25	0,5	0,75	1,00

Table 11.3. Weight measures of each mixture prism specimens.

Weights [g]	Plain concrete	PP fibers	PE 'yellow' fibers	PE 'green' fibers
Average weight	556,93	556,87	553,74	550,74
Theoretical weight	588,8	588,49	585,60	585,60
Weight error [%]	5,41	5,37	5,43	5,95

Concerning the average dimensions, height and breadth, the difference between theoretical and experimental values is not significant. Indeed, the error in the breadth and height's comes mostly from the dimensions of the molds which have been made by hand.

However, the errors between theoretical and experimental weights are stronger. These differences come mainly from the demolding process of the specimens, a difficult step in which specimens can be damaged, especially in the edges, where it is caused small losses of material and roughness, as it is shown on figure 11.3.

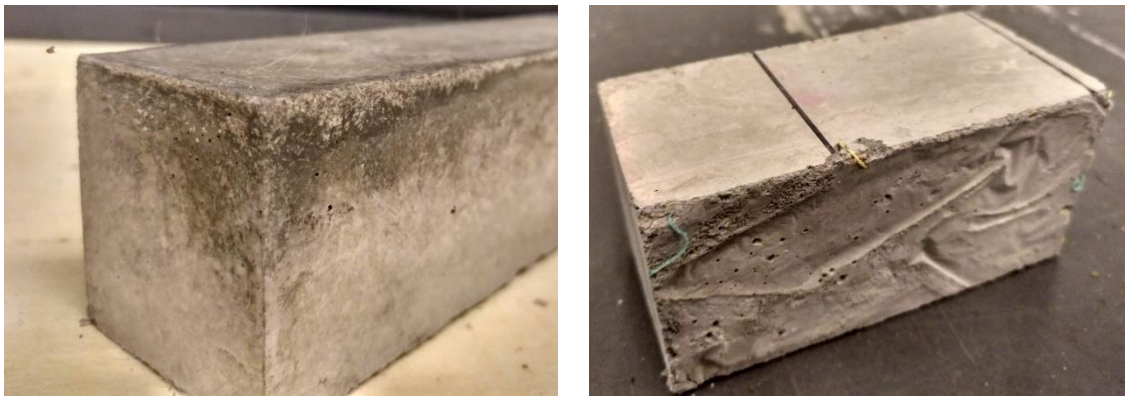

(a) Example 1. **(b) Example 2.**

Figure 11.3. Loss of material in the edges of the samples.

11.2. Results- Methods I

This section includes the results of the hardening properties tests carried out in the project, as the bending strength and compressive strength tests, as well as the SEM analysis of the bonding between the fibers and the cement-based matrix.

11.2.1. Bending

The objective of carrying out the bending test was to analyze the effect of the different type of fibers in the mortar mixture over the curing period. This was done by comparing the bending strength of mortar samples with the three different fibers for 1, 2, 7 and 28 days of curing, and later, compare with the reference samples. The average bending strengths values for 1, 2, 7 and 28 days samples are presented later on table 11.4.

All the working curves can be obtained in Appendix 5 as individual working curves separated by curing days and references.

From figure 11.4. to figure 11.7., it is presented the working curves grouped by curing days. Different colors are used for each reference sample: red for plain concrete, Ref- day, blue for PP reinforced mortar samples, Ref PP, yellow for PE reinforced mortar samples, Ref PE and green for PE2 reinforced mortar samples, Ref PE2.

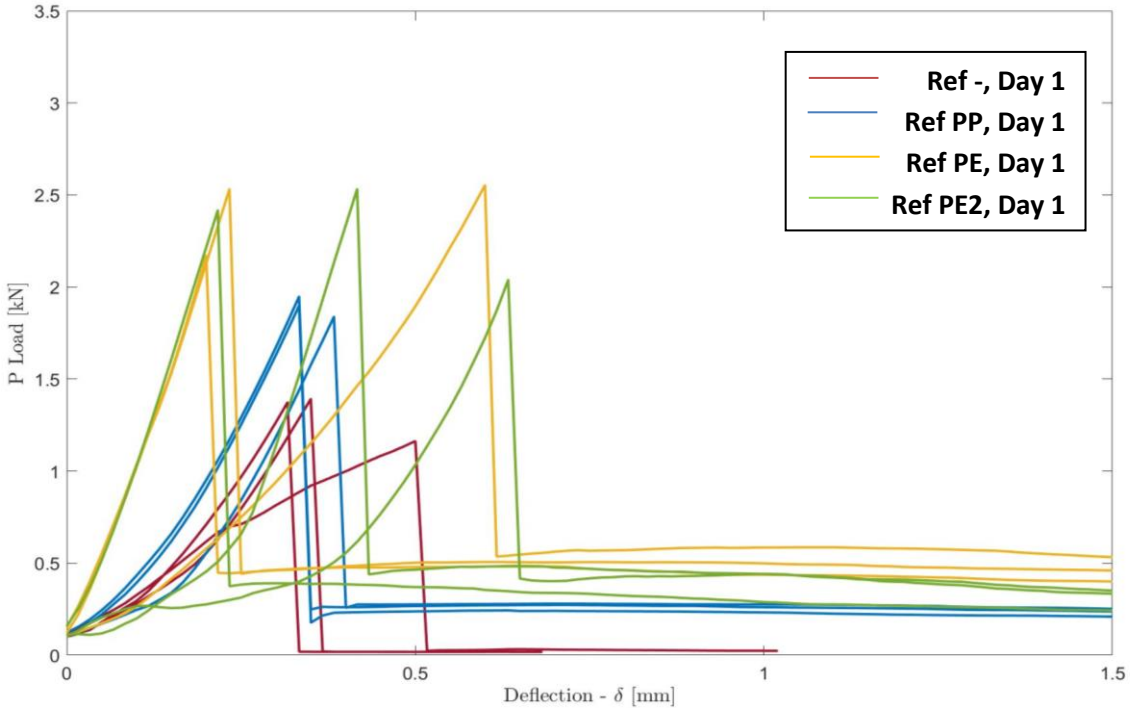

Figure 11.4. Working curve for all 1 day samples.

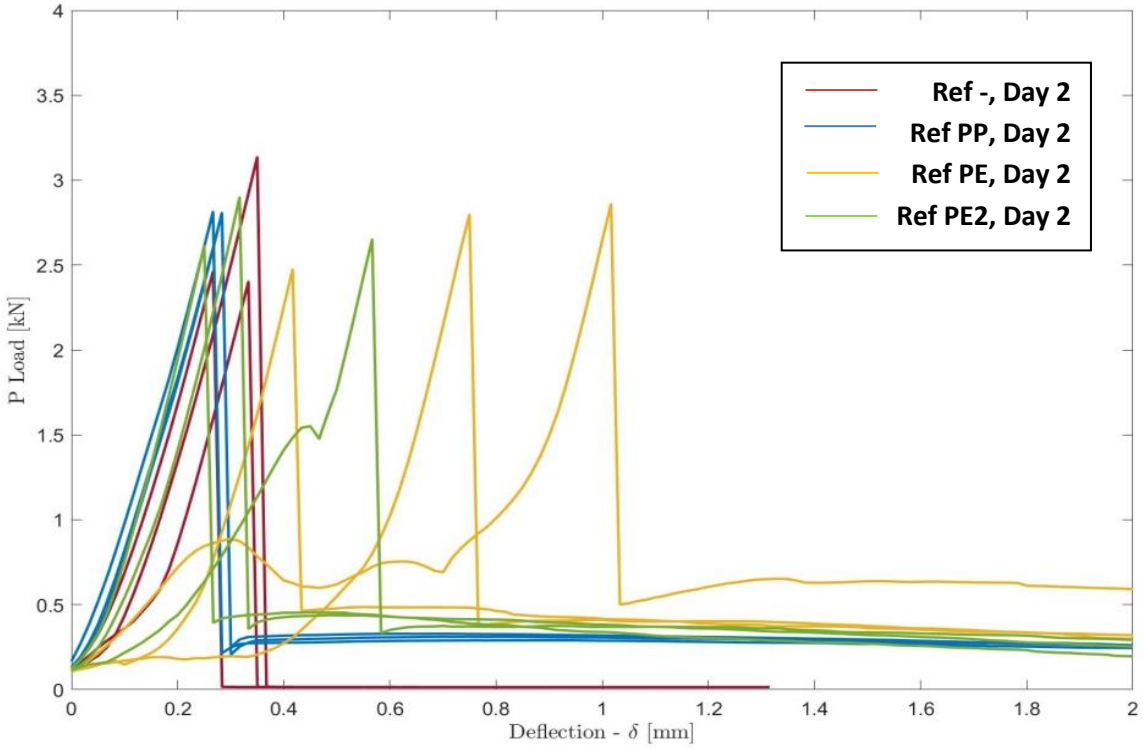

Figure 11.5.Working curve for all 2 day samples.

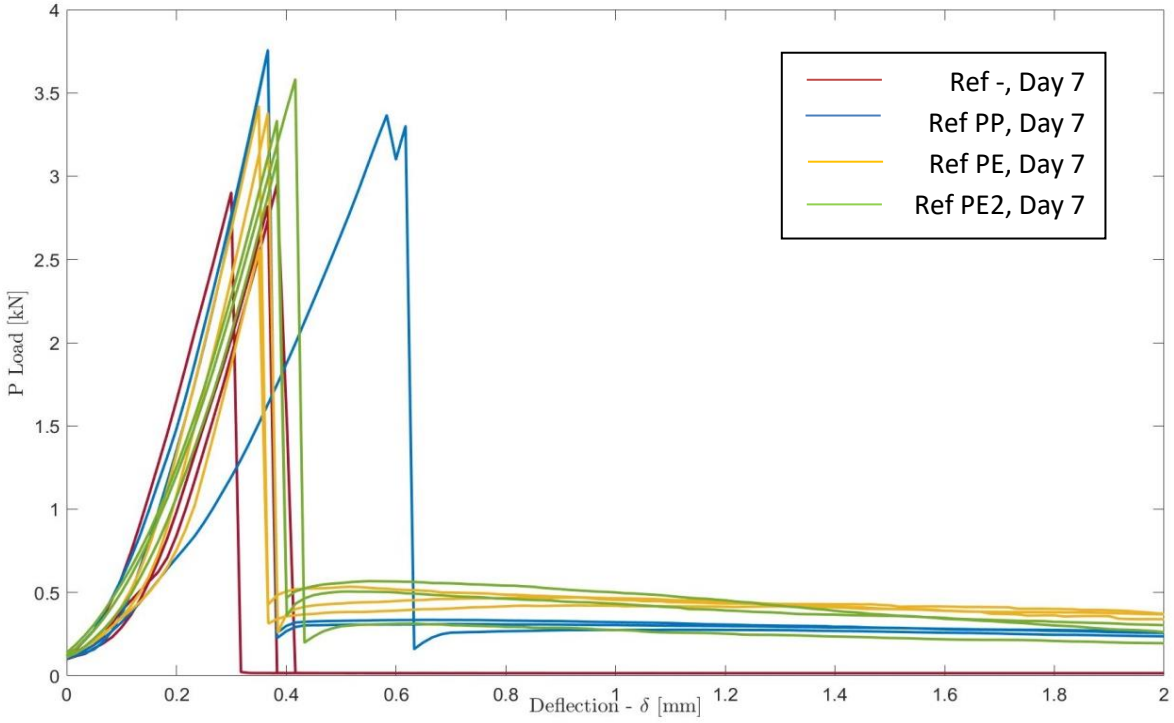

Figure 11.6. Working curve for all 7 days samples.

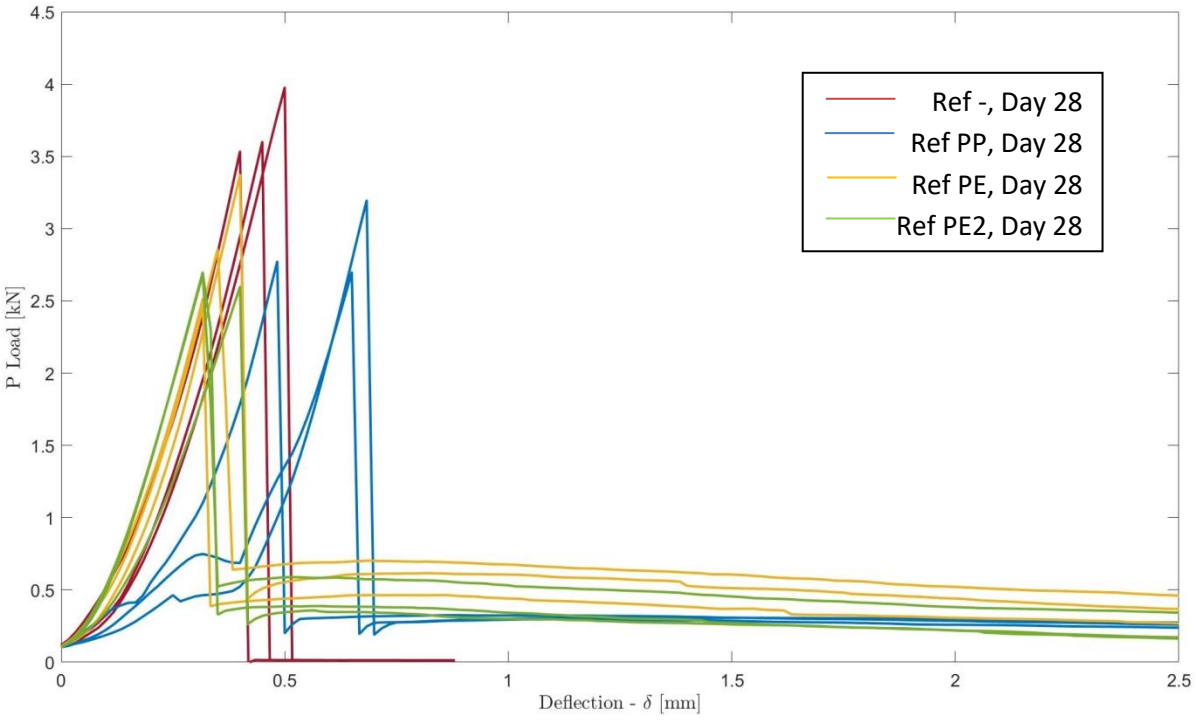

Figure 11.7. Working curve for all 28 days samples.

From 11.4 to figure 11.7. can be observed that as it is commented in the theory in section 10.1.1., there is an increase in energy that can be absorbed by the fiber reinforced mortar samples, whereas the plain mortar samples with no fiber content goes immediately to zero after the initial crack.

It can be observed that the strength during the post crack behavior increases over time due to the curing of the cement in the mortar samples. Moreover, the post cracking strength results for the 'yellow' and 'green' PE fiber reinforced samples look similar. However, as can be observed, the post cracking strength for 'yellow' PE fiber reinforced samples stayed superior during the curing days tested.

Below, on figure 11.8, it is presented the development of strength over time of the mortar samples for the different types of fibers, included reference samples, plain concrete. Each bar shows the mean initial crack strength along with the corresponding standard deviation. Different colors are used for each curing day: red for day 1, blue for day 2, green for day 7 and yellow for day 28.

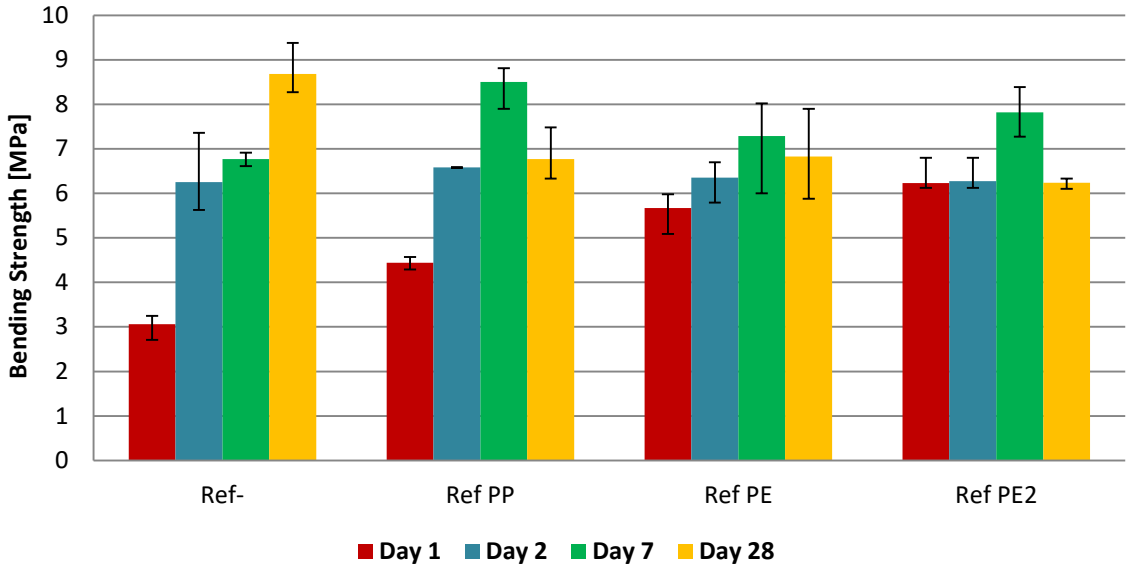

Figure 11.8. Bar chart showing the flexural strength of the samples during the different curing period.

The bar chart shows an increase in the first crack strength over time for the reference sample. Furthermore, it can be seen that the fiber reinforced samples, both, PP or PE fibers, shown an increase in the first crack strength during 1, 2 and 7 days of curing, being the results for each day higher than the results from the reference samples. However, during the 28 days of curing this first crack strength decreases for the reinforced samples comparing with the previous results, while for the reference samples, the maximum first crack strength is achieved.

The results could be attributed to small changes that are very sensitive as the mix design, the movement of the samples during the curing period or the use of cleaned or uncleaned fibers. However, the same mix was used for casting the twelve prisms for each mortar reference, and the results shown the decrease for the three reinforced cases, which were casting in different dates. Moreover, the samples were left immobilized during the curing period and cleaned fibers were used for all the castings.

The analysis of the standard deviations did not show any specific correlation due to all of them oscillate different for each mortar sample.

On table 11.4. is provided an overview of significant data points from the working curves. It is presented the results from all the mortar samples tested as the critical mid span deflection, δ_{cr}, the initial crack load, P_{cr}, the initial crack strength, R_F , with the standard deviation, as well as percentage of the strength compared to the corresponding reference samples. Furthermore, the maximum post-break load, P_{pb}, and the maximum post-break strength, R_{pb} with the standard deviation and the fiber efficiency factor, FEF, are presented.

The strengths have been found using equation (10.1). The results for all the samples tests can be seen in Appendix 5.

Table 11.4. Results for flexural strength. Mean values and standard deviations (SD) from three tests are given.

Reference	Curing period [days]	δ_{cr} [mm]	P_{cr} [kN]	R_F [Mpa]	SD	% of Ref	P_{pb} [kN]	R_{pb} [Mpa]	SD	FEF
Ref-	**1**	0,39	1,31	3,06	0,13	100,00[1]	-	-	-	-
	2	0,32	2,67	6,25	0,41	100,00[2]	-	-	-	-
	7	0,35	2,89	6,77	0,07	100,00[3]	-	-	-	-
	28	0,45	3,70	8,68	0,24	100,00[4]	-	-	-	-
Ref PP	**1**	0,35	1,90	4,44	0,05	145,04[1]	0,26	0,62	0,05	0,12
	2	0,28	2,81	6,58	0,01	105,24[2]	0,31	0,73	0,05	0,08
	7	0,44	3,62	8,50	0,23	125,26[3]	0,31	0,73	0,04	0,06
	28	0,60	2,89	6,77	0,27	78,11[4]	0,31	0,73	0,04	0,07
Ref PE	**1**	0,34	2,42	5,67	0,22	184,73[1]	0,53	1,23	0,13	0,20
	2	0,73	2,71	6,35	0,21	101,49[2]	0,52	1,21	0,28	0,15
	7	0,36	3,12	7,29	0,49	107,96[3]	0,48	1,12	0,10	0,11
	28	0,36	2,91	6,83	0,43	78,65[4]	0,60	1,40	0,31	0,17
Ref PE2	**1**	0,42	2,33	6,23	0,26	177,86[1]	0,44	1,03	0,12	0,15
	2	0,44	2,67	6,27	0,06	100,00[2]	0,43	1,02	0,10	0,12
	7	0,39	3,34	7,82	0,24	115,57[3]	0,46	1,07	0,30	0,10
	28	0,35	2,66	6,24	0,05	71,89[4]	0,46	1,08	0,25	0,14

It should be indicated that during the testing only the plain mortar samples were totally split in half by the Istron 10 kN machine, while FRM samples had to be manually separated after the post cracking behavior period to prepare the samples for the compression test.

11.2.2. Toughness

The flexural toughness is used to measure the flexural capacity of the FRM samples before and after the initial crack.

The toughness values have been found using equation 10.3., 10.4. and 10.5. for the critical value of δ_{cr}, $T_{\delta cr}$, $T_{2\delta cr}$ and $T_{3\delta cr}$. The mean toughness values were extracted from the graphs from figure 10.4 to figure 10.7. Furthermore, the toughness indexes I_5 and I_{10} have been found using equation 10.6. and 10.7., and the residual strength factor, $R_{10,5}$ has been found using equation 10.8. The results of the mean values are presented on table 11.5., below. All toughness values for each individual sample can be obtained in Appendix 6.

Table11.5. Results for toughness. Mean values and standard deviations (SD) from three tests are given.

Reference	Curing days	$T_{\delta cr}$ [Nm]	SD	$T_{3\delta,cr}$ [Nm]	SD	$T_{5\delta,cr}$ [Nm]	SD	I_5 [-]	I_{10} [-]	$R_{10,5}$ [-]
Ref-	1	0,289	0,081	-	-	-	-	-	-	-
	2	0,402	0,096	-	-	-	-	-	-	-
	7	0,436	0,022	-	-	-	-	-	-	-
	28	0,683	0,075	-	-	-	-	-	-	-
Ref PP	1	0,327	0,015	0,523	0,013	0,728	0,043	1,61	2,24	12,7
	2	0,389	0,013	0,579	0,029	0,785	0,045	1,49	2,02	10,6
	7	0,650	0,142	0,968	0,243	1,246	0,272	1,48	1,92	8,67
	28	0,582	0,073	0,962	0,120	1,342	0,152	1,65	2,31	13,1
Ref PE	1	0,411	0,225	0,785	0,487	1,143	0,667	1,87	2,77	17,9
	2	0,588	0,301	1,300	0,714	1,851	0,994	2,18	3,12	18,9
	7	0,467	0,097	0,908	0,209	1,336	0,305	1,94	2,88	18,9
	28	0,437	0,085	0,779	0,124	1,143	0,137	1,79	2,64	17,1
Ref PE2	1	0,356	0,069	0,703	0,236	0,996	0,329	1,96	2,75	15,7
	2	0,426	0,119	0,741	0,217	1,020	0,289	1,73	2,39	13,1
	7	0,582	0,075	0,938	0,013	1,222	0,094	1,63	2,15	13,5
	28	0,428	0,041	0,751	0,060	1,038	0,140	1,76	2,44	13,5

From the table 11.5. can be observed that there is an increase in toughness for the FRM samples comparing with the reference samples, as the reference samples only have toughness until the initial crack. At 28 days of curing, $T_{\delta,cr}$ is largest for the reference samples.

Further, it can be seen that as with the flexural strength the commercial PP fibers are slightly performing better than the PE recycled fibers. However, like in the flexural strength results, there is a decrease in the toughness for the critical deflection in all the FRM samples from the day 7 to day 28 of curing. The same decrease can be seen for the $T_{3\delta cr}$ values and the $T_{5\delta cr}$ values from day 7 to day 28. As it has been already exposed, these results can be attributed to small changes that are very sensitive.

The analysis of the I_5, I_{10} and $R_{10,5}$ indices did not show any specific pattern/correlation due to all of them oscillate different for each mortar sample. As all the values are in the range 1,49-2,88, the indices proved the improvement in flexural toughness compared with the flexural toughness obtained when the first crack appears.

11.2.3. Compression

The objective of carrying out the compression test was to analyze the effect of the different type of fibers in the mortar mixture over the curing period. The fiber reinforced mortar samples with 'yellow' and 'green' PE fibers are compared with plain mortar samples with no fiber content and samples with commercial PP fibers, Fibrin.

Figures from 11.9 to 11.12. present the compression strength averages for the 1, 2, 7 and 28 days compression tests carried out for all the samples groups with corresponding standard deviation. The strength was calculated using equation 10.9.The compressive strength results for all the mortar sample tests can be seen in Appendix 7.

Ref-

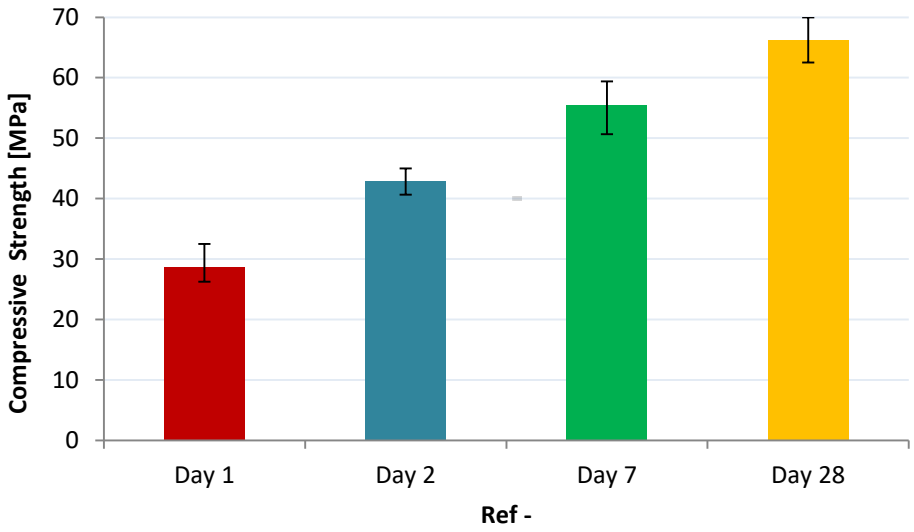

Figure 11.9. Bar chart showing the compressive strength of Ref- samples (plain concrete).

Ref PP

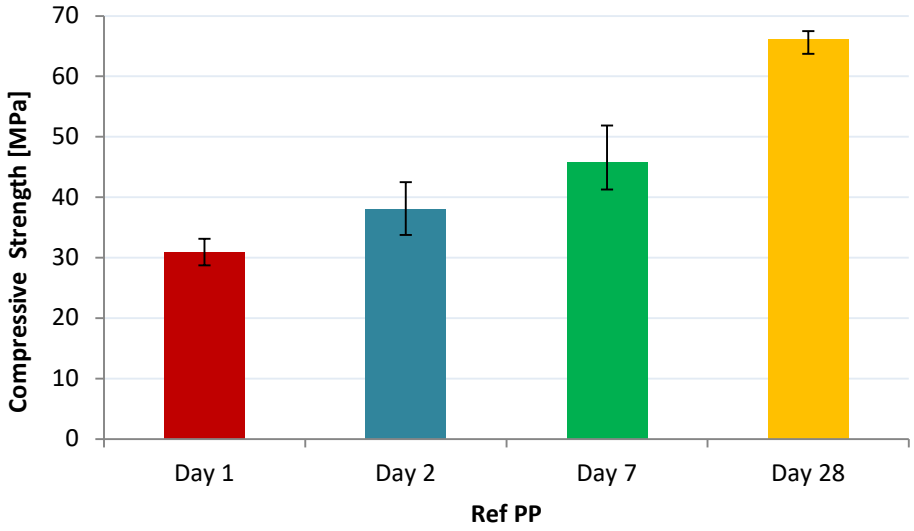

Figure 11.10. Bar chart showing the compressive strength of Ref PP samples.

Ref PE

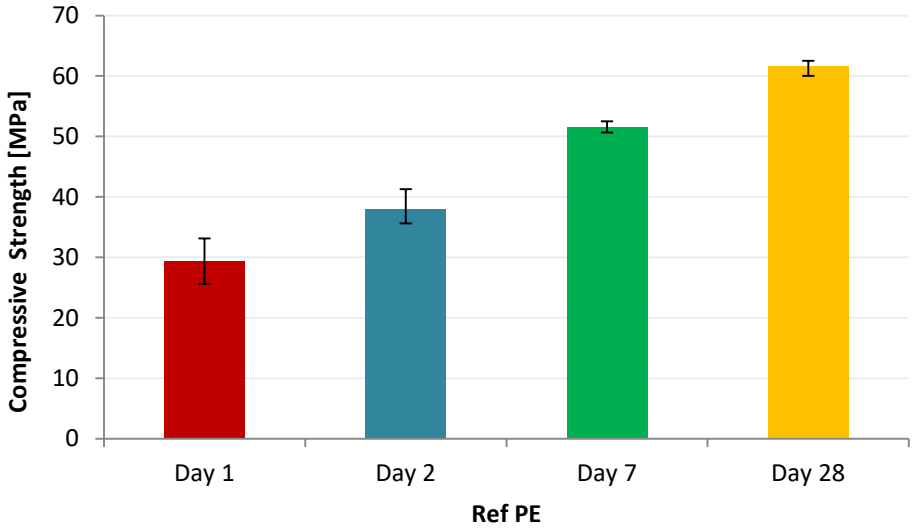

Figure 11.11. Bar chart showing the compressive strength of Ref PE samples.

Ref PE2

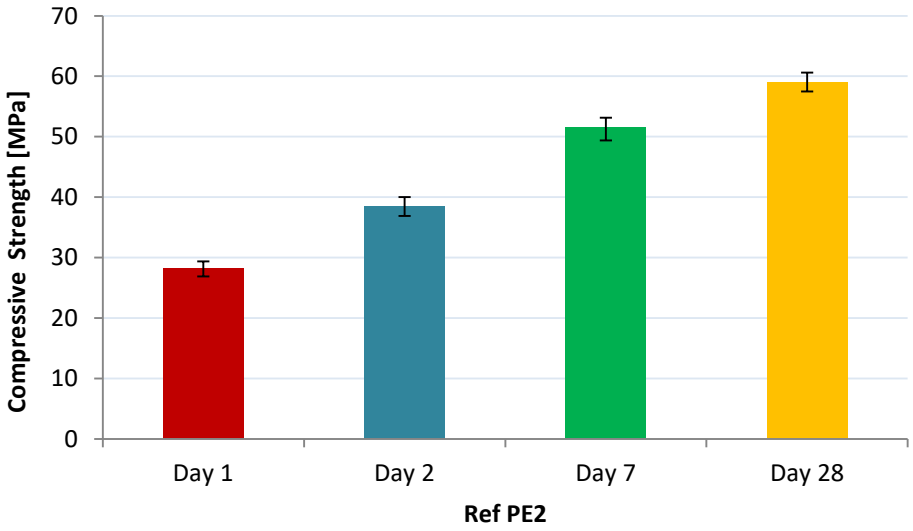

Figure 11.12.Bar chart showing the compressive strength of Ref PE samples.

As it is presented from figure 11.9. to figure 11.12., the compressive strength increases over the 28 days curing period for all the mortar samples. A decrease in compressive strength is produced when fibers are added to the mixture, so plain mortar samples showed the highest compressive strength comparing with FRM samples, except in the results obtained during day 1, which can be associated to small sensitive changes.

The results obtained from 'yellow' and 'green' PE FRM samples are similar for all the curing period, being the maximum result variation of -4,4% during the day 28 (PE2 respectively to PE). Comparing PE FRM samples with PP commercial FRM samples, the maximum variation for day 1 is +8,7% and during day 2 is +1,4% (both cases PP respectively to PE2). However, it is characteristic that during day 7 PE FRM samples have a higher compressive strength average than PP FRM with a maximum variation of -11,3% (PP respectively to PE and PE2), but during day 28, the results are inverted, having PP FRM samples the highest compressive strength, with a maximum variation of +10,1% (PP respectively to PE2).

On table 11.6. is provided an overview of the exact values from the compressive tests that can be seen from figure 11.9. to figure 11.12..

Table 11.6. Compression strengths of 1, 2, 7 and 28 days mortar samples.

Reference	Curing period [days]	Fc [kN]	Rc [Mpa]	SD [Mpa]	% of Ref
Ref-	1	46,00	28,75	3,30	100,00[1]
	2	68,67	42,92	2,19	100,00[2]
	7	88,67	55,42	2,09	100,00[3]

	28	106,00	66,25	3,75	100,00[4]
Ref PP	1	49,33	30,83	2,20	107,23[1]
	2	60,67	37,92	4,39	88,35[2]
	7	73,33	45,83	5,46	82,70[3]
	28	105,67	66,04	2,01	99,68[4]
Ref PE	1	47,00	29,38	3,06	102,19[1]
	2	60,67	37,92	2,95	88,35[2]
	7	82,33	51,46	0,95	92,85[3]
	28	98,67	61,67	1,44	93,08[4]
Ref PE2	1	45,00	28,13	1,25	97,84[1]
	2	61,67	38,54	1,57	89,79[2]
	7	82,33	51,46	1,90	92,85[3]
	28	94,33	58,96	1,57	89,00[4]

It should be indicated that the plain mortar samples during the compression test were separated into small parts, while the FRM samples did not detached any part and were kept entirely due to the fibers addition.

11.2.4. Interface bonding with SEM analysis

The objective of the samples' surface SEM analysis after the bending test was to study the different interface bonding generated by shear deformation between the fibers and the cement-based material matrix.

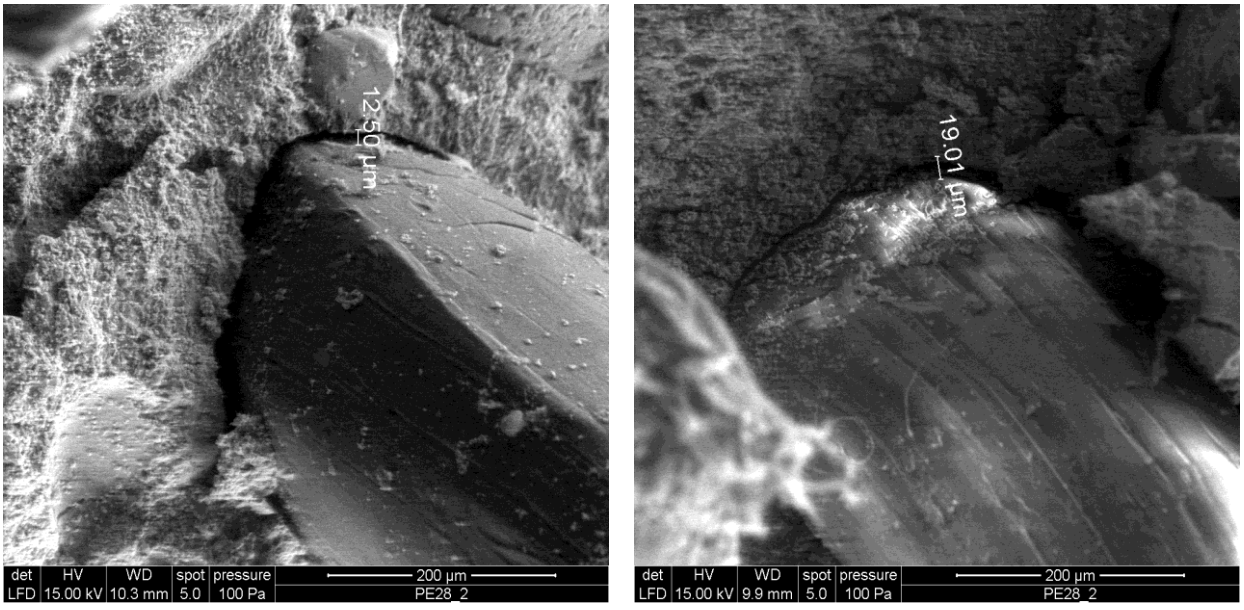

(a) 'yellow' PE fiber I **(b) 'yellow' PE fiber II**

Figure 11.13. SEM of interface bonding between yellow PE fiber and cement-based matrix, zoom x240.

Figures 11.3 and 11.14. present the SEM Images selected of the interface bonding of different 'yellow' and 'green' PE fibers with the cement-based material matrix. Figure 11.15. present the interface bonding between de commercial PP fibers and the cement-based material matrix.

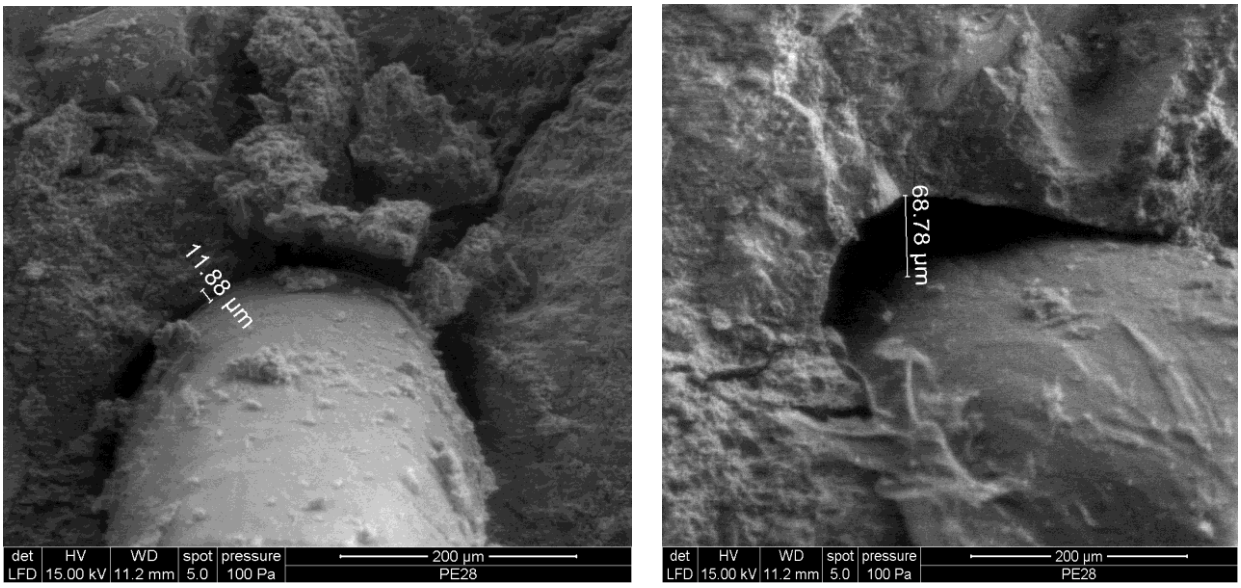

(a) 'green' PE fiber I **(b) 'green' PE fiber II**

Figure 11.14. SEM of interface bonding between green PE fiber and cement-based matrix, zoom x240.

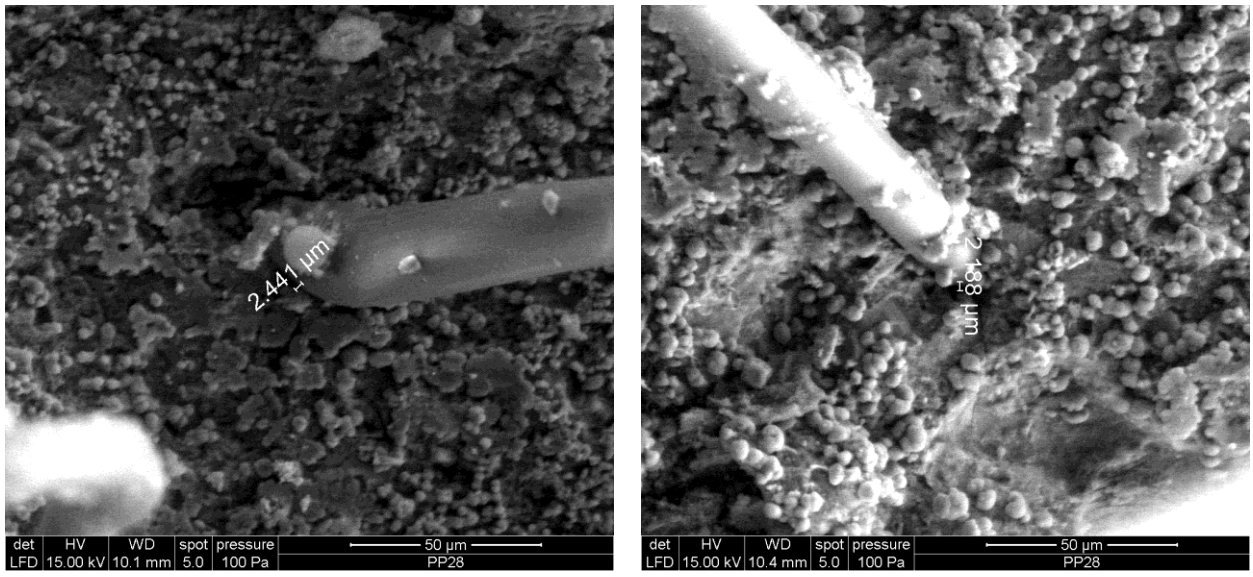

(a) Commercial PP fiber **(b) Commercial PP fiber**

Figure 11.15. SEM of interface bonding between PP fiber and cement-based matrix, zoom x800.

As can be seen comparing the figures 11.13. and 11.14. with figure 11.15., the debonding generated by shear deformation is more pronounced in the PE reinforced mortar samples. The debonding holes measured (µm) are in the order of tens, whereas for the PP fibers

the debonding holes (µm) are in the order of units. The small diameter and the fibrillated form of the PP fibers causes the fiber-to-matrix bonding to be stronger than with PE fibers, as it has been shown in the results of the compression and bending tests.

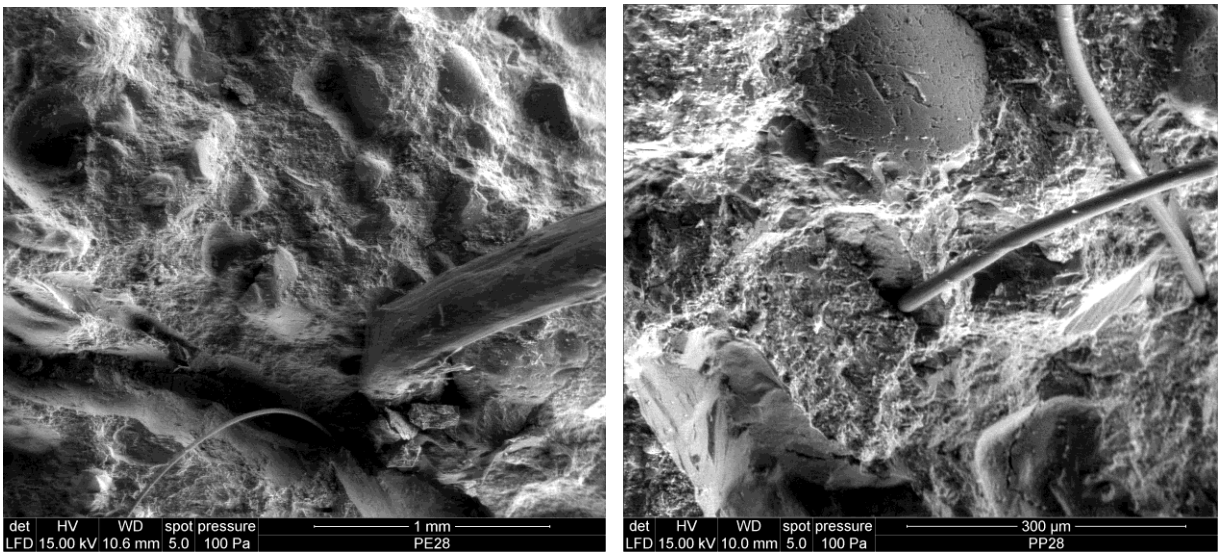

(a) Fracture surface of 'green' PE fiber mortar samples-. **(b) Fracture surface of commercial PP fiber mortar samples.**

Figure 11.16. Fracture surface of 'green' PE and PP fiber mortar samples- 28 days of curing.

The analysis of the surfaces showed that fibers were mainly pulled out of the matrix, proving a poor fiber-to-matrix bonding. Furthermore, as can be observed from figure 11.13. to figure 11.15., the fibers that were pulled out of the matrix show small particles of mortar mix on the fiber surface, but without any signs of fracture or degradation.

The samples analyzed were hydrating during 28 days, after that, they lost water mass while stabilizing. As can be seen on figure 11.16., the mortar fracture surfaces of the samples don not appear very porous. This parameter is affected by the w/c ratio, which was 0,5 for all the mix samples made during this project. However, the majority of holes were caused by the pulled out of fibers.

11.3. Results- Methods II

This section includes the results of the durability-related properties test carried out in the project, the analysis of the free dry shrinkage, through the measurement of the microstrain of different mortar samples.

11.3.1. Shrinkage cracking analysis

11.3.1.1. Linear Variable Displacement Transducer Test

The objective of the LVDT test was to measure the length variation (microstrain) of the bars samples, for at least 28 days with an absolute linear displacement transducer, to later compare the data with the measures obtained by GOM correlate program from the DIC method.

The microstrain measured over the 28 days for each mixture over the time is plotted in figure. All the results for each individual day measures can be obtained in Appendix 8.

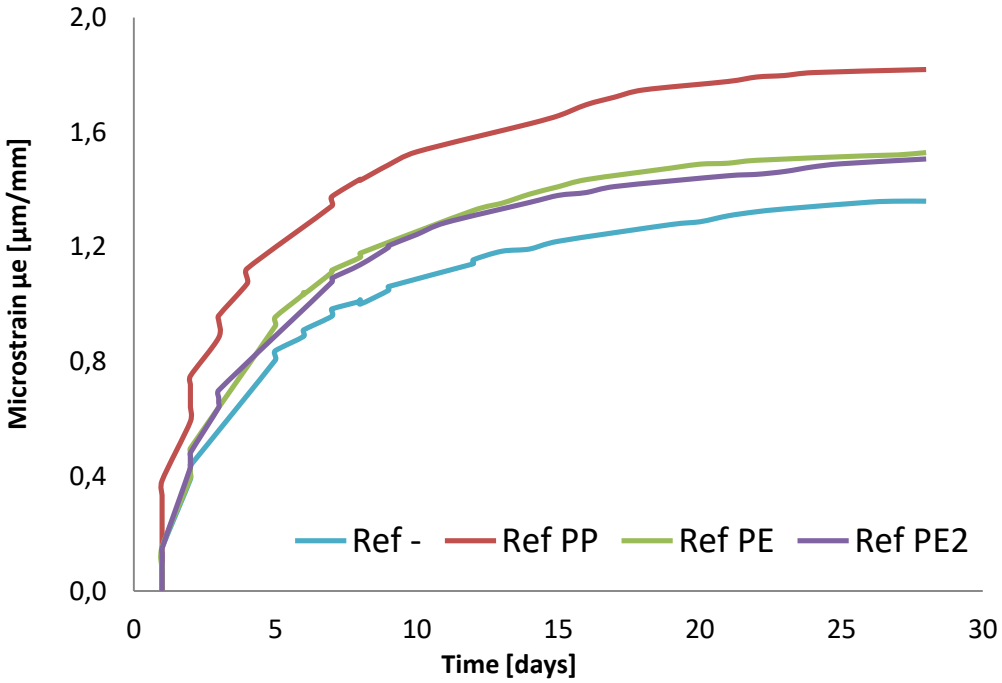

Figure 11.17. Microstrain mortar samples during free drying period.

As it is presented on figure 11.17., the shrinkage strain is increasing over the curing time for all the mixes but the rate is decreasing. Indeed, the shape of the curves shows that the shrinkage is developing fast in the first days of measurement and slowing down after around 7 days of free drying. The reference samples resulted in suffering less microstrain comparing with the FRM samples, in which PP reinforced mortar samples presented the highest microstrain.

The maximum microstrain achieved with the PP samples is 1,8 μm/mm, whereas for the maximum microstrain achieved with reference samples is 1, 32 μm/mm. So the results presents that the non- addition of fibers in the mix tends to decrease the shrinkage strain for a same exposure time, and do not seem to affect the rate.

Furthermore, 'yellow' and 'green' PE reinforced mortar samples presented similar results during the 28 days of experimentation, as can be observed on figure 11.17 with the

overlap of both curves, green and violet curves. The maximum microstrain achieved was 1,47 µm/mm for both bars. This means that both fibers shrinked equally during the free drying period and proved the reliability of the test carried out.

11.3.1.2. Digital Image Correlation

The objective of using a DIC method to measure the free drying shrinkage was to find the microstrain pattern over the bar's mortar surface and test the accuracy and validity of the DIC test with the results obtained from the LVDT test.

Figure 11.18. shows the surface area defined in GOM Correlate on top of the pictures taken of the different specimen. On the first picture, corresponding to day 1, the surface area is completely green, which means that it is set as the reference (0,00 mm in the scale) to start to measure the different displacements in the following pictures. As can be seen in the pictures corresponding to day 7, 16 and the last day of experimentation (among 24-28 depending on the samples), colors start to appear indicating the moves that have been in the picture.

Micro-strain

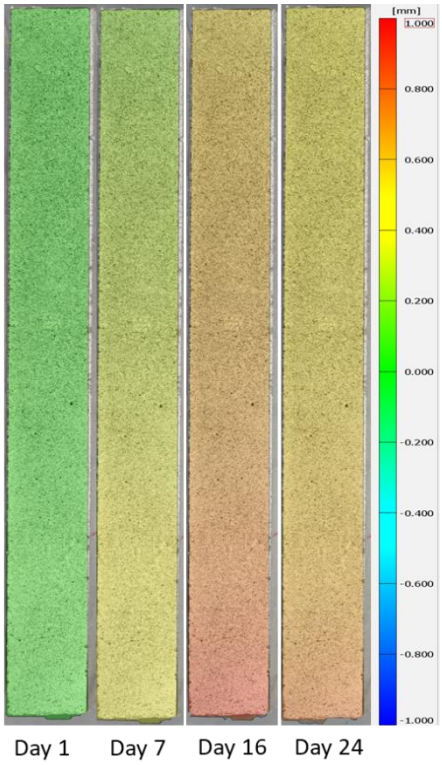

(a) PE samples microstrain displayed in GOM Correlate.

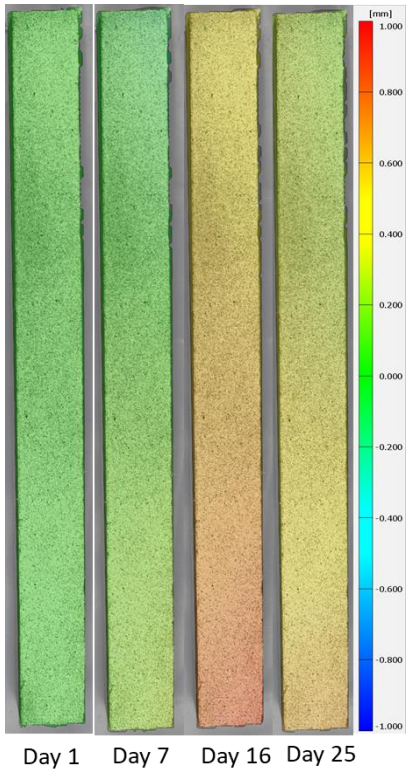

(b) PE2 samples microstrain displayed in GOM Correlate.

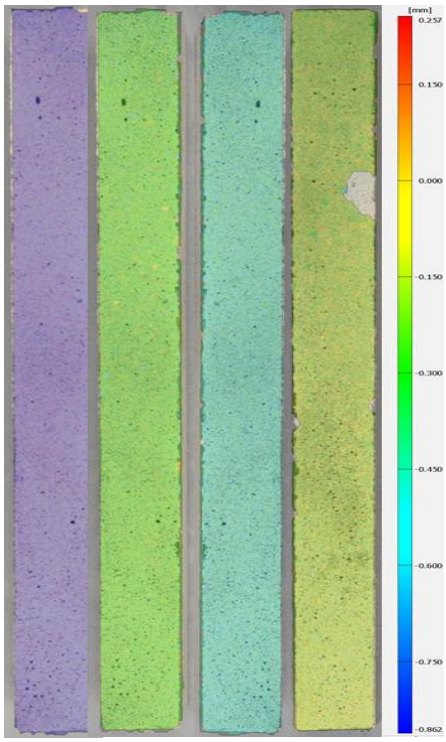

(c) Reference samples microstrain displayed in GOM Correlate.

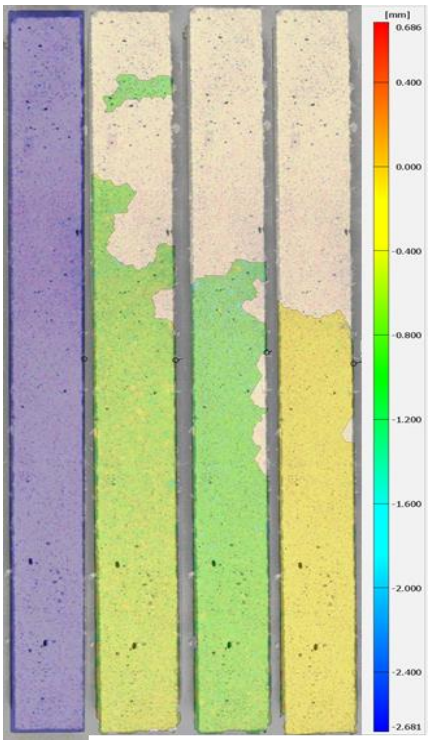

(d) PP samples microstrain displayed in GOM Correlate.

Figure 11.18. Development of microstrain in Y direction in GOM Correlate.

The analysis of the displacement in the direction Y of all the PE and PE2 bars shown a similar pattern. As it is shown on figure 11.18. (a) and (b), the microstrain of the bars was found to be higher at the bottom part of the bars (nearer to the edge of the cage) during the free drying process.

However the same pattern is not observed in figure c and d, corresponding to reference and PP reinforced mortar samples, respectively. The intensity of the colors is the same along the whole sample, although the same environment conditions were used as for the PE samples. Moreover, as it is observed, especially on figure 11.18 (c) and (d), the GOM Correlate program could not recognize some parts during the analysis of the displacement in Y of the different surfaces. This failure could be related to the quality of the photos taken during the DIC test or the precision of the painting made to cover the surface of the bars before the DIC test. Despite the procedure failure, a slight change of color comparing both sides of the samples, can be observed during day 7 and 16 in the PP bar. Analyzing the scale of colors can be observed that the same pattern followed by the PE bars in presented.

Controversially, comparing the pictures selected from 4 days, it was shown that the highest microstrain produced during the free drying was measured during the day 16th of the experiment for PE and PE2 bars. The PE and PE2 samples' microstrain measured

increased from day 1 until the 16th day and then, a decrease in the microstrain values from day 16th to day 28th is presented on the surfaces. These controversial results can also be observed on figure 11.19 and figure 11.20, in which different valleys and peaks are presented in curves that were supposed to increase slightly during the whole period.

For the reference and PP fiber bars, the highest microstrain presented was during the last day of experiment, which would be the normal result. However, in the analysis of the surfaces during the 4 days, a decrease is observed from day 7th to day 16th , increasing again until day 28th. Again, these controversial results can also be observed on figure 11.21 and figure 11.22, in which different valleys and peaks are presented in curves that were supposed to increase slightly during the whole period.

From figure 11.19. to figure 11.22., it is plotted the graphs of the microstrain in y-direction for each mixture, measured with the software GOM Correlate and processed in Matlab later. Only the data of two or three different bars was able to be used for the plotting.

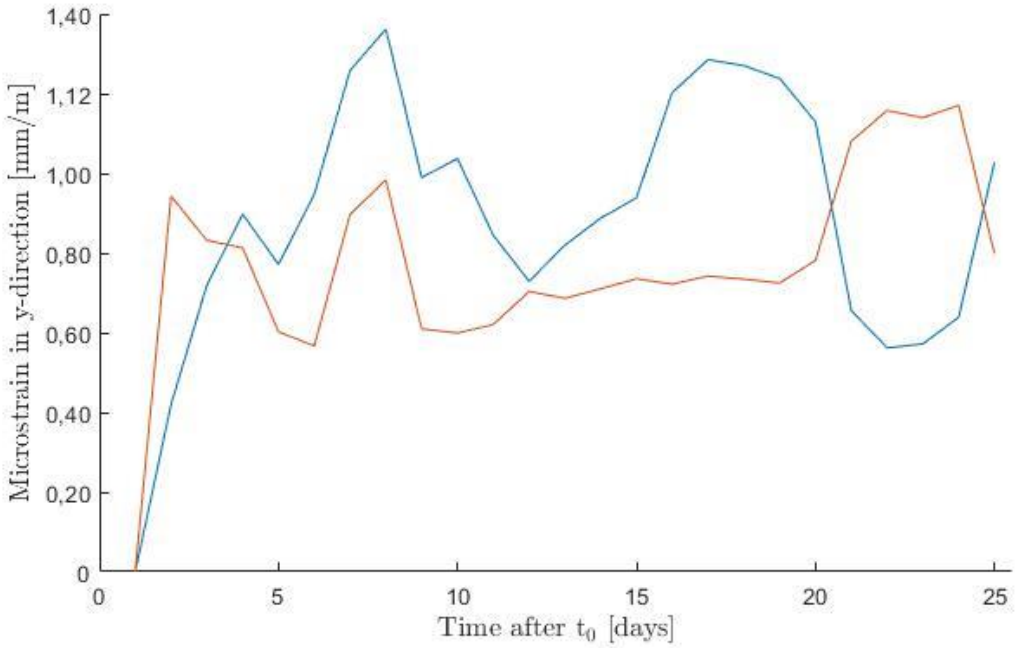

Figure 11.19. Microstrain in y-direction for 'yellow' PE mortar bar samples.

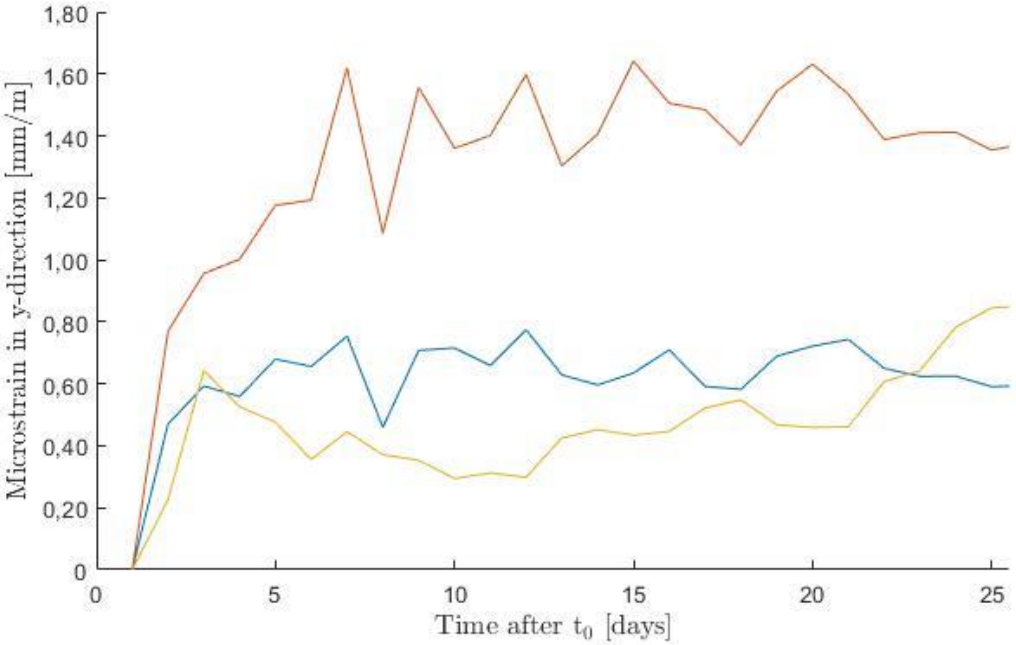

Figure 11.20. Microstrain in y-direction for 'green' PE mortar bar samples.

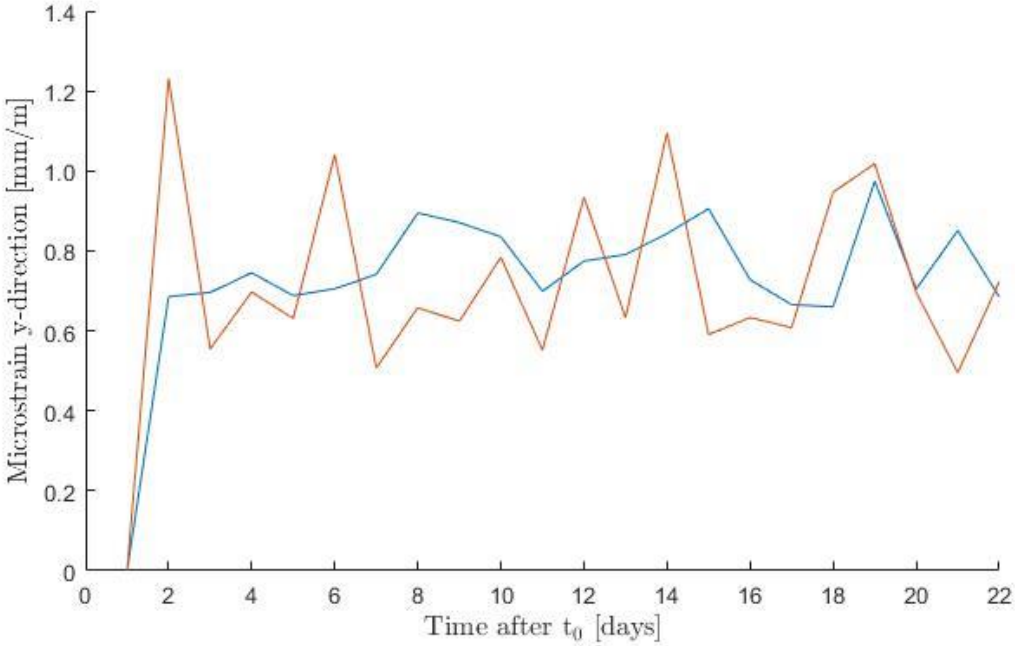

Figure 11.21. Microstrain in y-direction for PP mortar bar samples.

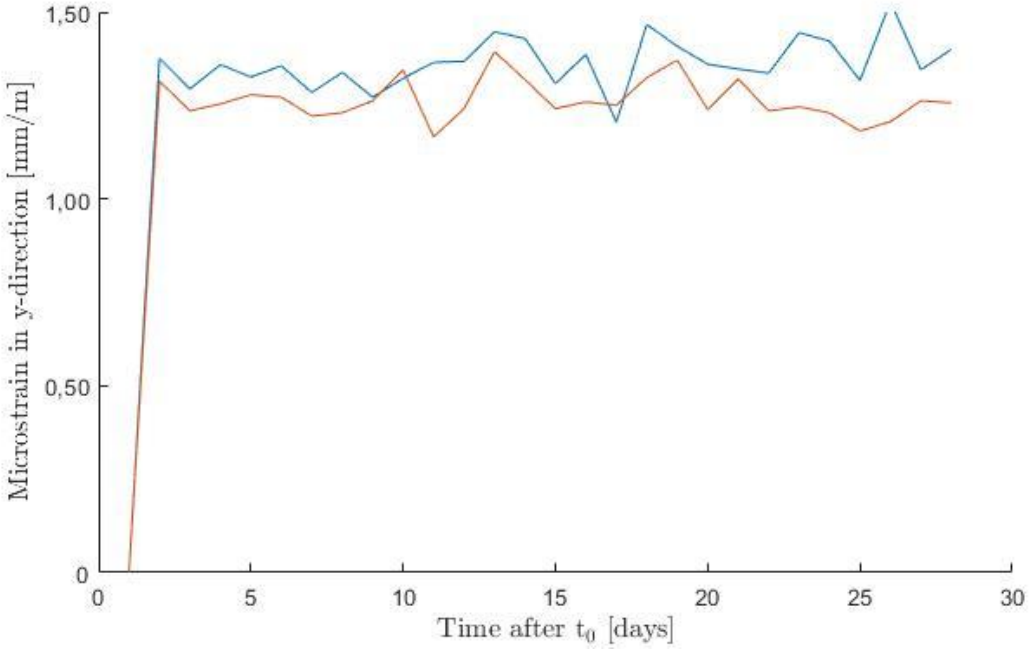

Figure 11.22. Microstrain in y-direction for reference mortar bar samples.

The graphs plotted show the vagueness of the DIC method used to quantify the microstrain. The curves follow a similar shape as the LVDT test curves (Figure 11.17), increasing quickly the microstrain rate during the first days and then, increasing slightly the microstrain until day 28 of free drying. However, the curves do not follow the slight increase tendency, showing peaks and valleys along the 28 days period. These results totally contradict the measures achieved with the LVDT test, in which an increase in the microstrain values is shown over the whole experiment period, demonstrating that the DIC test results are not reliable for making the comparison.

Furthermore it can be observed a big difference among the bars' microstrain curves for the same mix. So even, calculating the average for each mix bar, it would not be a reliable result for comparing the results with the LVDT test.

Figure 11. 22. presents the microstrain for the reference bars. Both reference bars showed similar results, they can be considered the most accurate results for the four mixtures analyzed. Furthermore, the biggest microstrain is observed, achieving the maximum microstrain around 1,50 µm/mm. Comparing with the LVDT test, on figure 11.17, the reference bar showed the maximum microstrain of 1,32 µm/mm. Results from the LVDT test showed the lowest microstrain for reference bars compared with the other bars' mixtures.

Figure 11.21 shows the microstrain for the PP samples. Both PP bars analyzed showed a slight difference concerning to the microstrain during the free drying. Although only 22 of curing days were measured, it was observed that the last days of free drying did not affect overly the microstrain of the bars. However, the maximum microstrain achieved with one

of the bars, it was observed to be around 1,20 µm/mm whereas the maximum microstrain achieved in the LVDT test was 1,80 µm/mm. Apart from showing completely different values between the LVDT test and the DIC test, during the DIC test, the PP bars showed a lower maximum microstrain comparing with the reference bars' maximum microstrain.

Figure 11.19. presents the microstrain for the 'green' PE bars. Three different bars were analyzed and the results did not show similarity. The date taken from two bars (curves blue and yellow on Figure 11.19) resulted in similar order of numbers, achieving a maximum microstrain around 0,80 µm/mm, which is lower compared to the third bar analyzed with a maximum microstrain of 1,60 µm/mm (curve red on Figure 11.19). The maximum microstrain measured during the LVDT test was of 1,47 µm/mm. These results demonstrate the inaccuracy of the DIC test carried out.

Figure 11.19. shows the microstrain for the 'yellow' PE bars. Both bars analyzed showed different values. Whereas in the first bar a maximum microstrain of 1,00 µm/mm was achieved, in the second one a maximum microstrain of 1,40 µm/mm was achieved and the curves did not show a similar pattern. The maximum microstrain measured during the LVDT test for the 'yellow' PE bar was of 1,47 µm/mm. Moreover, the equal microstrain found during the LVDT test regarding the PE bars it was not observed in the DIC test results.

The results of the DIC test showed the biggest maximum microstrain for the reference bars and the lowest maximum microstrain for the PP bars, just the opposite observed in the LVDT test results. However, the same tendency regarding the different mixtures was observed in the Literature used in this section, in which were proved that the addition of fibers in the mix tends to decrease the shrinkage strain for a same exposure time. The inaccuracy between the two measurement methods indicates that the DIC method is inefficient for obtaining displacement and strain fields during a long period of drying.

12. Discussion

This chapter includes the discussion of the results from Chapter 11. The chapter includes more in-depth discussion of the results internally, as well as a perspective and a comparison to previous related studies and research. As there are very few studies using fibers from recycled fishing nets, other waste materials used as fiber reinforcement will be considered and used for comparison.

12.1. Discussion- Casting

12.1.1. Distribution of PE fibers in mixture

The mechanical behavior of fiber reinforced concrete is strongly influenced by the distribution and the fibers orientation (N. Sebaibi et al., 2014). As was analyzed in section 11.1.1., the PP fibers resulted in a more homogeneous distribution on the samples' surfaces, comparing them with the PE reinforced mortar samples. The effect, as is exposed by S. Svensson (2016), is caused by the addition of fibers in the mixing. The greater the quantity of fibers added, the greater the loss of fluency in the casting process. In this project 0,2% of PP fibers were added to the mix samples comparing with the 2,0% of recycled PE fibers addition. The difference explains the difference observed in the distribution of fibers.

Furthermore, during the mixing process, it was found that the fibers were floating in the surface or stuck on the mixing shovel. The density of fibers is other parameter affecting the mixing properties as it is confirmed by S.Yin et al. (2015). The study exposes that fibers with a density of 0,9 g/cm^3 or lower, have a tendency to float on the surface during the mixing, which leads to a heterogeneous surface distribution of fibers. The PE fibers have a density of 0,950 g/cm^3, which makes them to be better distributed along the sample, allowing the use of a bigger quantity of PE fibers, comparing with the commercial PP fibers, which density is 0,910 g/cm^3, and consequently the maximum fibers addition is lower.

The transverse and longitudinal measurements showed that the percentage of longitudinal fibers in the fracture surfaces analyzed was higher than 70% for all the specimens, which concluded that, mostly, the orientation of the fibers was the ideal for performing better in compression and flexural strength. The homogenous distribution and the good orientation of fibers achieved in all the samples casted in the project could be attributed as one of the advantages when a High Speed Movement (HSM) is used during the last step of the casting process, as it is proved by N. Sebaibi et al. (2014). One of the disadvantages of using HSM in the casting exposed also in the study, is the increase of the porosity in the concrete samples. As it was shown in section 11.1.1., the porosity of the surfaces analyzed was not very perceptible.

Finally, it was observed a negative effect in the samples after the casting process, both fibers, PE and PP, were protruding from the edges and creating an uneven surface,

altering the physical characteristics, as can be seen on figure 11.2. The fiber protruding was more notable in the top surfaces, which are not in contact with mold surfaces. The same effect occurred during the casting for samples analyzed in the study carried out by S. Svensson (2016), in which Durus PP fibers were added and the same molds were used.

12.1.2. Specimens' weights and dimensions

As it has been shown in section 11.1.2., the difference between theoretical and experimental height and breadth values is not significant, whereas the difference between theoretical and experimental weight it is higher and mainly caused by the demolding process, producing material loss, which is also confirmed by G. Cardinaud (2017). The difference on the dimensions of the samples is mostly caused because of the molds' tolerances which were processed manually (G. Cardinaud 2017). Furthermore, the weight differences come mainly from the demolding part of the specimens, resulting on a loss of weight and length (G. Cardinaud 2017). Although different shapes and bigger molds were used with a distribution of small polyamide pieces of discarded fishing nets, the phenomena can be attributed to all the manual demolding processes for mortar or concrete samples.

12.2. Discussion- Methods I

12.2.1. Bending

The literature often exposes that plastic fibers as reinforcement in bending, have a positive effect on the first crack strength and during the post-cracking behavior compared with no reinforcement mortar mixes as it is proved by K.Kobayashi and R.Cho (1981) and by B.S.Al-Tulaian et al. (2016).

The results on section 11.2.1. showed an increase over time for 1, 2 and 7 days of curing in the first crack strength in PP, 'green' and 'yellow' PE fibers' samples, comparing with the plain concrete samples. The same increasing tendency in the flexural strength results was achieved by S. Svensson (2016). In the study, Durus and Fibrin PP fibers and recycled nylon fibers from fishing nets were used. The samples containing nylon fibers were tested during day 7, 14 and 28 of curing, whereas the Durus and Fibrin PP fibers were tested only after day 28 of curing. However, in the study the increasing on the first crack strength followed the same tendency from day 1 to day 28 of curing. Contrarily, in this project, all the FRM samples tested on the day 28 of curing suffered a decreased on the first crack strength comparing with the results from the same FRM samples tested on the day 7 of curing. However, for the reference samples, the maximum first crack strength was achieved during day 28 of curing, overcoming even the values obtained for FRM samples tested the same day of curing.

The decrease showed for the 28 days curing samples could be attributed to small changes that are very sensitive, especially if they are related with the curing temperature or the curing time as it is shown by S.Hong (2017). The study shows that the concrete's strength

decreases with an increase in temperature, particularly at high curing temperatures. The flexural strength lows from 45, 85 to 33, 95 Mpa when the temperature of curing goes from 20 ^{o}C to 40 ^{o}C. The phenomenon would explain the results obtained in the flexural test in this project about the drop in flexural strength from day 7 to day 28 in the FRM samples. The room where samples were curing during the whole period was converted into an environmental room after the samples of day 7 of curing were tested. The temperature and the relative humidity were increased, probably affecting the mechanical properties of the samples that were tested during the day 28 of curing.

In this project, an increase on flexural strength was presented on the FRM samples used in the project comparing with the reference samples and the sensitive changes that were produced due to the rise of temperature. The literature is divided in several studies that showed an increase on the flexural strength as B. S.Al-Tulaian et al. (2016), in which waste PET fibers were used; a decrease as S. Svensson (2016), in which waste PA6 fibers were used; or no affectation of the FRM samples as Silva et al. (2005), who used that PET fibers. It can be concluded that the fibers' material, the percentage of fibers added to the mix, the curing time and the curing temperature could be presented as the main factors affecting the mechanical properties of the FRM samples. Regarding to flexural strength, recycled PE fibers used in the project in a volume percentage of 2,0% , performed well as reinforcement.

Comparing the results with the project by S. Svensson (2016), and although different sizes and volume percentages of fibers were used, can be observed that during day 7 of curing, the values of the initial crack strength obtained for the waste PE reinforced mortar samples are higher than the values obtained for the waste PA6 reinforced mortar samples. However, due to the change suffered in the environment conditions during the curing period, the initial crack strength values obtained during day 28 of curing were higher for the PA6 reinforced mortar samples than for the PE reinforced mortar samples. Probably, if the conditions would be maintained equally during the curing period, the PE fibers would have performed better. However, the post cracking strength results showed higher values during day 7 for the PA6 reinforced mortar samples (2 cm, 1.0 % and 2.0 %) than PE reinforced mortar samples, and similar values during day 28 for both reinforced mortar samples.

The change in temperature and relative humidity conditions during the curing period seems not affect the post cracking behavior of the FRM samples, but nevertheless, affects first crack strength, compressive strength (12.2.3.) and toughness (12.2.2.).

12.2.2. Toughness

As it has been well documented in the section 10.1.2., fibers have a great positive influence on the toughness of fiber reinforced cement mortar and concrete samples. This is also proved on section 11.1.1 of this project, in which all the FRM samples presented a post-cracking well performed behavior comparing with the plummeted to zero that reference samples had. S.Orasutthinkul et al.(2017) and B.S.Al-Tulaian et al. (2016), also

exposed an improvement in toughness using recycled nylon fiber and recycled PET fibers, respectively.

Moreover, the flexural toughness of the commercial PP fibers showed a better performance than the PE recycled fibers. An increasing in the length-diameter ratio of the fibers usually augment the flexural strength and toughness of the concrete (V.S.Parameswaran, 1991) . The values of this ratio are usually restricted between 100 and 200 since fibers which are too long tend to "ball" in the mix and create workability problems. Commercial PP reinforced mortar samples performed better because of the higher ratio, 12 mm to 12 µm (ratio=667), comparing them with the recycled PE fibers, 348 µm to 17, 96 mm (ratio= 51, 72). However, with the commercial PP fibers, the value of the ratio presented by V.S.Parameswaran (1991), 200, was overcome.

The same tendency shown in the flexural strength results appeared in the toughness results. There was a decrease in the toughness for the critical deflection in all the FRM samples from the day 7 to day 28 of curing, and consequently for $T_{3\delta cr}$ values and the $T_{5\delta cr}$ values. These small changes were attributed to high temperature and relative humidity exposure in the environmental chamber.

Comparing the results with the values obtained by S. Svensson (2016), and although different sizes and volume percentages of fibers were used, can be observed that during day 7 of curing, the toughness performed by the PE reinforced mortar samples are higher than the values obtained with the PA6 fibers. However, during day 28 of curing, the toughness values resulted higher for the PA6 than for the PE fiber mortar samples, which can be attributed to the environment conditions exposed above. It can be concluded, that toughness results are similar for both types of fibers and if the environment conditions would remain steady during the curing process of this project, probably the toughness would have resulted higher for the PE reinforced mortar samples, which would prove that these fibers work better.

12.2.3. Compression

The results in compression strength in the project presented an increase over the 28 days curing period for all the mortar samples. Although, the effect of plastic fibers as reinforcement in compression is often debated, and the literature is divided, the same tendency was exposed by S.Hong (2017), where the compression strength of FRM samples increased from 36, 0 Mpa (day 1 of curing) to 51,41 Mpa (day 28 of curing).

The samples tested in compression during day 28 are the same showing a decrease on flexural strength during day 28 in section 11.2.3., conditioned by the possible exposure to high temperature and high relative humidity on the environmental chamber during the curing period. However, they did not show a decrease in compression strength comparing with the results achieved on day 7 of curing, as it was observed on the flexural strength results. S. Hong (2017) exposed that existed a decrease in compression strength on the same samples when they were tested on day 28 of curing and they were curing at different temperatures, going from 56,40 Mpa at -10 ^{o}C to 16,07 at 60 ^{o}C. A comparison

among the same samples tested the same day of curing and exposed at different temperatures during the whole period would be interesting to analyze in this project, but there is not enough data for doing it.

A decrease in compressive strength resulted when fibers were added to the mixture, so plain mortar samples showed the highest compressive strength comparing with FRM samples. This was also proved by S. Svensson (2016) and S.Orasutthikul (2017). In both studies, the reference samples were only tested during the day 28 of curing, showing the biggest compressive strength. V.C. Li (1992) investigates the effect of fiber addition on compressive strength of cementitious composites and explained that a decrease of compressive strength is a result of low resistance to sliding of crack faces which is exerted by bridging force of fiber. Moreover, the values obtained in the project carried out by S. Svensson (2016) with the PA6 fibers during day 28 of curing are slightly slower than the values obtained in this project with the PE fibers, although different sizes and volume percentages were used.

Furthermore, recycled PE fibers showed similar results, proving that their origin from different type of fishing nets with different color, size and braided form does not affect different their workability. PP commercial fibers, that has a smaller length average than recycled PE fibers showed the biggest compression strength comparing with the other FRM samples. The addition of fiber, especially long fiber, leads to an increase in the volume of interfacial transition zone which results in reduction of strength and stiffness of fiber reinforced mortar bonding documents folder (S.M.Palmquist et al., 2011).

The effect of plastic fibers as reinforcement in compression is often debated, and the literature is divided as some studies report an increase in compressive strength, some a decrease, and others no effect, as for the flexural strength and toughness.
However, concerning to the compressive strength, there are many parameters that affect the strength, such as the type of cement, the w/c ratio and other additional filler materials used. Therefore it is easy to compare the fibers in this study, as the difference between the FRM samples in this study was the fibers' material, PP Fibrin and recycled PE, and the curing days, 1, 2, 7 or 28. All samples used the same cement, same w/c ratio, same sand type and same casting procedure. This enabled a much more accurate comparison among the three fibers used and the days curing tested.

12.2.4. SEM analysis

The post peak behavior is directly affected by bond strength between fiber and matrix (S.Orasutthikul et al., 2017). On section 11.2.4. it was presented that the debonding generated by shear deformation in different samples was measured and resulted in more pronounced for the recycled PE reinforced mortar samples. The bonding strength between fiber and matrix is related to many factors as properties (fiber strength, stiffness, and Poisson's ratio), fiber geometry (fiber surface and cross section), fiber volume

content, matrix properties (matrix strength, stiffness, Poisson's ratio), and interface properties (adhesion, frictional and mechanical bond). (H.R. Pakravan et al., 2012)

Fibrillated fibers, as the PP commercial fibers used in the project, showed a better bonding comparing with the PE fibers. Some surface treatment techniques have been developed, as fiber fibrillation, to enhance the interfacial bond strength between the fiber and the cement composite matrix (W.C. Choi et al.,2015). The fiber geometry on bond behavior with hydrated cement matrix is affected by fiber geometry (Kim et al.,2012). In the mechanical bond test carried out in the study, the embossed R-PET fiber had considerably superior performance to the other types, as straight and crimped. Moreover, the study exposed that R-Nylon and R-PET fiber are softer than the surrounding cement matrix, and as consequence a part of their surfaces were peeled. In case of the PVA fiber, fragments of cement matrix were found on its surfaces. In this project, the PE and Fibrin PP fibers that were pulled out of the matrix showed a similar performance as the PVA fibers in the study Kim et al (2012). Small particles of mortar mix were found on the fiber surface, proving a chemical bonding between the PE and Fibrin PP fibers and the cementitous matrix. Furthermore, any signs of fracture or degradation were presented in the fibers.

The analysis of the surfaces showed that fibers were mainly pulled out of the matrix, demonstrating a poor fiber-to-matrix mechanical and chemical bonding between PE fibers and the cementitious matrix. As Kim et al. (2012) presented in the study, strong chemical bond between the PVA fibers and the hydrated cement matrix leads to break of the fiber rather than pulled out from the hydrated cement matrix. However, as V.S.Parameswaran, (1991), exposed, in the post-cracking stage, the failure is by a pull-out rather than by fiber yielding or fracture.

Finally, it should be cited that as S.Hong (2017) presented, the curing temperatures affects also the performance of the different bonding strength, going from 6, 06 Mpa at -10 ^{o}C to 1, 82 Mpa at 60 ^{o}C for polymer concrete matrix and steel reinforcement. However, there is no data available in the project to make a comparison of the bonding strength values because no bonding test was carried out.

12.3. Discussion- Methods II

12.3.1. Shrinkage analysis

12.3.1.1. Linear Variable Displacement Transducer Test

The microstrain results of the different samples measured with the LVDT along 28 days inside the environmental chamber seems very contradictory comparing them with the results obtained in the projects carried out by G.Cardinaud (2017) and C.M. Larsen (2017), in which were proved that the addition of fibers in the mix tends to decrease the shrinkage strain for a same exposure time and did not seem to affect the rate.

In G.Cardinaud (2017) project, the plain mortar or reference samples presented the highest microstrain rate with the maximum microstrain achieved on 1,7 µm/mm, whereas in this project the maximum microstrain achieved with the plain concrete samples was

1,38 µm/mm. Moreover, the PP reinforced mortar samples tested by G.Cardinaud (2017) presented the lowest microstrain rate comparing with the other mixtures. The maximum microstrain achieved during day 28 was 1, 25 µm/mm, whereas in this project the maximum microstrain achieved with the PP samples was 1,80 µm/mm. Similar results as G.Cardinaud (2017) were presented by C.M. Larsen (2017). However, a same tendency for the three projects was observed, the shrinkage strain presented was increasing over the curing time for all the mixes but the rate was decreasing. Indeed, the shape of the curves shows that the shrinkage was developing fast in the first days of measurement and slowing down after around day 7.

A different volume percentage of 'yellow' PE fibers was used in the samples made by G.Cardinaud (2017), 0,2% of PE fibers, and a microstrain of 1,40 µm/mm was presented . The microstrain results of the 'yellow' and 'green' PE reinforced mortar samples of this project with a volume percentage of 2,0%, were 1,51 and 1,53 µm/mm, respectively. As it is exposed in section 11.3.1.1., these results showed that both fibers affect similarly the microstrain performance. It can be concluded that the percentage of fibers added to the mix affects the strain of the mortar samples, as it is presented by G.Cardinaud (2017).

Analyzing the microstrain graphs presented by C.M. Larsen (2017), two differences can be found regarding to G.Cardinaud (2017) project. Firstly, although the volume percentage of PE and PP fibers is the same used by G.Cardinaud (2017), (0,2% for both mixes), the microstrain achieved slightly surpass a microstrain higher than 1 µm/mm, whereas in G.Cardinaud (2017) and this project some values around day 28 are close to 1,80 µm/mm. Secondly, C.M. Larsen (2017) showed graphs with 5 different bars' measures done for each mixture, and it can be observed that the difference among the bars' microstrain is very wide, although all the bars were casted the same day and the same mix proportions were used. The variation of microstrain in the same bars could be related to the variation of the environment conditions as the temperature and the humidity, but also to the placement of the bars during the free drying affected by the light exposure.

Finally, it should be cited, that due to the controversial results achieved, the LVDT test and DIC test was repeated for plain mortar bars and PP fibers mortar bars. During the second test, the resulting tendency achieved varied from the previous results, but the tendency showed in G.Cardinaud (2017) and C.M. Larsen (2017) was observed. The microstrain obtained for the PP fiber bars was much lower than the previous results, 1,1 µm/mm against 1,8 µm/mm measured during day 23 of free drying. However, the microstrain obtained for the reference bars was lower but similar to the previous result, 1,20 µm/mm against 1,36 µm/mm during day 28 of curing.

The discussion presented above would explain the controversial results achieved during the LVDT test. Although, as it was presented by C.M. Larsen (2017), the values corresponding to different bars from the same mix can plenty vary depending on very

sensitive small changes. However, for future studies and to improve the methodology to follow during the experimentation, it is suggested to:

- Use more than one bar to measure the microstrain in the LVDT test to calculate the average and compare the value with the results from the DIC test. With the current molds available in the concrete laboratory, it is only possible to cast 6 bars at the same time, so three bars could be used for the DIC test and the other three for the LVDT test. However, more moulds are needed in order to carry out the LVDT test, the DIC test and the water evaporation test at the same time and using bars from the same mix design.
- Place the bars used to measure with the LVDT in the same conditions as the bars used for the DIC test to have the same variables as temperature, humidity and light exposure and not alter the mechanical properties results with sensitive changes.
- Maintain certain distance among the bars placed in the environmental cage to allow the water evaporation to be equally, as this could be one of the sensitive factors affecting the samples properties.
- Improve the environmental chamber characteristics to maintain the temperature and humidity steadily. A deeper improvement suggestion concerning the environmental chamber is presented in section 14.1.

12.3.1.2. Digital Image Correlation

The aim of the DIC test was compare the results obtained with the LVDT test results, to prove the reliability and accuracy of the method as was compared in some studies as F. Lagier et al. (2011) and T. Mauroux et al. (2012). In these studies, the DIC method was carried out and the software Correli was used for the microstrain analysis, instead of the GOM Correlate software. In both studies the methods were contrasted and a good concordance between them was obtained, proving that the DIC method was efficient for obtaining displacement and strain fields during a several days long drying.

However, the results achieved from the DIC test showed contradictions regarding to the results from the LVDT test in this project. During the LVDT test, the biggest maximum microstrain achieved was showed in the PP bars, whereas the lowest maximum microstrain achieved was showed in the reference samples, and the opposite was observed in the DIC test results. The values from the DIC test were compared day per day with the values from the LVDT test, but they did not coincided. The same tendency was analyzed by G.Cardinaud (2017) and C.M. Larsen (2017), in which were proved that the addition of fibers in the mix tends to decrease the shrinkage strain for a same exposure

time and did not seem to affect the rate. Specially, in the FRM bars, the results achieved by G.Cardinaurd (2017), although different volume of fibers were used, showed that the maximum microstrain obtained in the PP bars was lower than the maximum microstrain achieved in the PE bars. The same tendency was observed in the DIC test results of this project.

However, the graphs plotted in Matlab showed the inaccuracy of the DIC method carried out in the environmental chamber used to quantify the microstrain of the different bar mixtures. The curves do not follow the slight increase tendency presented on the curves plotted with the results from the LVDT test (Figure 11.17.) and in G.Cardinaurd (2017) and C.M. Larsen (2017) projects, which are the usual shrinkage curves created by the constant water evaporation. However, from figure 11.19. to figure 11.22. several peaks and valleys are presented, meaning that the bars were contracting and expanding in the Y-direction along the 28 days experiment period. After the analysis of the possible sensitive causes that affected the microstrain results, it was concluded that the relative humidity was the main cause of the variation of the shrinkage in the bars. On figures 11.23. and 11.24. , the relative humidity and the microstrain evolution graphs for the PE and PE2 FRM samples are compared.

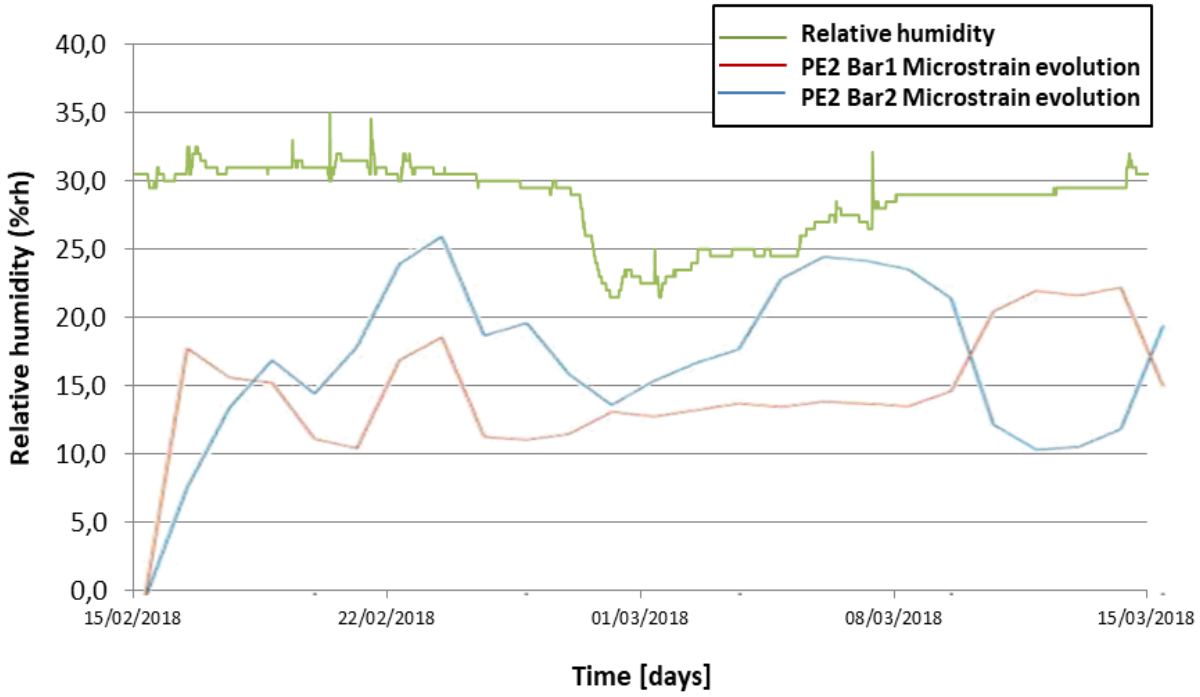

Figure 11.23. Relative humidity (%rh) and microstrain evolution for PE FRM samples (without scale).

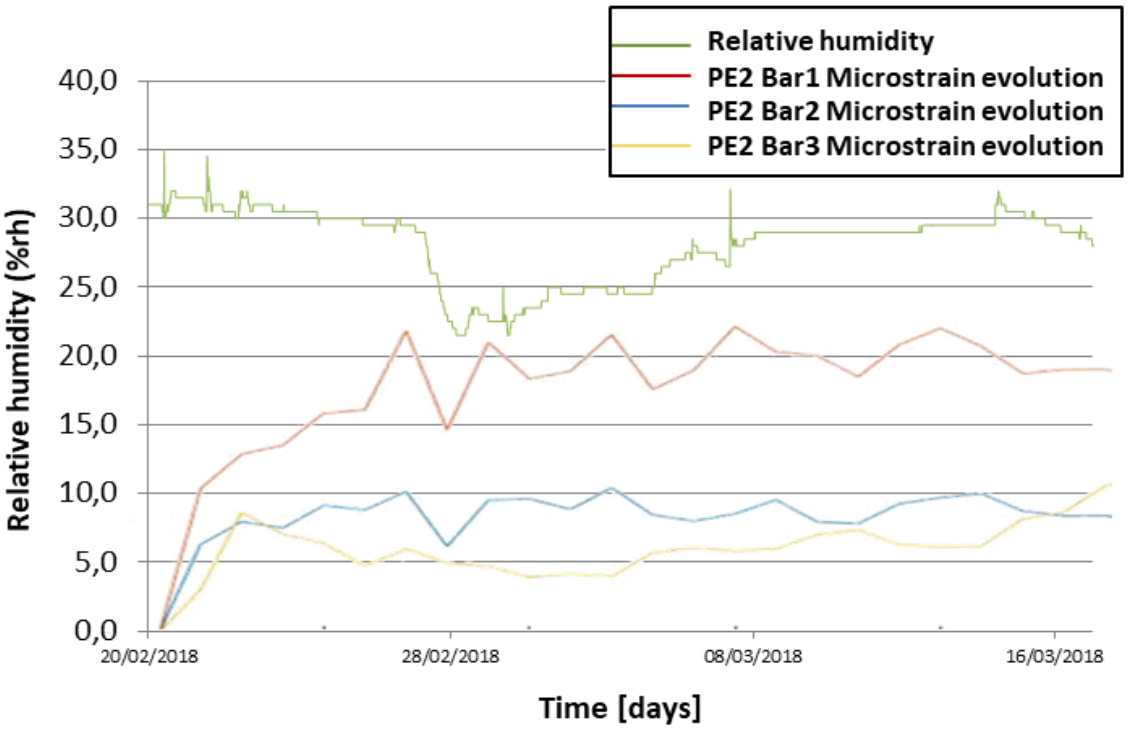

Figure 11.24. Relative humidity (%rh) and microstrain evolution for PE2 FRM samples (without scale).

As can be observed the majority of peaks and valleys in the microstrain evolution of the bars matched with the relative humidity points, proving that the wicked conditions of the environmental chamber to maintain the environment parameters as temperature and relative humidity steadily is the main cause of the DIC experiment failure. However, it can be observed that the microstrain values obtained with the DIC test vary from one bar to another, even coming from the same mixture. Small sensitive changes regarding the position, light exposure, vibration or water evaporation could be some of the factors affecting these variations. It is also surprising that the LVDT test was carried out during the same period, with the same environment variations, but no peaks or valleys were observed in the microstrain results plotted, but a slightly increase tendency. The placement of the bars out of the cage not being directly exposed to the LED light and the movement suffered each time they were measured could be some of the causes to obtain different results. It is concluded that having the exactly same conditions for all the samples tested is the primordial factor to take into account when the experiment is performed in order to get the most accurate data to contrast then both tests and obtained the match among the curves of the microstrain evolution.

Some factors related with the set-up of the camera and the environmental cage of the experiment, or some previous procedure steps as the painting process could have affected

the workability of the DIC test and would explain the variable results achieved. Regarding to the paint process, in order for GOM Correlate to detect points at the surface of the bars, the surface must have a clear stochastic pattern. During the previous painting process, the white layer seemed to be absorbed a little, making the surface look more grey than white. The addition of the black dots on top was done when the white layer was still wet, because the painting has to be done quickly. This sometime resulted in color mixing with the white layer making the black dots less prominent. Due to the precision of the deformation measurements by DIC is significantly dependent on the quality of image texture, and although 4 bars of each mixture were used for the DIC test, GOM Correlate was not able to detect the entire surface for some bars, so only 2 or 3 bars were analyzed. Similar conclusions regarding to the paint process were presented by C.M. Larsen (2017). For this reason, the use of GOM Correlate for measuring the microstrain can be really unpractical, even though it is a smart tool.

For future studies and to improve the methodology to follow during the test and the set-up, it is recommended to

- Improve the painting process by finding a specific method that specify distances and times to try to make possible to paint always with the most similar pattern possible. Although, it is very difficult to reproduce the same paint in the different surfaces, the mesh should be more regular to make GOM Correlate able to recognize and analyze the entire surface. As the painting it is considered one fundamental step to achieve accurate results, by improving the procedure, a breakthrough could be made in the DIC methodology used and reliable results could be obtained.

- Change the frequency of the photo shooting for the 28 days free drying period. During this project one photo was taken each hour during 28 days, proving later the inability of the GOM software to analyse more than 650 photos. It is recommended to take a photo each hour during the first 7 days and then change the frequency to one picture to each 6 hours until the day 28. On figure 11.17. and from figure 11.19. to figure 11.22. can be observed that day 7 is the date around the microstrain rate slowed. This frequency would offer accurate results and would save time of microstrain post-analysis.

- A better comprehension of the camera's setups would help to adapt the adjustments depending on the samples used and get the best pictures. It should be checked that the light of the chamber is off during the photo shot to no alter the quality of the photos and allow a better post-analysis in GOM Correlate.

Furthermore, it would be interesting to build a new set-up that allow a perpendicular movement of the camera, but that also keeps it fixed on the top of the cage, to be able to catch a perpendicular surface of the entire cage bottom and have only one face from each sample visually in the photo.

- Place the bars used during the LVDT test in the same conditions as the bars used for the DIC test to have them submitted to the same environment variables as temperature, humidity and light exposure, avoiding the alteration of the mechanical properties with small sensitive changes.
- Maintain certain distance among the bars placed in the environmental cage to allow the water evaporation to be equally in all directions. The water evaporation process could be one of the sensitive factors affecting the mechanical properties of the samples.
- Improve the environmental chamber characteristics to maintain the temperature and humidity steadily. It would be ideal to carry out this experimentation having the exactly same conditions for all the bars. A deeper improvement suggestion regarding the environmental chamber is presented in section 14.1.

13. Economic analysis and alternative solutions

In this section a brief economic analysis is provided regarding the different types of fibers used along this project. The data of the different fibers was obtained from industrial suppliers and the affectation by the economy of scale was taken into account to do the analysis.

The price per kilogram of the PE fibers was provided by the company Plastix and is 3 DKK/kg fiber cleaning not-included. After asking for the price to some PP commercial fibers suppliers as PP Nordica, Cemex, Roadstone & CRH and Danish Fibres, the range of 20-30 DKK/kg was selected as an average from the range provided. However, it was checked that PP commercial fibers can be purchased in the Asian market cheaper than 15 DKK/kg. The difference of price could be attributed mostly because in the first case the raw material, coming from the discarded fishing nets thrown into the ocean, is free of charge, whereas costly raw material is being used for the manufacture of virgin fibers. However, the action of collecting the nets and carrying them ashore is the extra cost affecting the price for PE fibers, but not the PP commercial fibers.

Figure 13.1. Reparation of broken fishing nets.

Figure 13.2. Processing and cutting of discarded fishing nets in Plastix installation.

Although the price for the PE recycled fibers is more than the quarter of the PP commercial fibers, different percentages of volume of fibers are needed for the same quantity of each mixture. In this project a percentage of 0,2% volume was used for PP fiber mixtures and a percentage of 2,0% volume was used for both, 'yellow' and 'green' PE fibers mixtures. This means that for example for 1 m3 of mixture 1, 82 kg of PP commercial fibers are required while 19 kg of PE fibers are required. Passing the amount required to the equivalent price means that for 1 m3 of mixture, the cost for the PP commercial fibers required would be in the range of 36,4 – 54,6 DKK, and for the recycled

PE fibers required would be 57 DKK. Looking at these numbers, it can be seen that there is not a huge difference of prices when the price of PP commercial fibers is 30 DKK/kg (54, 6 VS 57), as fibers delivered by PP Nordica and used in this project. However, when we talk of an order of tons and when a variation in the price thanks to scale of economies can occur, millions of Danish crones can be saved. This situation could explain why recycled fibers are not very used in the construction world nowadays despite the good mechanical properties they have shown to have.

As long as the environmental and circular economy awareness does not profoundly affect the building sector, and the economic benefit remains as the priority for companies, the use of recycled PE fibers as concrete reinforcement probably will be restricted to small-scale experiments in the laboratories or to some particular building case where recycled materials should be used. A first option to reduce the amount of discarded fishing nets thrown into the ocean each year would be to face the question 'Why the fishing nets are being thrown into the ocean?'. The arrangement of old fishing nets is not worth comparing the price and duration with new fishing nets. So, one solution to the problem would be offer cheaper fishing nets reparation in the ports, so more fishing companies would carry them ashore to fix them before throwing them into the ocean because it is not worthwhile to carry them in the ship. If the recovery of the fishing net is not possible, at least, a system of incentives to fishing companies could be implemented in order to encourage them to return the nets ashore, were companies as Plastix can take and process them without having to go out to sea to pick the discarded nets. Furthermore, one of these two ideas along with a hardening of fines addressed to fisheries because of the marine environment pollution they are generating with waste plastics would complement an efficient solution to the problem treated here.

A second option, figuring that the first optional scenarios exposed in the previous paragraph regarding to fisheries could not be achieved, would be to boost the use of PE recycled fibers as reinforcement by building companies through implementing a system of incentives by the government. As a first option, the incentives would be given to those companies that decide to bet for the use of recycled fibers as concrete reinforcement. As a second option, the incentives could be given to the discarded fishing nets collecting companies as the Danish company Plastix. Whereas with the first solution, companies are provided with a higher budget for the purchase of the recycled fibers, the second solution would allow to low the price of the PE recycled fibers to be able to compete in the market with the PP commercial fibers and overcome them in terms of usability.

Tabla 13.1. Overview of alternative solutions for the problem presented in this project.

State	Option	Advantages
'How to avoid or reduce fishing nets discarded into the ocean'	Cheaper fishing nets reparation.	1. Companies will carry the nets onshore to repair them instead of throwing them into the ocean. 2. Increase in jobs. 3. Increase in sailors and fisheries awareness.
	System of incentives for returning the fishing nets ashore.	1. Companies will carry the nets onshore to repair them instead of throwing them into the ocean. 2. Reduction of PE fibers' cost due to the elimination of the collecting process in the sea by companies as Plastix.
	Harder fines for marine pollution.	1. Companies will carry the nets ashore to repair them instead of throwing them into the ocean. 2. Government commitment.
'How to boost the idea of the project commercially'	System of incentives for construction companies.	1. PE recycled fibers used as concrete reinforcement impulse. 2. Market increase for PE fibers and increase of competitiveness with commercial PP fibers. 3. Government commitment.
	System of incentives for fishing nets' collecting companies.	1. Government commitment. 2. Reduction of PE fibers' cost. 3. Market increase for PE fibers and competitiveness with commercial PP fibers.

Finally, the Scandinavian region seems to be a good scenario for the construction and concrete companies that could be interested in the use of waste fibers from fishing nets that this project presents. The Danish architecture firms Lendager Group, pioneer within sustainability, circular economy and resource efficiency, could be a good partner when promoting the initiative of this project commercially More and more companies are willing to enter or improve their commitment with the circularity and the upcycling of products in the construction sector, and this is reflected in the increase in research related to the recycling of waste products in the Civil Engineering and Materials departments at the University.

14. Conclusions

Two different parts were carried out in this project. The first part was focused on analyzing the marine impact of the microplastics generated from the discarded fishing nets, and the second part was focused on the use of recycled fibers as reinforcement into concrete. The two types of fishing nets investigated were delivered by the company Plastix and they were made of PE. The recycled fibers were held against the commercial PP fibers called Fibrin delivered by the company PP Nordica.

From the experimental work of the first part of the project the following conclusions were derived:

- The analysis of the impurities coming together with the PE fibers delivered by the company Plastix showed a high quantity of impurities as particles of sand, salt, and clay, as well as PE microplastics and other white filament microplastics with an unknown origin. The average percentage of impurities smaller than 1 mm measured in the samples was of 76%. The high number proved the necessity of a washing process before the addition of the fibers into the mortar mix, in order to not alter the mechanical properties and the workability of the FRM samples.
- The results obtained in the microplastics release tests demonstrated the environmental problem represented by abandoned fishing gear. It was proved the microplastics release from the fishing nets that can enter directly in the marine food chain. The microplastics creation process was surprisingly quick considering that the experiment was running only 2 months and that the PE degradation is a very slow process. Furthermore, the results proved that the wave friction and the UV light conditions are the main factors speeding the degradation of the PE nets and fibers, so nets and fibers floating on sea surface conditions degrade quicker than if they are floating under the surface.
- Two different types of PE fibers and nets were used for the simulation of the nets degradation into the ocean, ‘yellow’ and ‘green’ PE. The degradation speed of the nets was higher for the ‘yellow’ nets, which had bigger mesh dimension and a braided less compressed, which are proved factors to affect the degradation rate. Moreover, the quantity of impurities, as clay and sand, observed in the filter’ samples at the end of the simulation was higher in the ‘green’ PE nets.

From the experimental work of the second part – Methods I of the project the following conclusions were derived:

- The distribution of the recycled PE fibers into the mortar resulted very homogenous and the percentage of longitudinal fibers in the fracture surfaces analyzed was higher than 70% for all the specimens, which concluded that, in general, the orientation of the fibers was the best option for performing better in compressive and flexural strength. However, in all the FRM samples, fibers protruding from the edges of the samples were observed, which created an uneven surface.
- Concerning the specimens' weight and dimension test it was concluded that the difference between theoretical and experimental height and breadth values was not significant, whereas the difference between theoretical and experimental weight was higher and mainly caused by the manual demolding process, in which some material was lost.
- The results achieved in the compressive and flexural strength tests showed that the PE fibers from discarded fishing nets were performing similarly to the commercial PP fibers. Furthermore, it was proved that the PE fiber reinforcement significantly improves the toughness by sustaining useful load beyond the first crack load. These results were satisfactory, since they prove that commercial fibers could be replaced by fibers from the PE discarded fishing nets.
- During the 28 days of curing period, some environmental conditions in the curing chamber as temperature and relative humidity, were changed. This fact could have affected the workability of the samples as was observed in the flexural strength and toughness results. A decreasing tendency in flexural strength and consequently in flexural toughness was observed in tests carried out from day 7^{th} to day 28^{th} of curing. Comparing with some studies from the Literature, the tendency should have been an increase of strength until day 28^{th} of curing, as was presented in the compressive test results.
- The analysis of the surfaces showed that fibers were mainly pulled out of the matrix, demonstrating a poor fiber-to-matrix mechanical and chemical bonding between PE fibers and the cementitious matrix. Moreover, small particles of mortar mix were found on the fiber surface and no signs of degradation were showed in the fibers.
- Two different types of PE fibers were tested into the mortar samples, 'yellow' and 'green' PE fibers, coming from fishing nets with different color, mesh dimension and braided. Results showed similar workability regarding to compressive and flexural strength, flexural toughness and bond strength between fiber and matrix, which

proved that PE fishing nets with different characteristics can be collected and processed together.

From the experimental work of the second part – Methods II of the project the following conclusions were derived:

- The LVDT test results observed along the 28 days showed that the shrinkage strain is increasing over the curing time for all the mixes but the rate is decreasing, being higher during the first days of free drying. The PP fiber bars showed the highest microstrain and the reference bars showed the lowest, contradicting the Literature used, in which it is exposed that the addition of fibers in the mix tends to decrease the shrinkage strain for a same exposure time and do not seem to affect the rate. The microstrain results of the 'yellow' and 'green' PE fibers showed that both fibers affected similarly the shrinkage strain performance.
- In the DIC test, the reference bars showed the highest microstrain and the PP bars showed the lowest, agreeing with the Literature used. However, no similarity was found in the microstrain values of the different 'yellow' and 'green' PE bars. Furthermore, results were considered not reliable and accurate. Firstly, because of the peaks and valleys showed in the microstrain curves instead of a slight rise during the 28 days and secondly, because of the different microstrain values achieved for the bars within the same mixture. The disavowal of the test results are attributed to several causes that should be improved as the camera and the environmental chamber settings, but especially the previous painting process, which conditioned the accuracy of the GOM Correlate surface analysis.
- Both test results were compared day per day, but not match was found. Furthermore, opposite results were presented; in the LVDT test the plain mortar bars presented the lowest maximum microstrain comparing with the FRM bars, whereas in the DIC test the contrary results were presented. Both methods should be improved in order to get reliable data to compare them and conclude if the DIC method is valid to quantify the microstrain produced in the bars.

From the economic analysis the following conclusions were derived:

- The main Scandinavian companies supplying commercial PP fibers sell these fibers at 30 DKK / Kg. The Scandinavian company Plastix, which is one of the responsible for the

collection and processing of the fishing nets discarded in the Northern Periphery and Arctic region, plans to sell the recycled PE fibers for 3 DKK / Kg. Although the percentages of volume needed for each type of fiber in the mix vary, there can be a clearly economic competition in the construction sector. Furthermore, taking into account the growing willingness of Scandinavian companies to make a transition to more sustainable state, recycled fibers would take advantage.

- It is necessary to enhance the circular economy awareness affecting the building sector to boost the use of recycled fibers from fishing nets as concrete reinforcement. Alternatives solutions for the fishing nets problem are presented as: cheaper reparation taxes for the nets in the ports, the use of incentives to make fisheries to transport the nets ashore, or set harder legislation concerning marine pollution. Other alternatives proposed are: to implement a system of incentives for construction companies that decide to bet for the use of waste fibers, or to the collecting companies as Plastix to allow to lower the prices and make the PE recycled fibers able to compete in the market with the commercial fibers.

14.1. Future studies or improvements

In this section it is presented some interesting questions and improvements for future studies that appeared throughout the project. It would be necessary to improve or interesting to carry out:

- A deep characterization of the microplastics found in the impurities in order to have a better overview of the current plastic pollution in the Arctic Region where the nets are collected. Study the origin of the microplastic and prove their link to the fisheries industry could be something beneficial for the creation of future plans to fight against marine pollution.

- Further studies to obtain a higher number of data to establish connections between marine environment stress on the nets and the release of microplastics. It would be interesting to carry out the repetition of the microplastics release experiment in a bigger scale, using glass or plastic cages and new pieces of nets, totally covered to avoid the water evaporation. In this way, the blades of the mixers would have more space and would not be in direct contact with the nets, avoiding the possible collapse of the experiment. It would be very appropriate to run this experiment for a long period, between 6 months and one year. The fishing nets degradation and the microplastics release into the ocean water is a long

process, so by extending the experiment life, the measurement of the results would be facilitated.

- A test and analysis of the affectation of the curing temperature and humidity variation to the different mortar samples. The flexural strength, flexural toughness and compression strength results achieved in this project were negatively affected by small sensitive changes. It was concluded that the main cause was the increase of temperature and relative humidity suffered during the curing process. During these project the samples were test taking into account the variable curing time, but it would be interested to carry out a test to have a better understanding about how different temperatures and humidifies can affect the mechanical properties of the samples.
- In the environmental chamber, the specific conditions set for temperature and humidity rate must be maintained steadily. The creation of a closed cage, in which the DIC test could be performed, and in which the variables could be controlled easily with different sensors, it would be a possible solution. Moreover, the environment parameters could be varied easily in each cage by students, creating new possibilities to study specimens under different temperature, relative humidity and wind velocity parameters. There is enough space to place more cages in the same space and allow more students to perform experiment at the same time, avoiding reservation problems. The specimens used to study the shrinkage cracking are only positioned inside the cage, so there is no reason to maintain these conditions in all the room because the main space it is used as warehouse.
- A water evaporation test for the different samples bars. It would be interesting to place several weight machines inside one environmental cage with the same conditions as the cage used for the DIC test, and monitor all the data in smaller and simpler devices instead of using a big computer. More than one bar from the same mix should be used for the measurement.
- Improvements in the set-up or experimentation about the LVDT test and the DIC method can be found more explicit in section 12.3.1.1. and section 12.3.1.2., respectively.

15. Bibliography

A. Al-manaseer and T.r. Dalal. Concrete Containing Plastic Aggregates. Concrete International, Vol. 19, 1997, Pages 47-52.

A. K. Jassim. Recycling of Polyethylene Waste to Produce Plastic Cement. University of Basrah, College of Engineering, Materials Engineering Department, Basrah, Iraq. Procedia Manufacturing Vol. 8, 2017, pages 635 – 642.

A. Montarsolo, R. Mossotti, A. Patrucco, M. Zoccola, R. Caringella, P. D. Pozzo and C. Tonin. Study on Microplastics Release from Fishing Nets. Proceedings of the International Conference on Microplastic Pollution in the Mediterranean Sea, 2017, Pages 81-88.

A.M. Neville, J.J. Brooks. Concrete technology. Pearson, second edition, 2010.

ASTM C1018-97. Standard Test Method for Flexural Toughness and First-Crack Strength of Fiber-Reinforced Concrete (Using Beam With Third-Point Loading). American Society for Testing and Materials. 1998.

B.S. Al-Tulaian, M.J. Al-Shannag and A.R. Al-Hozaimy. Recycled plastic waste fibers for reinforcing Portland cement mortar. Construction and Building Materials Vol. 127, 2016. Pages 102–110.

C.M.Larsen. Plastic shrinkage cracking of cement based materials reinforced with waste fibres. Master Thesis, Byg department, DTU, 2017.

D. Silva, A. Betioli, P. Gleize, H. Roman, L. Gomez, and J. Ribeiro. Degradation of recycled pet fibers in Portland cement-based materials. Cement and Concrete Research, Vol. 35- Pages 1741-1746, 2005.

Dr. B. Harbor. Standard Practice for the Preparation of Substitute Ocean Water. American Society for Testing and Materials. ASTM D1141, Reapproved 2013, Pages 1-3.

Dr. P. J. Kershaw. Marine plastic debris and microplastics. Global lessons and research to inspire action and guide policy change. UNEP, 2016.

DS / EN ISO 17892-1. Geotechnical survey and testing - Laboratory testing of soil - Part 1: Determination of water content. 2014

DS/EN 12390-3. Compressive strength of test specimens. 2012.

DS/EN-196-1. Methods of testing cement – part 1: Determination of strength. Dansk Standard. 2005.

F. Lagier, X. Jourdain, C. De Sa , F. Benboudjema and J.B. Colliat. Numerical strategies for prediction of drying cracks in heterogeneous materials: Comparison upon experimental results. Engineering Structures 33, 2011, Pages 920–931.

G.Cardinaud. Reuse of waste plastic fibres from discarded fishing nets in cement-based specimens. Master Thesis, Byg department, DTU, 2017.

H.R. Pakravan, M. Jamshidi, M. Latifi. A study on bonding strength of polymeric fibers to cementitious matrix. 3rd International Conference on Concrete & Development, 2009, Pages 149-158.

I.M. Gieysztor and L.M. Ottosen. Engineering properties of fibres from waste fishing nets. International Conference on Materials, Systems and Structures in Civil Engineering.2016

I.M. Gieysztor and L.M. Ottosen. Reuse of polyethylene fibres from discarded fishing nets as reinforcement in gypsum based materials. 2nd International Conference on Bio-based Building Materials & 1st Conference on Ecological behavior of Granular and Fibrous materials –Clermont-Ferrand, France. 2017. Pages 2-6.

J.H.J. Kim, C.G. Park, S.W. Lee, S.W. Lee and J.P. Won. Effects of the geometry of recycled PET fiber reinforcement on shrinkage cracking of cement-based composites. Composites B Vol. 39, 2008, Pages 442–450.

J.J.Kim, D.J. Kim, S.T. Kang and J.H. Lee. Influence of sand to coarse aggregate ratio on the interfacial bond strength of steel fibers in concrete for nuclear power plant. Nucl. Enf. Des., Vol. 252, 2012. Pages 1-10.

K. Kobayashi, R.Cho. Flexural behavior of polyethylene fiber reinforced concrete. International Journal of Cement Composites and Lightweight Concrete, Vol. 3, 1981, Pages 19-25.

M. Serdar, A. Baricevic, M. J. Rukavina, M. Pezer, D. Bjegovic, and N. Štirmer. Shrinkage Behavior of Fiber Reinforced Concrete with Recycled Tyre Polymer Fibres .Department of Materials, University of Zagreb Faculty of Civil Engineering, Fra Andrije Kacica Miosica 26, 10000 Zagreb, Croatia. 2015.

M. Sudhakar and M. Doble. Marine microbe-mediated biodegradation of low- and high-density polyethylene. Vol. 61, 2008, Pages 203-213.

N.Kalogerakis, K.Karkanorachaki, G. C.Kalogerakis, E. I. Triantafyllid, A. D. Gotsis , P. Partsinevelos and F. Fava. Microplastics Generation: Onset of Fragmentation of Polyethylene Films in Marine Environment Mesocosms. 2017.

N.Sebaibi, M. Benzerzour and N.E. Abriak. Influence of the distribution and orientation of fibres in a reinforced concrete with waste fibres and powders. Construction and Building Materials Vol. 65, 2014, Pages 254–263.

P. Kumar Mehta. Concrete: microstructure, properties and materials. Mc Graw Hill Education, fourth edition, 2014.

S. Hong. Influence of Curing Conditions on the Strength Properties of Polysulfide Polymer Concrete. Aplied sciences, MDPI, Vol. 7, 2017, Pages 1-13.

S. J. Svensson. Methodology and Testing of Waste Fishing Net as Fibre Reinforcement in Mortar. Master Thesis, Byg department, DTU, 2016.

S. Orasutthikul, D. Unno and H. Yokota. Effectiveness of recycled nylon fiber from waste fishing net with respect to fiber reinforced mortar. Construction and Building Materials Vol. 146 ,2017, Pages 594–602.

S. Spadea, I. Farina, A. Carrafiello and F. Fraternali. Recycled nylon fibers as cement mortar reinforcement. Construction and Building Materials, Vol. 80, 2015, Pages 200–209.

S. Thomas and C. Hidrayanathan. The effect of natural sunlight on the strength of polyamide 6 multifilament and monofilament fishing net materials. Fisheries Research , Vol. 81, 2006, Pages 326-330.

S. Yin, R. Tuladhar, T. Collister, M. Combe, N. Sivakugan, Z.Deng. Post-cracking performance of recycled polypropylene fibre in concrete. Construction and Building Materials Vol. 101, 2015, Pages 1069–1077.

S.M. Palmquist, E. Kintzel and K. Andrew. Scanning electron microscopy to examine concrete with carbon nanofibers. Proceedings of the 5th Pan American Conference for NDT, 2011. Pages 1-6.

T. Mauroux, F. Benboudjema, P. Turcry, A. Aït-Mokhtar and O. Deves. Study of cracking due to drying in coating mortars by digital image correlation. Cement and Concrete Research 42, 2012, Pages 1014-1023.

U. Oxvig and U.J. Hansen. Fishing gears. Fisheries circle. 2nd edition, 2007, Pages 11-22.

V. Hidalgo-Ruz, L. Gutow, R.C. Thompson and M. Thiel. Microplastics in the Marine Environment: A Review of the Methods Used for Identification and Quantification. Environ. Sci. Technol., Vol. 46 , 2012, Pages 3060–3075.

V.C.Li. A Simplified Micromechanical Model of Compressive Strength of Fiber-Reinforced Cementitious Composites. Cement & Concrete Composites Vol. 14, 1992, Pages 131 – 141.

V.S. Parameswaran. Fibre-reinforced Concrete: a Versatile Construction Material. Building and Environment, Vol. 26, Nº. 3, 1991, Pages 301-305.

W.C. Choi, S.J. Jang and H.D. Yun. Interface Bond Characterization between Fiber and Cementitious Matrix. International Journal of Polymer Science, 2015.

16. Appendix

This is the Appendix for Master Thesis Recycling Fishing Net into concrete by Edurne Suárez Lejardi at Technical University of Denmark. July 16, 2018.

The Appendix consists of the following appendixes:

Appendix 1- Experimental log

Appendix 2 – Microplastics- Filters' surface analysis pictures.

Appendix 3- Water content calculation.

Appendix 4- Specimens' theoretical weight calculation.

Appendix 5- Working Curves of Mortar Samples- Bending Strength.

Appendix 6- Flexural Toughness Data.

Appendix 7- Compressive Strength Test Data.

Appendix 8- LVDT test data.

16.1. Appendix 1- Experimental log

On table 16.1. it is presented the experimental log carried out during the whole project period.

Table 16.1. Experimental log of the project.

Date	Experiment	Standard	Location	Comment
07-02-18	Casting of plain concrete samples (REF-)	DS/EN-196-1	DTU Concrete Lab	-
08-02-18	Bending and compression test 1 day prism samples (REF-)	DS/EN-196-1	DTU Byg	Failure with one sample during the bending test.
08-02-18	Starting of LVDT and DIC tests with bar samples (REF-)	-	DTU Concrete Lab	-
09-02-18	Bending and compression test 2 day prism samples (REF-)	DS/EN-196-1	DTU Byg	-
12-02-18	Casting of concrete with PP reinforced mortar samples (REF PP)	DS/EN-196-1	DTU Concrete Lab	-
13-02-18	Bending and compression test 1 day prism samples (REF PP)	DS/EN-196-1	DTU Byg	Failure with one sample during the bending test.
13-02-18	Starting of LVDT and DIC tests with –bar samples (REF –PP)		DTU Concrete Lab	Failure on the demolding of bar samples. Shrinkage premature apparition. One bar is discarded.
14-02-18	Casting of concrete with PE ‘yellow’ reinforced mortar samples (REF PE)	DS/EN-196-1	DTU Concrete Lab	-
14-02-18	Bending and compression test 2 day prism samples (REF PP)	DS/EN-196-1	DTU Byg	-
14-02-18	Bending and	DS/EN-196-1	DTU Byg	-

	compression test 7 day prism samples (REF-)			
15-02-18	Bending and compression test 1 day prism samples (REF PE)	DS/EN-196-1	DTU Byg	-
15-02-18	Starting of LVDT and DIC tests with bar samples (REF PE)	-	DTU Concrete Lab	-
16-02-18	Bending and compression test 2 day prism samples (REF PE)	DS/EN-196-1	DTU Byg	-
19-02-18	Casting of concrete with PE 'green' reinforced mortar samples (REF PE2)	DS/EN-196-1	DTU Concrete Lab	-
19-02-18	Bending and compression test 7 day prism samples (REF PP)-	DS/EN-196-1	DTU Byg	-
20-02-18	Bending and compression test 1 day prism samples (REF PE2)	DS/EN-196-1	DTU Byg	-
20-02-18	Starting of LVDT and DIC tests with bar samples (REF PE2)	-	DTU Concrete Lab	-
21-02-18	Bending and compression test 7 day prism samples (REF PE)	DS/EN-196-1	DTU Byg	-
21-02-18	Bending and compression test 2 day prism samples (REF PE2)	DS/EN-196-1	DTU Byg	-
26-02-18	Bending and compression test 7 day prism samples	DS/EN-196-1	DTU Byg	-

	(REF PE2)			
27-02-18	Repetition of the casting of REF- and REF PP samples	DS/EN-196-1	DTU Concrete Lab	Only 3 prism specimens were casted for each mix
28-02-18	Repetition of the casting of REF PE and REF PE2 samples	DS/EN-196-1	DTU Concrete Lab	Only 3 prism specimens were casted for each mix
28-02-18	Bending test 1 day for prism samples (REF- Rep an REF PP Rep)	DS/EN-196-1	DTU Byg	Bending test repetition for the three specimens after have been weighed and measured
01-03-18	Bending test 1 day for prism samples (REF PE Rep an REF PE2 Rep)	DS/EN-196-1	DTU Byg	Bending test repetition for the three specimens after have been weighed and measured
7-03-18	Bending and compression test 28 day prism samples (REF -)	DS/EN-196-1	DTU Byg	-
7-03-18	End of LVDT and DIC tests with bar samples (REF -)	-	DTU Concrete Lab	-
12-03-18	Bending and compression test 28 day prism samples (REF PP)	DS/EN-196-1	DTU Byg	-
12-03-18	End of LVDT and DIC tests with bar samples (REF PP)	-	DTU Concrete Lab	Downloaded photos from camera card to computer
14-03-18	Bending and compression test 28 day prism samples (REF PE)	DS/EN-196-1	DTU Byg	-
14-03-18	End of LVDT and DIC tests with bar samples (REF PE)	-	DTU Concrete Lab	-
15-03-18	Starting of microplastics release test	-	DTU Byg	Done with help from Sabrina June Hvid

19-03-18	Bending and compression test 28 day prism samples (REF PE2)	DS/EN-196-1	DTU Byg	-
19-03-18	End of LVDT and DIC tests with bar samples (REF PE2)	-	DTU Concrete Lab	Downloaded photos from camera card to computer. Downloaded temperature and humidity data from USB measurer to computer
03-04-18	Visual inspection of the microplastic release test	-	DTU Byg	No microplastics observed in samples.
04-04-18	Casting of REF-bars for DIC repetition	DS/EN-196-1	DTU Concrete Lab	-
5-04-18	Starting of LVDT and DIC tests repetition I	-	DTU Concrete Lab	-
05-04-18	Preparation of samples for the SEM analysis	-	DTU Byg	Measurement and cutting
9-04-18	Visual inspection of the microplastic release test	-	DTU Byg	No microplastics observed in samples.
10-04-18	SEM Analysis of PE and PP fiber mortar samples	-	DTU Byg	Bonding measurement. Done with help from Ebba Cederberg
16-04-18	Casting of REF PP bars for DIC repetition	DS/EN-196-1	DTU Concrete Lab	-
16-04-18	Visual inspection of the microplastic release test	-	DTU Byg	Microplastics and impurities observed in sample nº 3. Impurities in the bottom of the glass (sand, silt…) and microplastics observed floating in the surface. No

				evolution from last day
17-04-18	Starting of LVDT and DIC tests repetition II	-	DTU Concrete Lab	-
23-04-18	Visual inspection of the microplastic release test	-	DTU Byg	Microplastics and impurities observed in sample nº 3. Impurities in the bottom of the glass (sand, silt…) and microplastics observed floating in the surface. No evolution from last day
30-04-18	Visual inspection of the microplastic release test	-	DTU Byg	Experiment spoilt. Addition of sea water. Some microplastics found in the remaining water.
01-05-18	SEM Analysis of PE and PP fiber mortar samples and impurities coming with fibers	-	DTU Byg	Surface fracture. Done with help from Ebba Cederberg
14-05-18	End of fishing nets degradation experiment.	-	DTU Byg	Cleaning of the experiment set-up and drying of nets in the oven at 50 ^{o}C during two days.
16-05-18	Water absorption and filtering of microplastics release tests.	-	DTU Byg	Filters of 0,45µm were used in the vacuum.
16-05-18	Microscope analysis of microplastics	-	DTU Byg	Analysis of microplastics found in sample nº1,3,5 and 7.

16.2. Appendix 2 – Microplastics- Filter' surfaces analysis pictures

From figure 16.1 to figure 16.8. some previous pictures taken to the filter' surfaces, used in the experiment in section 5.2.,with the microscope portable are shown. For the analysis

of the filters' surface finally the fix electronic microscope pictures were used because of the better quality.

Figure 16.1. Sample test nº1.

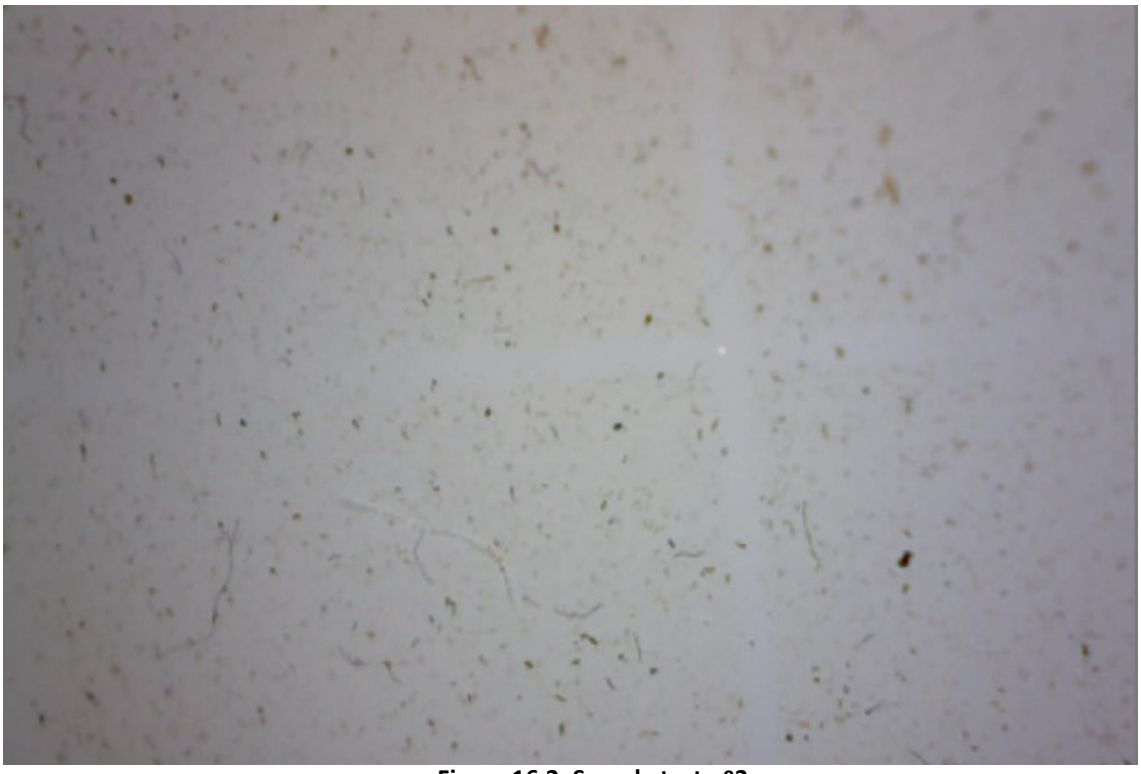

Figure 16.2. Sample test nº2.

Figure 16.3. Sample test nº3.

Figure 16.4. Sample test nº4.

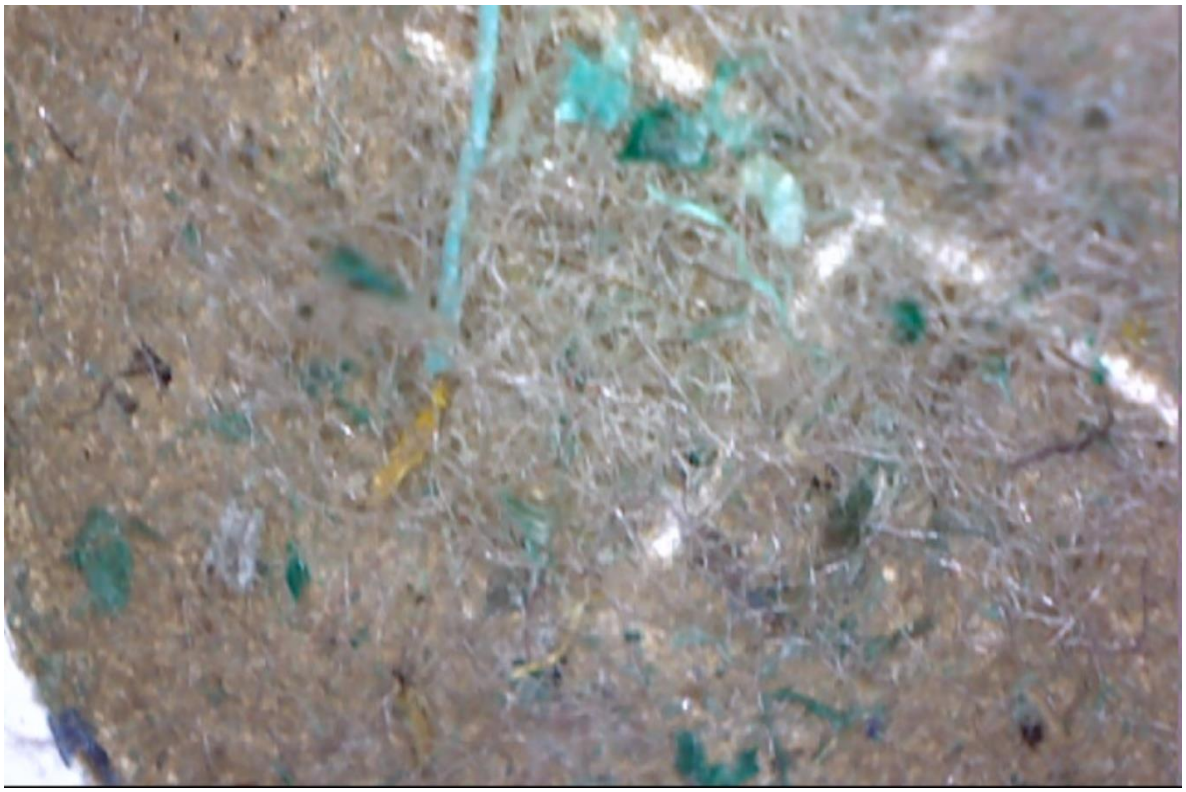

Figure 16.5. Sample test nº5

Figure 16.6. Sample test nº6

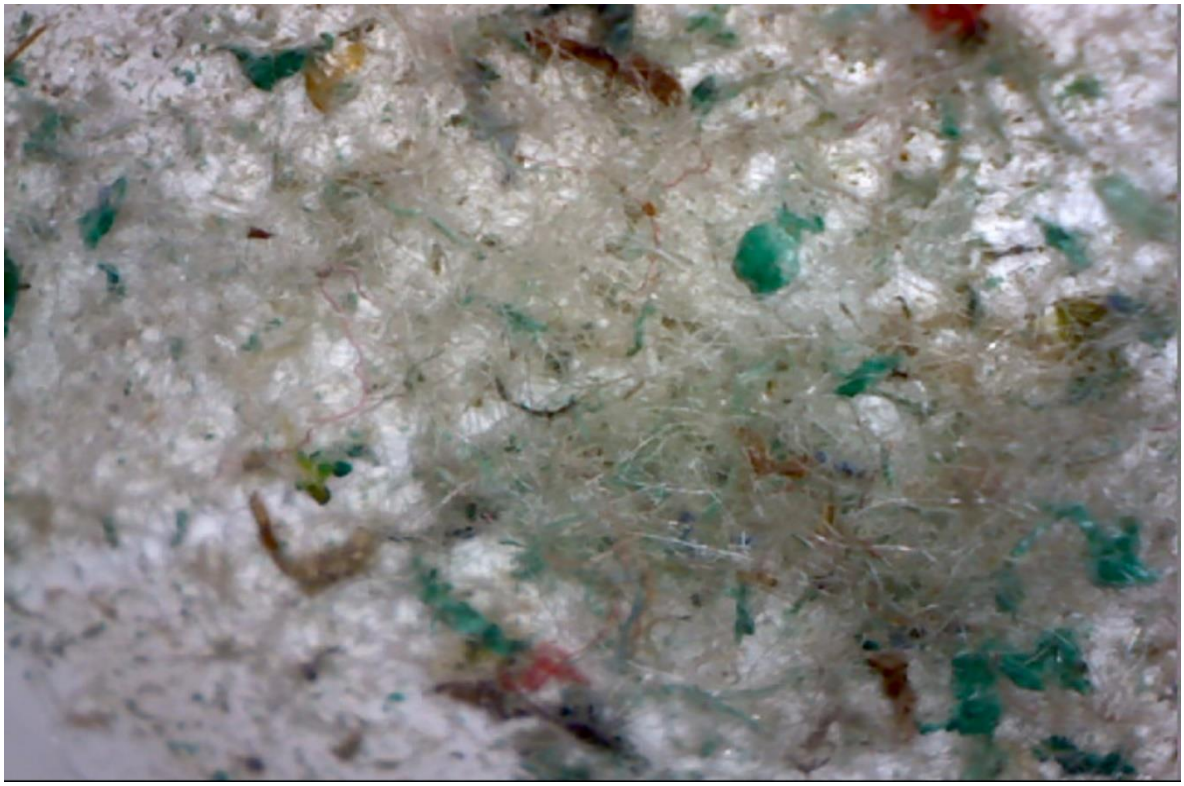

Figure 16.7. Sample test nº7.

Figure 16.8. Sample test nº8.

16.3. Appendix 3- Water content calculation

According to DS-EN-17892-1 (2014) the water content is calculated by placing a wet sample in a container of known mass. Then, the sample is weighted and placed in an oven at 105 °C during 24 hours until the mass is constant.

However in this project, the procedure followed to calculate the water content was carried out by placing three wet sand samples approximately of 300 g in three containers of known mass. Then the containers were weighted and placed in a microwave at a medium level during 5 minutes. After that the samples were weighted, and the content water was calculated using the average.

The different water content of each mix design are shown from table 16.2. to table 16.6.

Table 16.2. Water content in the sand for mix design 07/02/18- Ref -

Water content d. 7/02/2018 sand 0-4mm

	Bowl [g]	Wet [g]	Dry [g]	Water content [g]	Water content [%]
A	108,34	300,45	408,42	0,37	0,12
B	107,58	300,35	407,66	0,27	0,09
C	107,46	300,07	407,21	0,32	0,11
				avr.	**0,106561839**

Table 16.3. Water content in the sand for mix design 12/02/18 Ref PP

Water content d. 12/02-2018 sand 0-4mm

	Bowl [g]	wet [g]	dry	Water content [g]	Water content [%]
A	108,34	300,60	408,70	0,24	0,08
B	107,58	300,30	406,80	1,08	0,36
C	107,46	300,20	406,50	1,16	0,39
				avr.	**0,27529658**

Table 16.4 Water content in the sand for mix design 14/02/18 Ref PE

Water content d. 14/02-2018 søsand 0-4mm

	Bowl [g]	wet [g]	dry	Water content [g]	Water content [%]
A	108,34	300,39	408,07	0,66	0,22
B	107,58	300,09	407,13	0,54	0,18
C	107,46	300,24	407,07	0,63	0,21
				avr.	**0,203164174**

Table 16.5. Water content in the sand for mix design 19/02/18 Ref PE2

Water content d. 19/02-2018 søsand 0-4mm					
	Bowl [g]	**wet [g]**	**dry**	**Water content [g]**	**Water content [%]**
A	108,34	300,62	408,17	0,79	0,26
B	107,58	300,28	406,90	0,96	0,32
C	107,46	300,12	406,63	0,95	0,32
				avr.	**0,299677299**

The data of the repetition of the casting process for each mix is shown below.

Table 16.6. Water content in the sand for mix design repetition 27/02/18

Vandindhold d. 2/02/18 søsand 0-4mm					
	Bowl [g]	**wet [g]**	**dry**	**Water content [g]**	**Water content [%]**
A	108,34	300,02	405,92	2,44	0,81
B	107,58	300,14	405,35	2,37	0,79
C	107,46	300,00	405,17	2,29	0,76
				avr.	**0,788747984**

Table 16.7.Mix design for plain mortar mix repetition, Ref - Rep

Plain mortar [REF- Rep] 27/02/18	
Material	**Amount [g]**
Cement	1050 ± 2
Sand	1550 ± 5
Fibers	0
Water	523 ± 1
Total	**3124** ± 8

Table 16.7. Mix design for fiber reinforced mortar mixture with commercial PP fibers repetition, Ref PP Rep

Plain mortar [REF PP Rep] 27/02/18	
Material	**Amount [g]**
Cement	735 ± 2
Sand	1080 ± 5
Fibers	1,91
Water	367 ± 1
Total	**2183** ± 8

Table 16.8. Mix design for fiber reinforced mortar mixture with PE fibers repetition, Ref PE Rep

Plain mortar [REF PE Rep] 28/02/18	
Material	**Amount [g]**
Cement	735 ± 2
Sand	1030 ± 5
Fibers	19,95
Water	366 ± 1
Total	**2152** ± 8

Table 16.9. Mix design for fiber reinforced mortar mixture with PE2 fibers repetition, Ref PE2 Rep

Plain mortar [REF PE2 Rep] 28/02/18	
Material	**Amount [g]**
Cement	735 ± 2
Sand	1030 ± 5
Fibers	19,95
Water	366 ± 1
Total	**2152** ± 8

16.4. Appendix 4- Specimens' theoretical weight calculation

The calculation values of the theoretical density and theoretical weight used in section 11.1.2.are shown on the tables below.

Tabla 16.10 Data for the calculation of the theoretical density.

Reference	Mortar [g]	[%]	Density [kg/m^3]	Fiber [g]	[%]	Density [kg/m^3]	Theoretical density [kg/m^3]
-	-	-	2300	-	-	-	2300,00
PP	2181,04	99,90	2300	1,911	0,10	910	2298,78
PE	2131,90	99,07	2300	19,95	0,93	950	2287,48
PE2	2131,90	99,07	2300	19,95	0,93	950	2287,48

Tabla 16.11. Theoretical weight calculation for each mixture.

Reference	Theoretical volume [mm^3]	Theoretical density [kg/m^3]	Theoretical weight [g]
-	256000	2300,00	588,80
PP	256000	2298,78	588,49
PE	256000	2287,48	585,60
PE2	256000	2287,48	585,60

16.5. Appendix 5- Working Curves of Mortar Samples- Bending Strength

Appendix 5 contains the working curve for the three-point bending test performed for each mixture. The key values has been extracted from the figures to the tables presented in the Appendix. From figure 16.9. to figure 16.12 it is shown the bending strength curves for the samples tested on day 1 of curing.

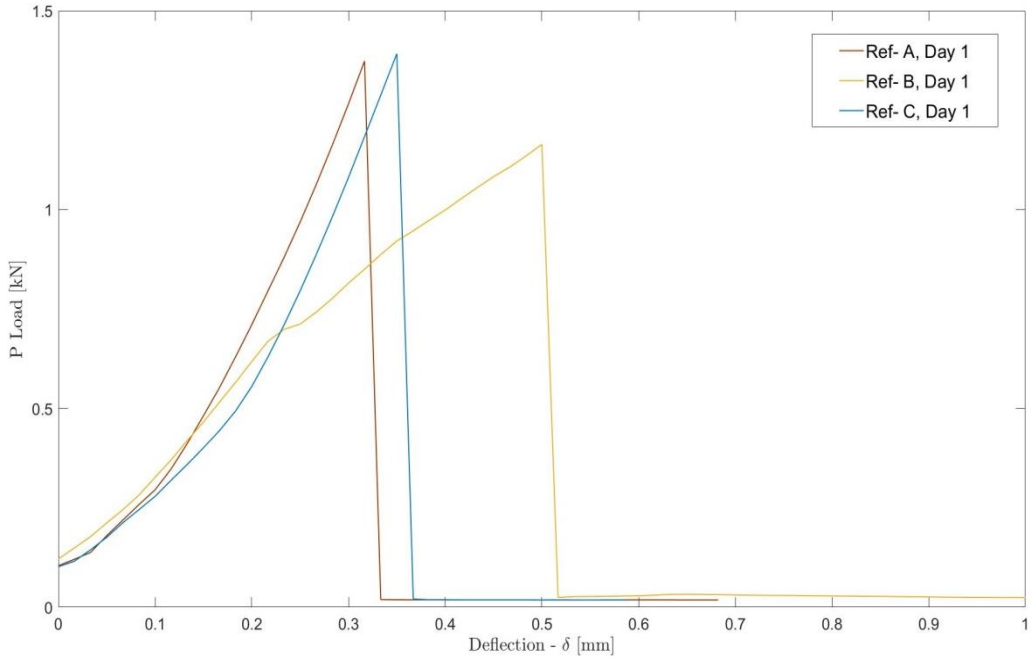

Figure 16.9. Working curve for plain mortar sample Ref-, Day 1.

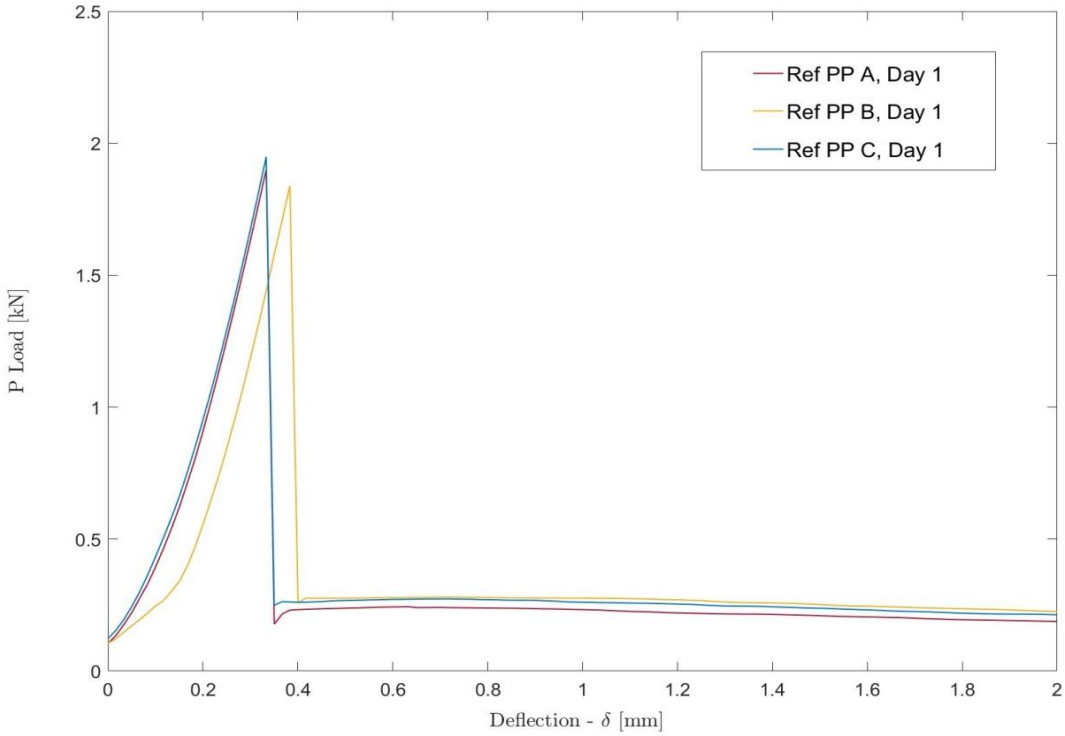

Figure 16.10. Working curve for Ref PP, Day 1.

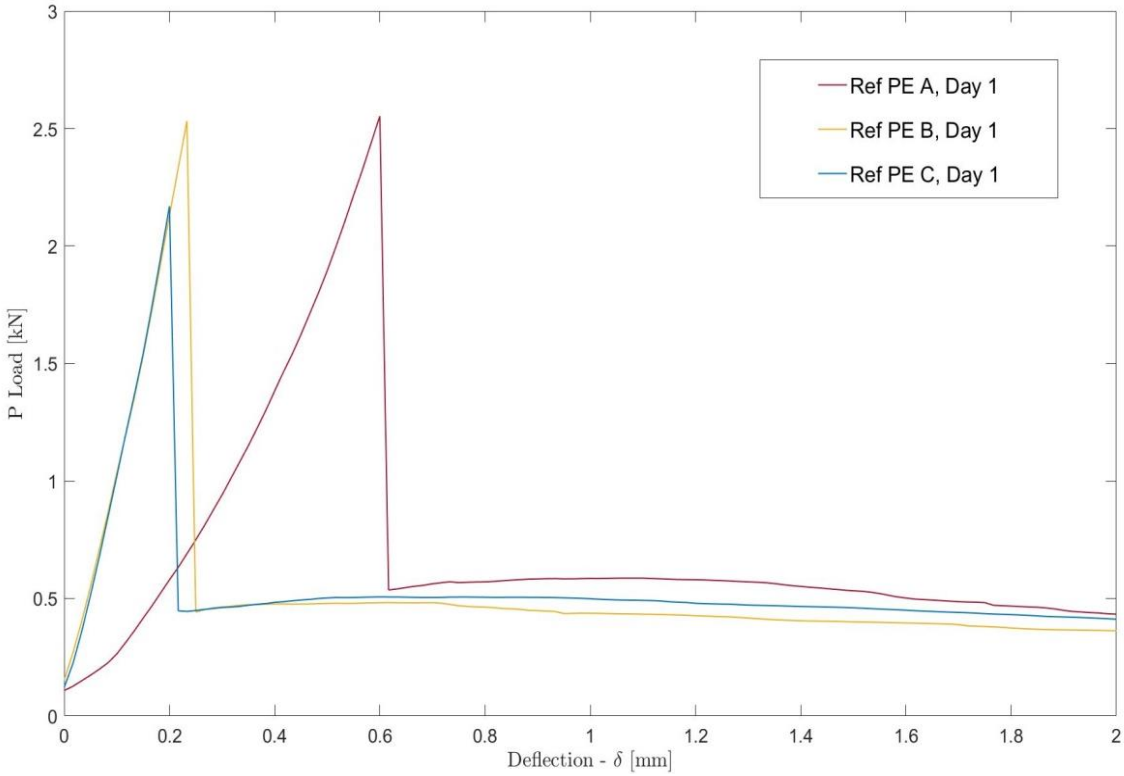

Figure 16.11. Working curve for Ref PE, Day 1.

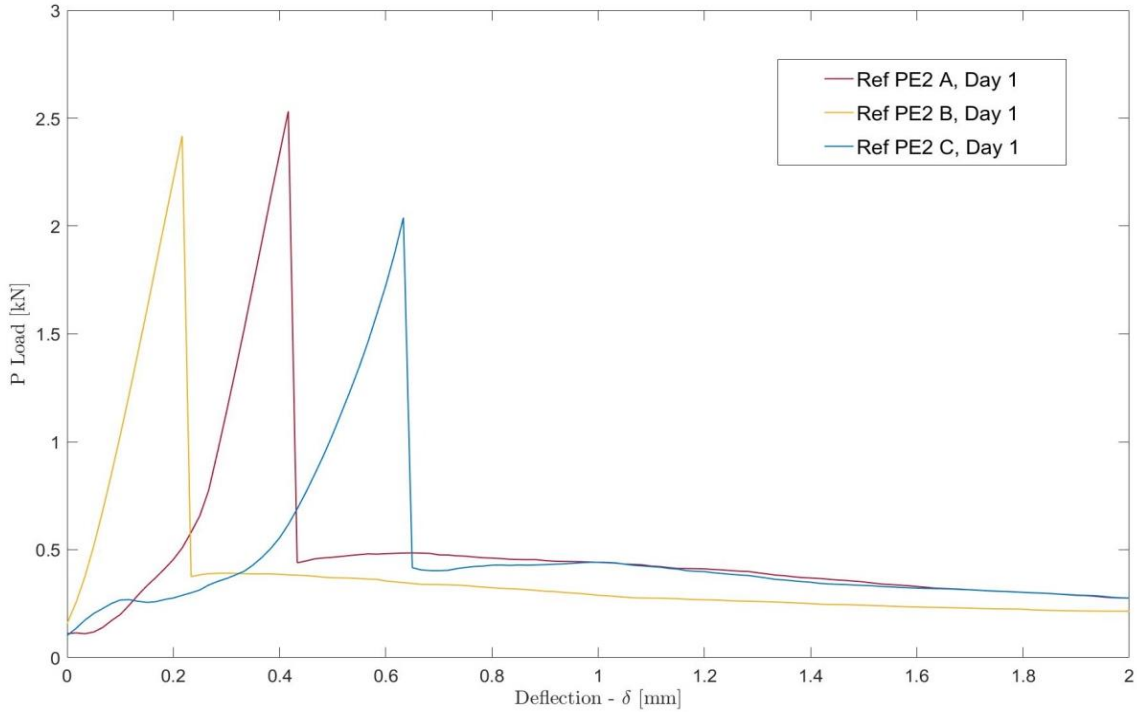

Figure 16.12. Working curve for Ref PE2, Day 1.

Table 16.12. Bending Strength test results for day 1 of curing.

Reference	δ_{cr} [mm]	P_{cr} [MPa]	R_F [MPa]	SD	P_{pb} [kN]	R_{pb} [MPa]	SD	FEF
Ref- 1	0,32	1,37	3,21	-	-	-	-	-
Ref- 2	0,50	1,16	2,71	-	-	-	-	-
Ref- 3	0,35	1,39	3,25	-	-	-	-	-
Ref - average	**0,39**	**1,31**	**3,06**	**0,13**	-	-	-	-
Ref PP 1	0,33	1,90	4,45	-	0,24	0,56	-	0,09
Ref PP 2	0,38	1,83	4,29	-	0,28	0,66	-	0,14
Ref PP 3	0,33	1,95	4,57	-	0,27	0,63	-	0,13
Ref PP average	**0,35**	**1,90**	**4,44**	**0,05**	**0,26**	**0,62**	**0,05**	**0,12**
Ref PE 1	**0,60**	**2,55**	**5,98**	**-**	0,59	1,38	-	0,21
Ref PE 2	**0,23**	**2,53**	**5,93**	**-**	0,48	1,13	-	0,17
Ref PE 3	**0,20**	**2,17**	**5,09**	**-**	0,51	1,20	-	0,21
Ref PE average	**0,34**	**2,42**	**5,67**	**0,22**	**0,53**	**1,23**	**0,13**	**0,20**
Ref PE2 1	**0,41**	**2,53**	**5,93**	**-**	0,49	1,15	-	0,16
Ref PE2 2	**0,21**	**2,41**	**5,65**	**-**	0,39	0,91	-	0,12
Ref PE2 3	**0,63**	**3,04**	**7,13**	**-**	0,44	1,03	-	0,17
Ref PE2 average	**0,42**	**2,33**	**6,23**	**0,26**	**0,44**	**1,03**	**0,12**	**0,15**

From figure 16.13. to figure 16.16 it is shown the bending strength curves for the samples tested on day 2 of curing.

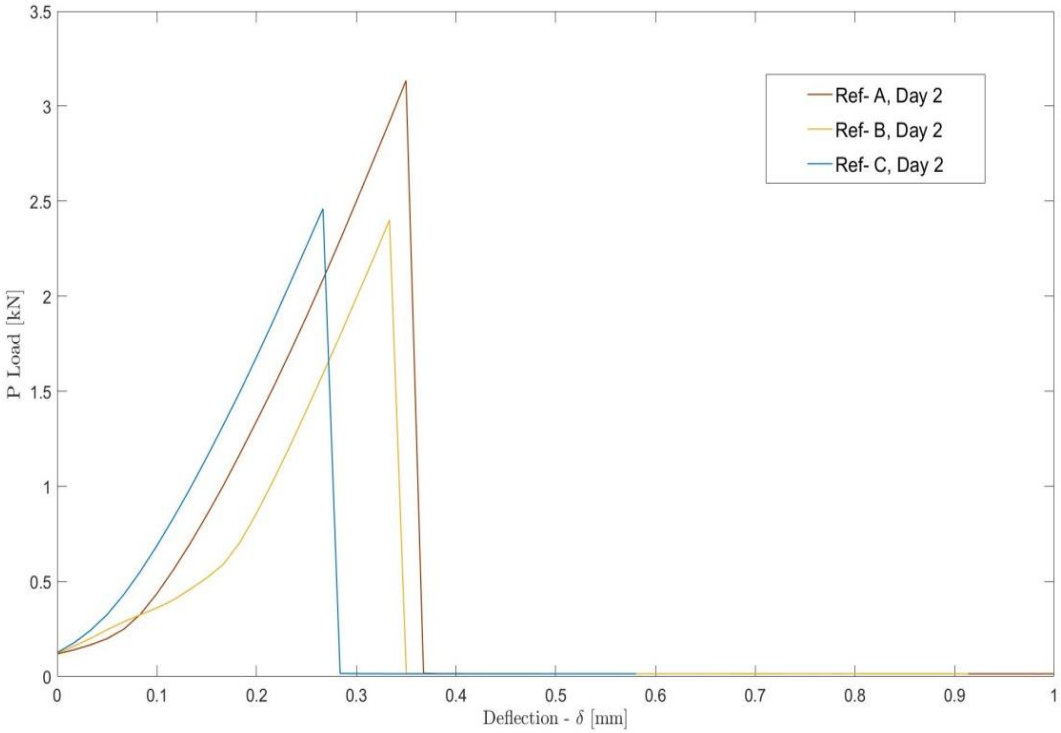

Figure 16.13. Working curve for Ref-, Day 2.

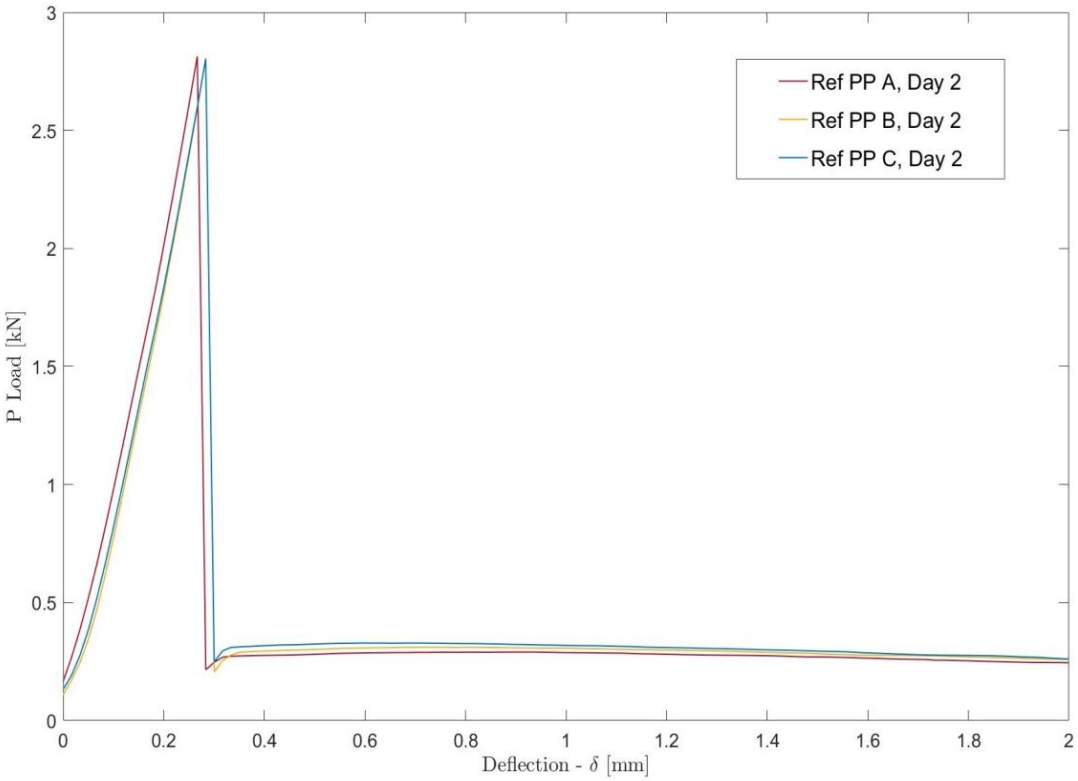

Figure 16.14. Working curve for Ref PP, Day 2.

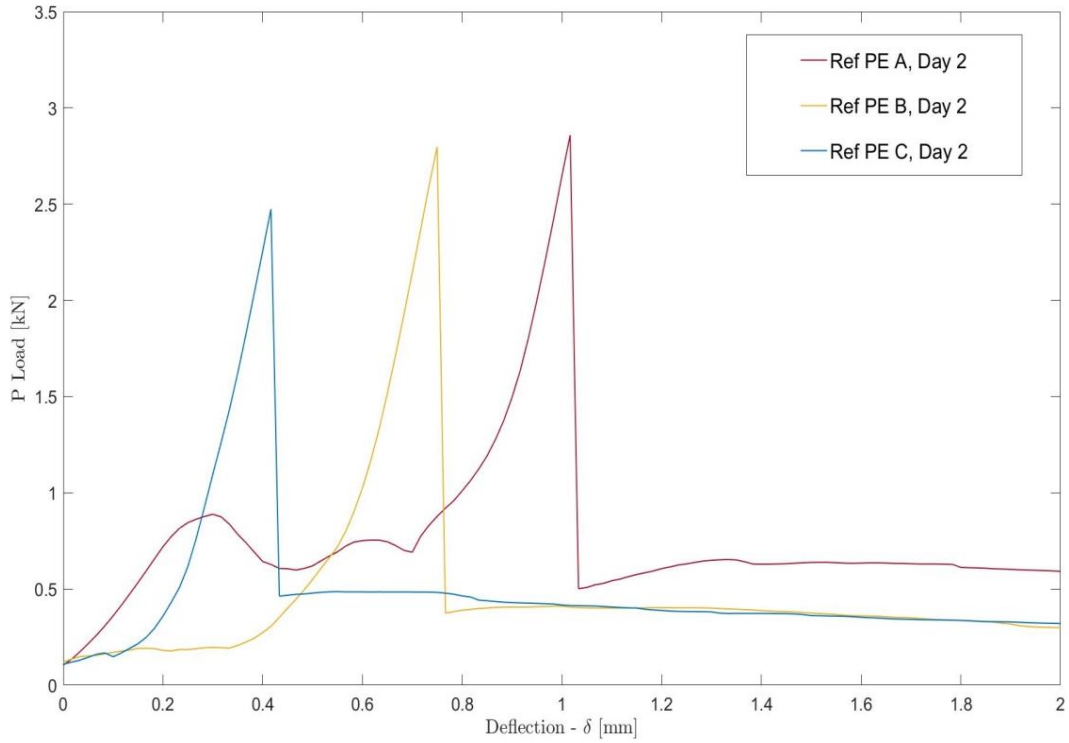

Figure 16.15. Working curve for Ref PE, Day 2.

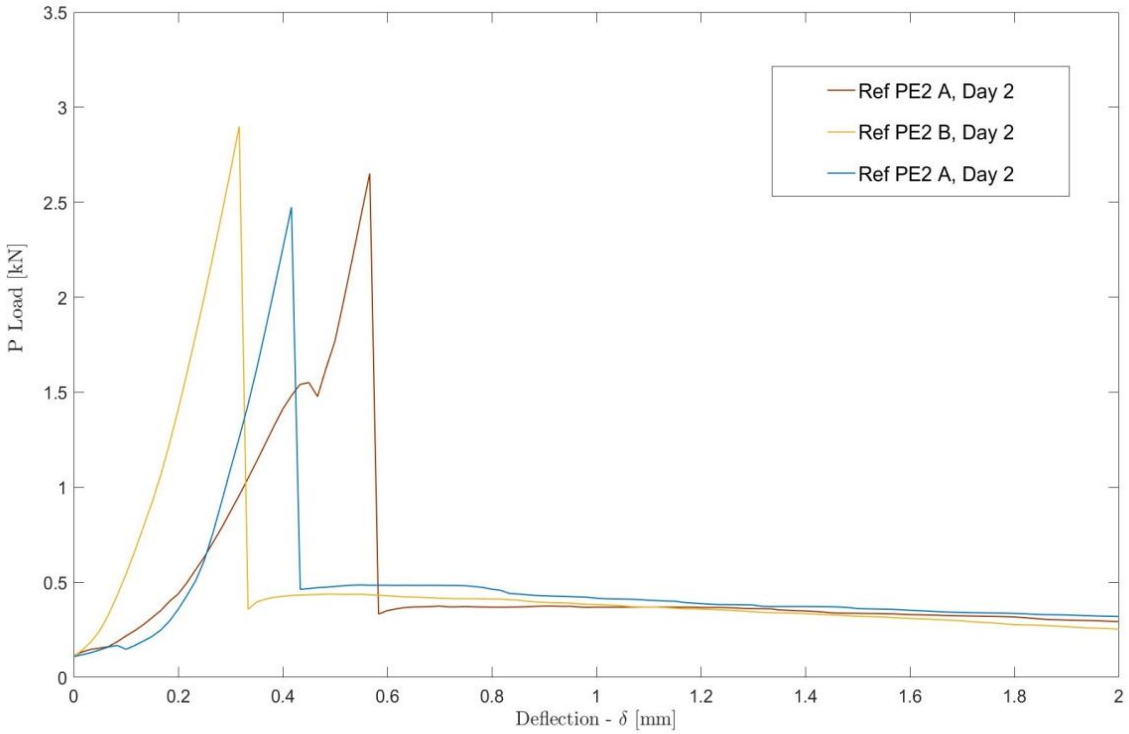

Figure 16.16. Working curve for Ref PE2, Day 2.

Table 16.13. Bending Strength test results for day 2 of curing.

Reference	δ_{cr} [mm]	P_{cr} [MPa]	R_F [MPa]	SD	P_{pb} [kN]	R_{pb} [MPa]	SD	FEF
Ref- 1	0,35	3,14	7,36	-	-	-	-	-
Ref- 2	0,33	2,40	5,63	-	-	-	-	-
Ref- 3	0,27	2,46	5,77	-	-	-	-	-
Ref - average	**0,32**	**2,67**	**6,25**	**0,41**	-	-	-	-
Ref PP 1	0,27	2,81	6,59	-	0,29	0,68	-	0,08
Ref PP 2	0,28	2,81	6,59	-	0,31	0,73	-	0,07
Ref PP 3	0,28	2,80	6,57	-	0,33	0,77	-	0,09
Ref PP average	**0,28**	**2,81**	**6,58**	**0,01**	**0,31**	**0,73**	**0,05**	**0,08**
Ref PE 1	1,01	2,86	6,70	-	0,65	1,52	-	0,18
Ref PE 2	0,75	2,80	6,56	-	0,41	0,96	-	0,13
Ref PE 3	0,42	2,47	5,79	-	0,49	1,15	-	0,15
Ref PE average	**0,73**	**2,71**	**6,35**	**0,21**	**0,52**	**1,21**	**0,28**	**0,15**
Ref PE2 1	0,57	2,65	6,21	-	0,38	0,89	-	0,13
Ref PE2 2	0,32	2,90	6,80	-	0,44	1,03	-	0,12
Ref PE2 3	0,25	2,61	6,12	-	0,46	1,08	-	0,12
Ref PE2 average	**0,38**	**2,72**	**6,38**	**0,42**	**0,43**	**1,00**	**0,10**	**0,12**

From figure 16.17. to figure 16.20 it is shown the bending strength curves for the samples tested on day 7 of curing.

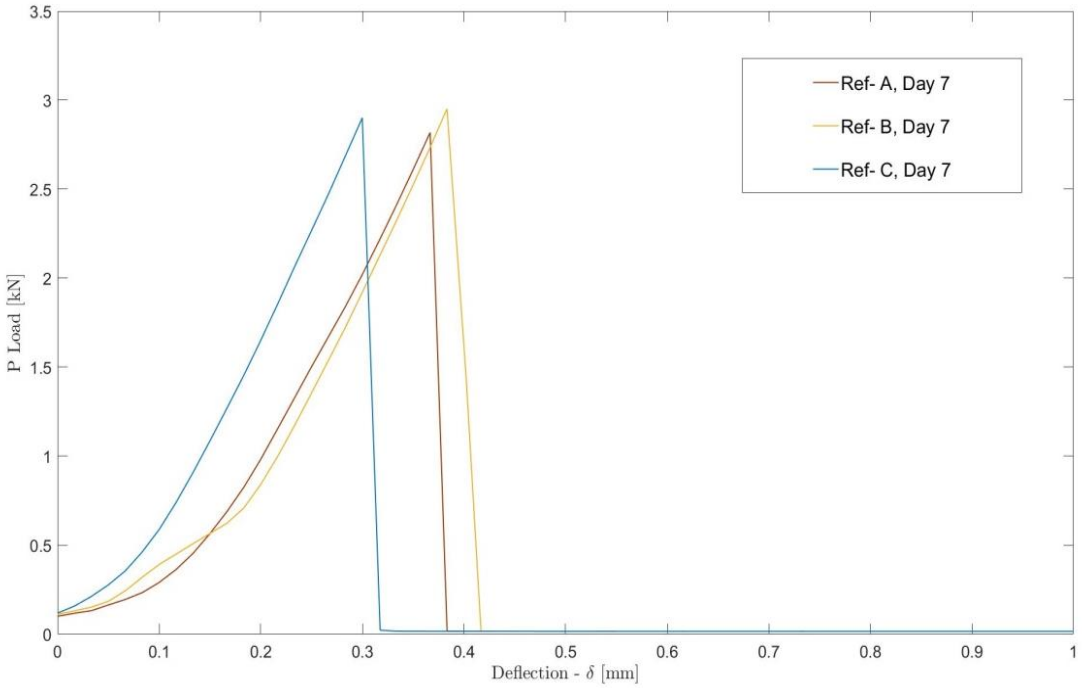

Figure 16.17. Working curve for Ref-, Day 7.

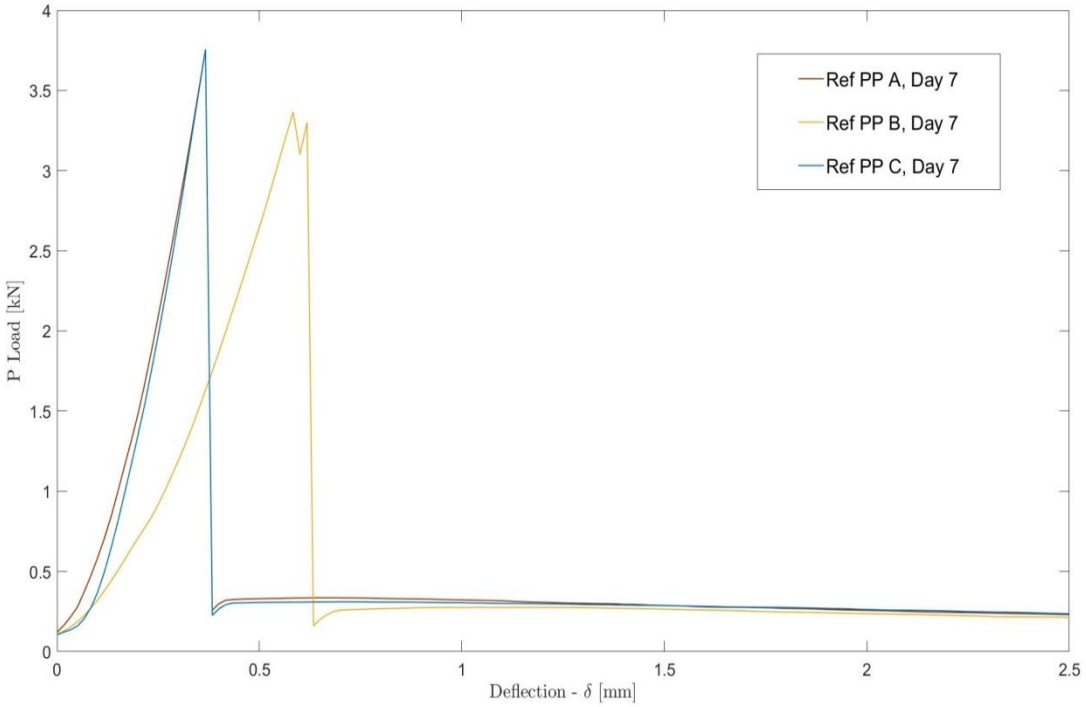

Figure 13.18. Working curve for Ref PP, Day 7.

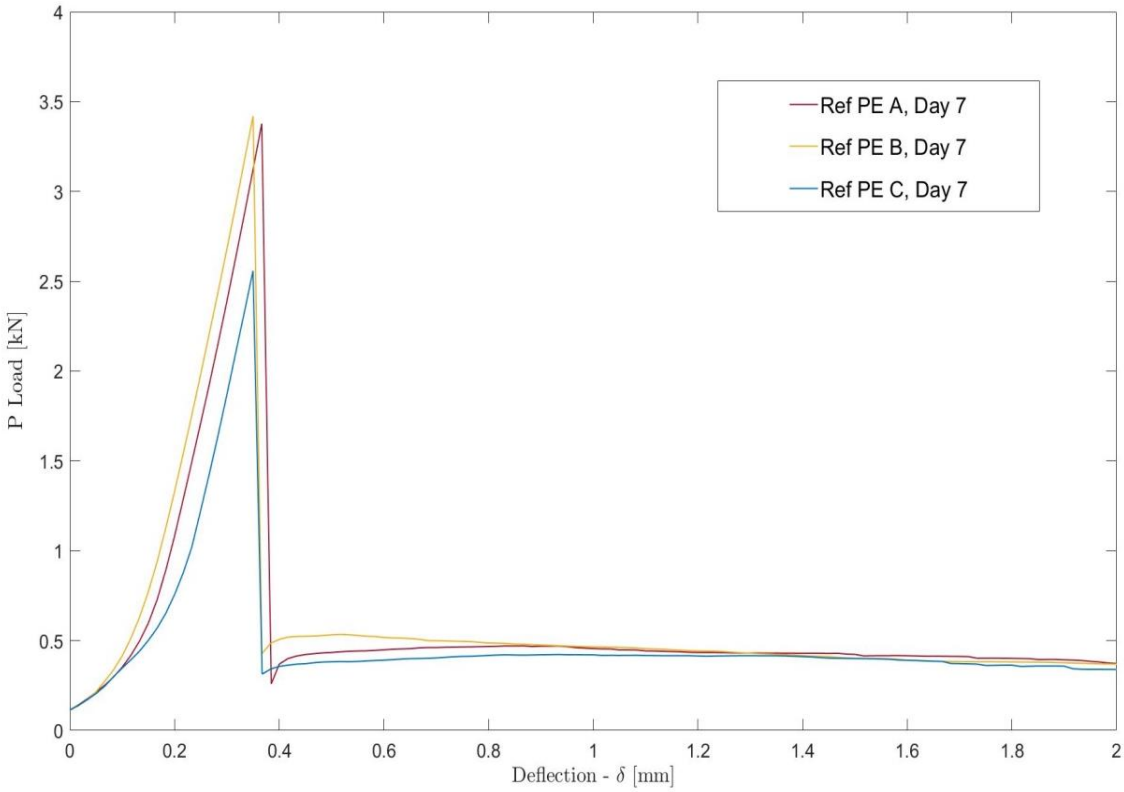

Figure 16.19. Working curve for Ref PE, Day 7.

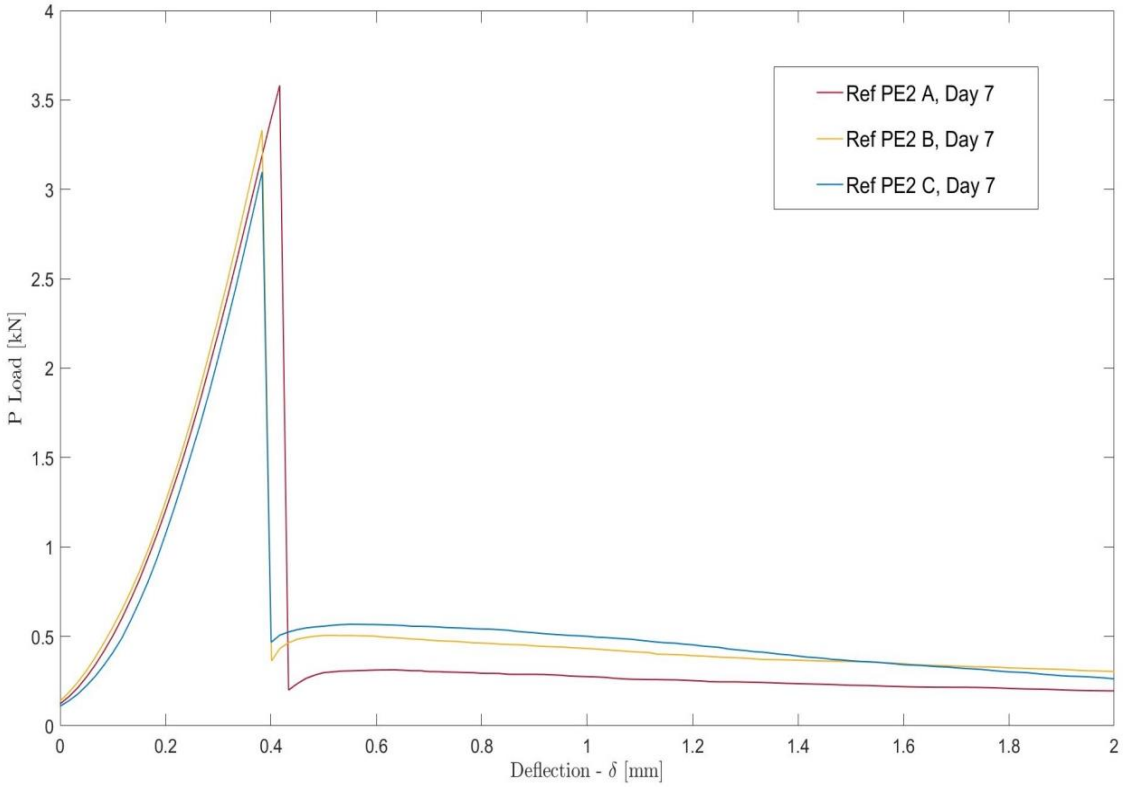

Figure 16.20. Working curve for Ref PE2, Day 7.

Table 16.14. Bending Strength test results for day 7 of curing.

Reference	δ_{cr} [mm]	P_{cr} [kN]	R_F [MPa]	SD	P_{pb} [kN]	R_{pb} [MPa]	SD	FEF
Ref- 1	0,37	2,82	6,61	-	-	-	-	-
Ref- 2	0,38	2,95	6,91	-	-	-	-	-
Ref- 3	0,30	2,90	6,79	-	-	-	-	-
Ref - average	**0,35**	**2,89**	**6,77**	**0,07**	-	-	-	-
Ref PP 1	0,37	3,76	8,81	-	0,30	0,70	-	0,07
Ref PP 2	0,58	3,37	7,90	-	0,33	0,77	-	0,05
Ref PP 3	0,37	3,76	8,81	-	0,31	0,73	-	0,06
Ref PP average	**0,44**	**3,62**	**8,50**	**0,23**	**0,31**	**0,73**	**0,04**	**0,06**
Ref PE 1	0,37	3,34	7,83	-	0,47	1,10	-	0,08
Ref PE 2	0,35	3,42	8,02	-	0,54	1,17	-	0,12
Ref PE 3	0,35	2,56	6,00	-	0,42	0,98	-	0,12
Ref PE average	**0,36**	**3,12**	**7,29**	**0,49**	**0,48**	**1,12**	**0,10**	**0,11**
Ref PE2 1	**0,42**	**3,58**	**8,39**	**-**	**0,31**	**0,73**	-	**0,06**
Ref PE2 2	**0,38**	**3,33**	**7,80**	**-**	**0,50**	**1,17**	-	**0,11**
Ref PE2 3	**0,38**	**3,10**	**7,27**	**-**	**0,56**	**1,31**	-	**0,14**
Ref PE2 average	**0,39**	**3,34**	**7,82**	**0,24**	**0,46**	**1,07**	**0,30**	**0,10**

Fromm figure 16.21. to figure 16.24. it is shown the bending strength curves for the samples tested on day 7 of curing.

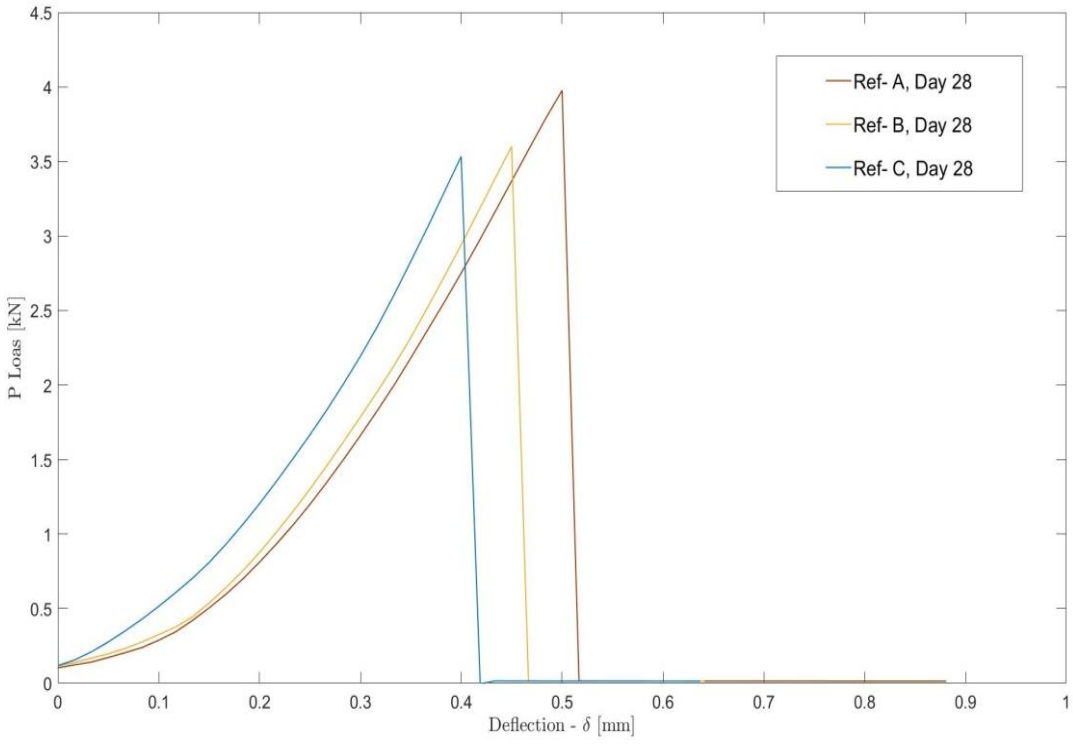

Figure 16.21. Working curve for Ref-, Day 28.

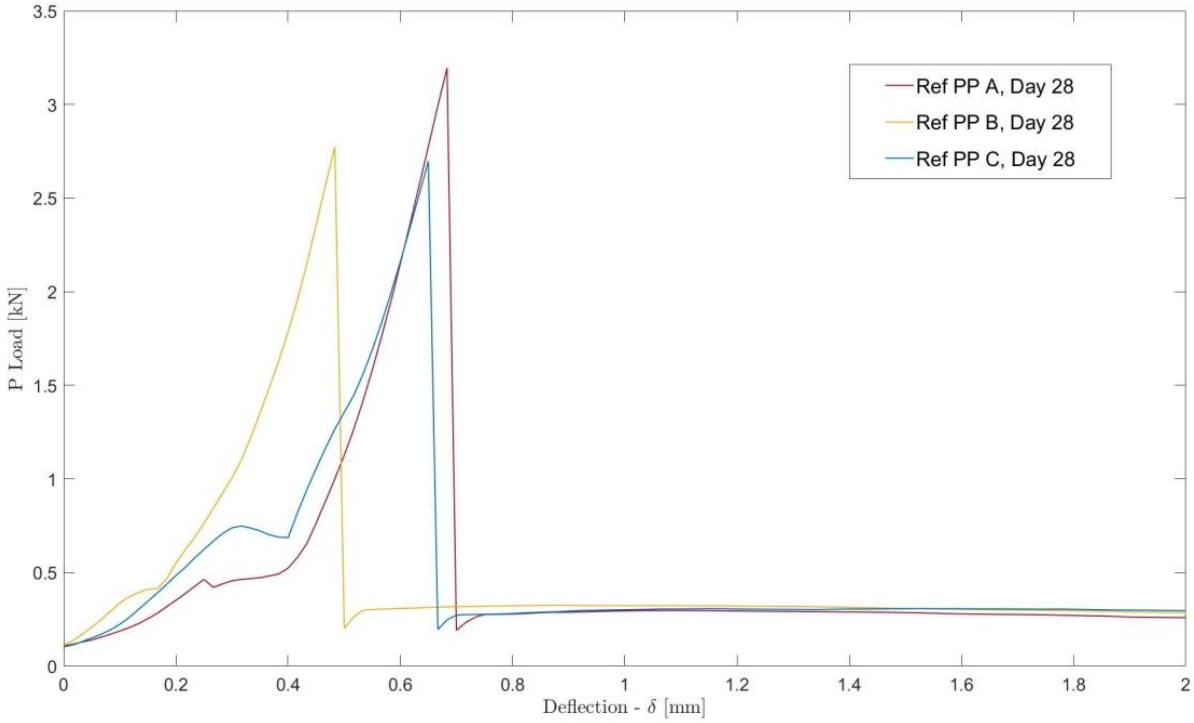

Figure 16.22. Working curve for Ref PP, Day 28.

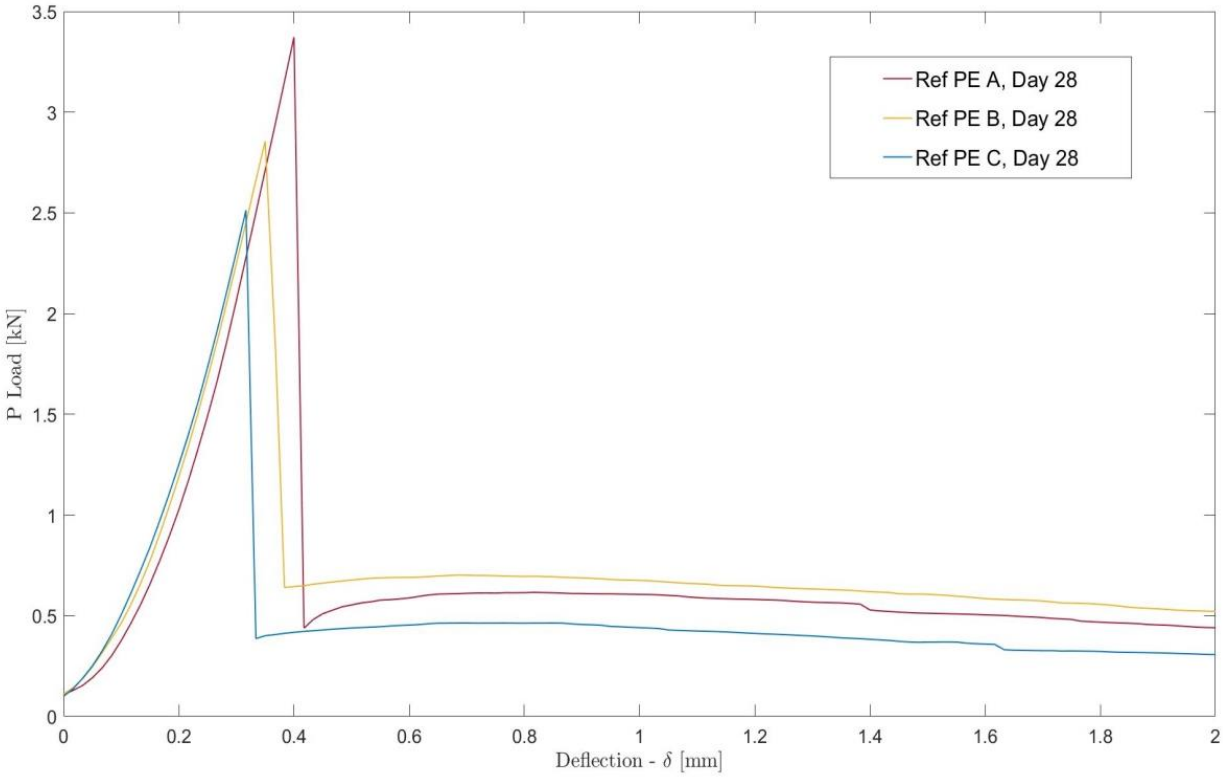

Figure 16.23. Working curve for Ref PE, Day 28.

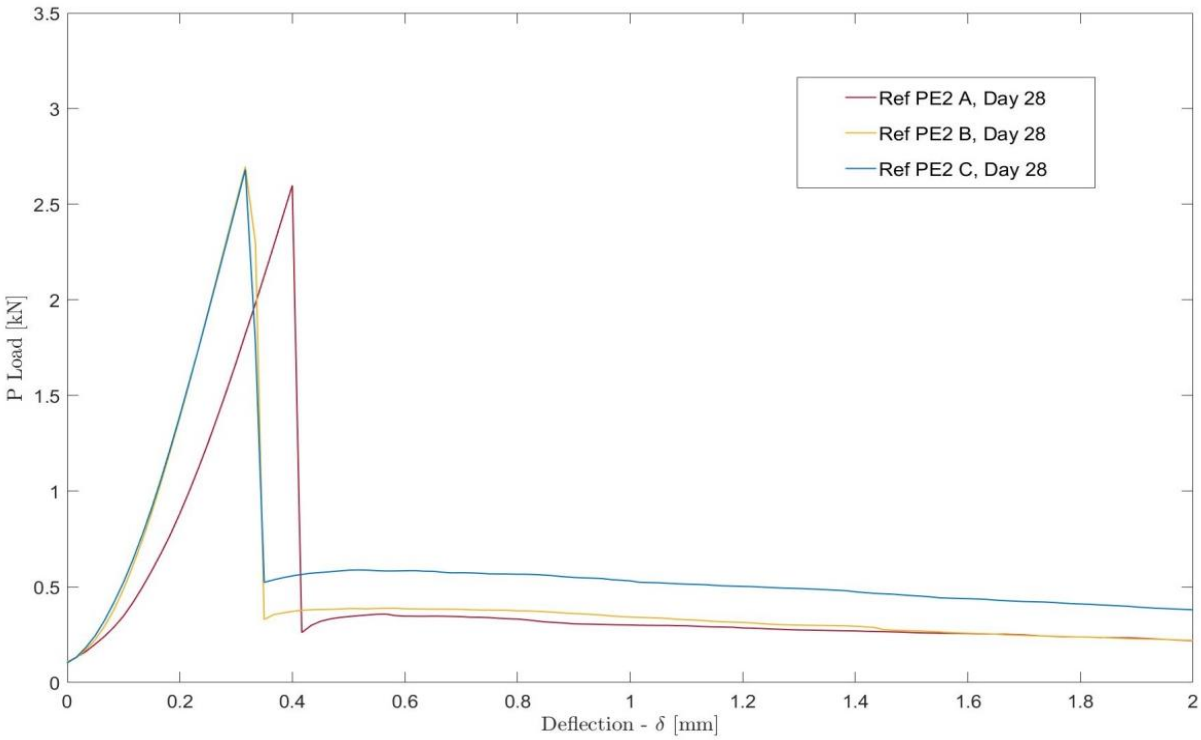

Figure 16.24. Working curve for Ref PE2, Day 28.

Table 16.15. Bending Strength test results for day 28 of curing.

Reference	δ_{cr} [mm]	P_{cr} [MPa]	R_F [MPa]	SD	P_{pb} [kN]	R_{pb} [MPa]	SD	FEF
Ref- 1	0,50	3,98	9,38	**-**	-	-	-	-
Ref- 2	0,45	3,60	8,44	**-**	-	-	-	-
Ref- 3	0,40	3,53	8,27	**-**	-	-	-	-
Ref - average	**0,45**	**3,70**	**8,68**	**0,24**	-	-	-	-
Ref PP 1	0,68	3,19	7,48	-	0,30	0,70	-	0,06
Ref PP 2	0,48	2,77	6,49	-	0,33	0,77	-	0,07
Ref PP 3	0,65	2,70	6,33	-	0,31	0,73	-	0,07
Ref PP average	**0,60**	**2,89**	**6,77**	**0,27**	**0,31**	**0,73**	**0,04**	**0,07**
Ref PE 1	0,40	3,37	7,90	-	0,61	1,43	-	0,13
Ref PE 2	0,35	2,86	6,70	-	0,72	1,69	-	0,22
Ref PE 3	0,32	2,51	5,88	-	0,46	1,08	-	0,15
Ref PE average	**0,36**	**2,91**	**6,83**	**0,43**	**0,60**	**1,40**	**0,31**	**0,17**
Ref PE2 1	0,40	2,60	6,10	-	0,36	0,84	-	0,10
Ref PE2 2	0,32	2,70	6,33	-	0,45	1,05	-	0,12
Ref PE2 3	0,32	2,68	6,28	-	0,57	1,34	-	0,19
Ref PE2 average	**0,35**	**2,66**	**6,24**	**0,05**	**0,46**	**1,08**	**0,25**	**0,14**

16.6. Appendix 6- Flexural Toughness Data.

Appendix 6 contains the tables with the flexural toughness values calculated from the figures on Appendix 5.

Table 16.16. Flexural toughness values for day 1 of curing.

Reference Day 1	$T_{\delta cr}$ [Nm]	SD	$T_{3\delta,cr}$ [Nm]	SD	$T_{5\delta,cr}$ [Nm]	SD	I_5 [-]	I_{10} [-]	$R_{10,5}$ [-]
Ref- 1	0,231	-	0,249	-	0,249	-	1,08	1,08	-
Ref- 2	0,381	-	0,406	-	0,406	-	1,06	1,06	-
Ref- 3	0,255	-	0,271	-	0,271	-	1,06	1,06	-
Ref - average	**0,289**	**0,081**	**0,309**	**0,085**	**0,309**	**0,085**	**1,07**	**1,07**	**-**
Ref PP 1	0,336	-	0,508	-	0,685	-	1,51	2,04	10,6
Ref PP 2	0,309	-	0,535	-	0,771	-	1,73	2,50	15,4
Ref PP 3	0,335	-	0,527	-	0,728	-	1,58	2,18	12,0
Ref PP average	**0,327**	**0,015**	**0,523**	**0,013**	**0,728**	**0,043**	**1,61**	**2,24**	**12,7**
Ref PE 1	0,666	-	1,345	-	1,910	-	2,02	2,87	17,0
Ref PE 2	0,322	-	0,561	-	0,819	-	1,74	2,55	16,2
Ref PE 3	0,244	-	0,450	-	0,701	-	1,85	2,88	20,6
Ref PE average	**0,411**	**0,225**	**0,785**	**0,487**	**1,143**	**0,667**	**1,87**	**2,77**	**17,93**
Ref PE2 1	0,357	-	0,751	-	1,077	-	2,10	3,02	18,4
Ref PE2 2	0,287	-	0,447	-	0,634	-	1,63	2,21	11,6
Ref PE2 3	0,425	-	0,912	-	1,278	-	2,15	3,01	17,2
Ref PE2 average	**0,356**	**0,069**	**0,703**	**0,236**	**0,996**	**0,329**	**1,96**	**2,75**	**15,7**

Table 16.17. Flexural toughness values for day 2 of curing.

Reference Day 2	$T_{\delta cr}$ [Nm]	SD	$T_{3\delta,cr}$ [Nm]	SD	$T_{5\delta,cr}$ [Nm]	SD	I_5 [-]	I_{10} [-]	$R_{10,5}$ [-]
Ref- 1	0,514	-	0,552	-	0,556	-	1,07	1,08	-
Ref- 2	0,345	-	0,374	-	0,374	-	1,08	1,08	-
Ref- 3	0,348	-	0,374	-	0,374	-	1,07	1,07	-
Ref - average	**0,402**	**0,096**	**0,42**	**0,085**	**0,435**	**0,105**	**1,07**	**1,08**	**-**
Ref PP 1	0,379	-	0,549	-	0,738	-	1,45	1,95	10,0
Ref PP 2	0,385	-	0,582	-	0,789	-	1,51	2,05	10,8
Ref PP 3	0,404	-	0,607	-	0,828	-	1,50	2,05	11,0
Ref PP average	**0,389**	**0,013**	**0,579**	**0,029**	**0,785**	**0,045**	**1,49**	**2,02**	**10,6**
Ref PE 1	0,927	-	2,104	-	2,977	-	2,27	3,21	18,8
Ref PE 2	0,487	-	1,058	-	1,485	-	2,15	3,05	18,0
Ref PE 3	0,350	-	0,738	-	1,091	-	2,11	3,11	20,0
Ref PE average	**0,588**	**0,301**	**1,300**	**0,714**	**1,851**	**0,994**	**2,18**	**3,12**	**18,9**
Ref PE2 1	0,555	-	0,980	-	1,334	-	1,77	2,41	12,8
Ref PE2 2	0,404	-	0,689	-	0,961	-	1,71	2,38	13,4

Ref PE2 3	0,320	-	0,555	-	0,764	-	1,73	2,39	13,2
Ref PE2 average	**0,426**	**0,119**	**0,741**	**0,217**	**1,020**	**0,289**	**1,73**	**2,39**	**13,13**

Table 16.18. Flexural toughness values for day 7 of curing.

Reference Day 7	$T_{\delta cr}$ [Nm]	SD	$T_{3\delta,cr}$ [Nm]	SD	$T_{5\delta,cr}$ [Nm]	SD	I_5 [-]	I_{10} [-]	$R_{10,5}$ [-]
Ref- 1	0,427	-	0,463	-	0,472	-	1,08	1,10	-
Ref- 2	0,461	-	0,525	-	0,540	-	1,14	1,17	-
Ref- 3	0,419	-	0,454	-	0,464	-	1,08	1,11	-
Ref - average	**0,436**	**0,022**	**0,481**	**0,039**	**0,492**	**0,041**	**1,10**	**1,23**	**-**
Ref PP 1	0,590	-	0,858	-	1,119	-	1,46	1,90	8,8
Ref PP 2	0,813	-	1,247	-	1,559	-	1,53	1,92	7,8
Ref PP 3	0,549	-	0,801	-	1,061	-	1,46	1,93	9,4
Ref PP average	**0,650**	**0,142**	**0,968**	**0,243**	**1,246**	**0,272**	**1,48**	**1,92**	**8,67**
Ref PE 1	0,566	-	1,071	-	1,551	-	1,89	2,74	17,0
Ref PE 2	0,464	-	0,981	-	1,513	-	2,11	3,26	23,0
Ref PE 3	0,372	-	0,673	-	0,984	-	1,81	2,65	16,8
Ref PE average	**0,467**	**0,097**	**0,908**	**0,209**	**1,336**	**0,305**	**1,94**	**2,88**	**18,93**
Ref PE2 1	0,662	-	0,924	-	1,144	-	1,40	1,73	6,6
Ref PE2 2	0,571	-	0,950	-	1,281	-	1,66	2,24	11,6
Ref PE2 3	0,513	-	0,940	-	1,271	-	1,83	2,48	13,0
Ref PE2 average	**0,582**	**0,075**	**0,938**	**0,013**	**1,222**	**0,094**	**1,63**	**2,15**	**13,5**

Table 16.19. Flexural toughness values for day 28 of curing.

Reference Day 28	$T_{\delta cr}$ [Nm]	SD	$T_{3\delta,cr}$ [Nm]	SD	$T_{5\delta,cr}$ [Nm]	SD	I_5 [-]	I_{10} [-]	$R_{10,5}$ [-]
Ref- 1	0,789	-	0,827	-	0,827	-	1,05	1,05	-
Ref- 2	0,647	-	0,680	-	0,680	-	1,05	1,05	-
Ref- 3	0,614	-	0,651	-	0,651	-	1,06	1,06	-
Ref - average	**0,683**	**0,075**	**0,719**	**0,094**	**0,719**	**0,094**	**1,05**	**1,05**	**-**
Ref PP 1	0,637	-	1,044	-	1,420	-	1,64	2,23	11,8
Ref PP 2	0,499	-	0,824	-	1,167	-	1,65	2,34	13,8
Ref PP 3	0,611	-	1,019	-	1,438	-	1,67	2,35	13,6
Ref PP average	**0,582**	**0,073**	**0,962**	**0,120**	**1,342**	**0,152**	**1,65**	**2,31**	**13,1**
Ref PE 1	0,478	-	0,833	-	1,213	-	1,74	2,54	16
Ref PE 2	0,495	-	0,867	-	1,230	-	1,75	2,48	14,6
Ref PE 3	0,339	-	0,637	-	0,985	-	1,88	2,91	20,6
Ref PE average	**0,437**	**0,085**	**0,779**	**0,124**	**1,143**	**0,137**	**1,79**	**2,64**	**17,1**
Ref PE2 1	0,475	-	0,751	-	0,994	-	1,58	2,09	10,2
Ref PE2 2	0,398	-	0,690	-	0,925	-	1,73	2,32	11,8

Ref PE2 3	0,412	-	0,811	-	1,195	-	1,97	2,90	18,6
Ref PE2 average	**0,428**	**0,041**	**0,751**	**0,060**	**1,038**	**0,140**	**1,76**	**2,44**	**13,53**

16.7. Appendix 7- Compressive Strength test Data.

Appendix 7 contains the key values for the compressive test performed on mortar samples for each mixture.

Table 16.20. Compressive Strength test results for day 1 of curing.

Reference	Fc [kN]	Rc [MPa]	SD [MPa]
Ref- 1	42,00	26,25	**-**
Ref- 2	44,00	27,50	-
Ref- 3	52,00	32,50	-
Ref - average	**46,00**	**28,75**	**3,30**
Ref PP 1	53,00	33,13	**-**
Ref PP 2	49,00	30,63	-
Ref PP 3	46,00	28,75	-
Ref PP average	**49,33**	**30,83**	**2,20**
Ref PE 1	41,00	25,63	**-**
Ref PE 2	47,00	36,88	-
Ref PE 3	53,00	51,25	-
Ref PE average	**47,00**	**29,38**	**3,06**
Ref PE2 1	45,00	28,13	**-**
Ref PE2 2	47,00	29,38	-
Ref PE2 3	43,00	26,86	-
Ref PE2 average	**45,00**	**28,13**	**1,25**

Table 16.21. Compressive Strength test results for day 2 of curing.

Reference	Fc [kN]	Rc [MPa]	SD [MPa]
Ref- 1	72,00	45,00	**-**
Ref- 2	65,00	40,63	**-**
Ref- 3	69,00	43,13	**-**
Ref - average	**68,67**	**42,92**	**2,19**
Ref PP 1	54,00	33,75	**-**
Ref PP 2	68,00	42,50	**-**
Ref PP 3	60,00	37,50	**-**
Ref PP average	**60,67**	**37,92**	**4,39**
Ref PE 1	59,00	36,88	**-**
Ref PE 2	57,00	35,63	**-**
Ref PE 3	66,00	50,63	**-**
Ref PE average	**60,67**	**37,92**	**2,95**
Ref PE2 1	62,00	38,75	**-**
Ref PE2 2	59,00	36,88	**-**
Ref PE2 3	64,00	40,00	**-**

Ref PE2 average	**61,67**	**38,54**	**1,57**

Table 16.22. Compressive Strength test results for day 7 of curing.

Reference	Fc [kN]	Rc [MPa]	SD [MPa]
Ref- 1	90,00	56,25	-
Ref- 2	95,00	59,38	-
Ref- 3	81,00	50,64	-
Ref - average	**88,67**	**55,42**	**2,09**
Ref PP 1	71,00	44,38	-
Ref PP 2	83,00	51,88	-
Ref PP 3	66,00	41,25	-
Ref PP average	**73,33**	**41,25**	**5,46**
Ref PE 1	82,00	51,25	-
Ref PE 2	81,00	50,63	-
Ref PE 3	84,00	52,50	-
Ref PE average	**82,33**	**51,46**	**0,95**
Ref PE2 1	83,00	51,88	-
Ref PE2 2	79,00	49,38	-
Ref PE2 3	85,00	53,13	-
Ref PE2 average	**82,33**	**51,46**	**1,90**

Table 16.23. Compressive Strength test results for day 28 of curing

Reference	Fc [kN]	Rc [MPa]	SD [MPa]
Ref- 1	112,00	70,00	-
Ref- 2	106,00	66,25	-
Ref- 3	100,00	62,50	-
Ref - average	**106,00**	**66,25**	**3,75**
Ref PP 1	102,00	63,75	-
Ref PP 2	107,00	66,88	-
Ref PP 3	108,00	67,50	-
Ref PP average	**105,67**	**66,04**	**2,01**
Ref PE 1	96,00	60,00	-
Ref PE 2	100,00	62,50	-
Ref PE 3	100,00	62,50	-
Ref PE average	**98,67**	**61,67**	**1,44**
Ref PE2 1	**94,00**	**58,75**	-
Ref PE2 2	**92,00**	**57,50**	-
Ref PE2 3	**97,00**	**60,63**	-
Ref PE2 average	**94,33**	**58,96**	**1,57**

16.8. Appendix 8- LVDT test data

Appendix 8contains the length variation values for all mortar samples measured with the LVDT test. The average of the measures and the microstrain rate used to plot the graph in section 11.3.1.1. are shown.

Table 16.24. LVDT data for reference bars.

REF -	Time	Measures					Average	Microstrain	
Date		1	2	3	4	5	mm	µm/mm	
08/02/2018	10:40:00	2,635	2,631	2,629	2,623	2,624	2,628	8,835	0,000
	11:40:00	2,621	2,62	2,62	2,62	2,617	2,620	8,805	0,030
	12:40:00	2,609	2,607	2,605	2,605	2,603	2,606	8,759	0,076
	13:40:00	2,597	2,596	2,596	2,596	2,595	2,596	8,726	0,109
	14:40:00	2,589	2,589	2,590	2,590	2,590	2,590	8,705	0,130
	15:40:00	2,585	2,585	2,583	2,583	2,583	2,584	8,685	0,150
09/02/2018	10:40:00	2,513	2,512	2,514	2,512	2,512	2,513	8,446	0,389
	11:40:00	2,507	2,508	2,508	2,508	2,508	2,508	8,430	0,405
	12:40:00	2,505	2,504	2,504	2,505	2,504	2,504	8,418	0,417
	13:40:00	2,501	2,501	2,501	2,501	2,500	2,501	8,406	0,429
	14:40:00	2,489	2,499	2,498	2,499	2,498	2,497	8,392	0,443
	15:40:00	2,498	2,499	2,498	2,498	2,498	2,498	8,397	0,438
12/02/2018	9:10:00	2,389	2,389	2,389	2,389	2,389	2,389	8,030	0,805
	11:55:00	2,384	2,385	2,385	2,384	2,385	2,385	8,015	0,819
	15:00:00	2,380	2,380	2,379	2,378	2,379	2,379	7,997	0,838
13/02/2018	9:10:00	2,363	2,364	2,365	2,366	2,364	2,364	7,948	0,887
	12:30:00	2,360	2,360	2,360	2,360	2,360	2,360	7,933	0,902
	15:15:00	2,357	2,358	2,358	2,357	2,358	2,358	7,925	0,910
14/02/2018	9:10:00	2,344	2,344	2,343	2,343	2,343	2,343	7,877	0,958
	12:30:00	2,338	2,338	2,338	2,339	2,338	2,338	7,859	0,975
	15:40:00	2,335	2,335	2,335	2,338	2,336	2,336	7,851	0,984
15/02/2018	9:12:00	2,327	2,328	2,329	2,328	2,327	2,328	7,825	1,010
	12:40:00	2,325	2,326	2,327	2,328	2,325	2,326	7,819	1,016
	15:35:00	2,33	2,331	2,332	2,332	2,329	2,331	7,835	1,000
16/02/2018	9:15:00	2,316	2,317	2,318	2,316	2,316	2,317	7,787	1,048
	12:35:00	2,315	2,315	2,314	2,314	2,314	2,314	7,779	1,055
	15:35:00	2,314	2,313	2,312	2,312	2,312	2,313	7,773	1,062
19/02/2018	9:06:00	2,288	2,289	2,289	2,289	2,290	2,289	7,694	1,141
	12:01:00	2,288	2,288	2,288	2,288	2,288	2,288	7,691	1,144
	16:30:00	2,285	2,286	2,285	2,285	2,283	2,285	7,680	1,155
20/02/2018	11:47:00	2,276	2,276	2,276	2,276	2,276	2,276	7,650	1,185
21/02/2018	12:47:00	2,271	2,275	2,274	2,275	2,273	2,274	7,642	1,193

22/02/2018	11:34:00	2,265	2,267	2,266	2,265	2,265	2,266	7,615	1,219
26/02/2018	10:25:00	2,249	2,248	2,248	2,248	2,248	2,248	7,557	1,278
27/02/2018	8:55:00	2,245	2,245	2,246	2,245	2,246	2,245	7,548	1,287
28/02/2018	9:15:00	2,240	2,239	2,239	2,239	2,239	2,239	7,527	1,308
01/03/2018	9:20:00	2,235	2,236	2,234	2,235	2,235	2,235	7,513	1,322
02/03/2018	13:39:00	2,232	2,232	2,232	2,232	2,232	2,232	7,503	1,332
05/03/2018	9:34:00	2,225	2,225	2,225	2,225	2,225	2,225	7,479	1,356
06/03/2018	9:21:07	2,224	2,224	2,224	2,224	2,224	2,224	7,476	1,359
07/03/2018	9:34:00	2,224	2,224	2,224	2,224	2,224	2,224	7,476	1,359

Table 16.25. LVDT data for PP FRM bars.

Ref PP	**Time**	**Measures**					**Average**	**Microstrain**	
Date		**1**	**2**	**3**	**4**	**5**	mm	µm/mm	
13/02/2018	10:30:00	2,186	2,170	2,159	2,151	2,144	2,162	7,267	0,000
	11:30:00	2,122	2,114	2,110	2,107	2,100	2,111	7,094	0,173
	12:40:00	2,099	2,098	2,092	2,093	2,092	2,095	7,041	0,226
	13:40:00	2,086	2,082	2,079	2,077	2,073	2,079	6,990	0,278
	14:40:00	2,067	2,063	2,064	2,060	2,060	2,063	6,934	0,333
	15:40:00	2,051	2,052	2,047	2,045	2,043	2,048	6,883	0,385
14/02/2018	9:10:00	1,991	1,988	1,982	1,985	1,985	1,986	6,676	0,591
	10:40:00	1,974	1,972	1,972	1,970	1,970	1,972	6,627	0,640
	11:40:00	1,973	1,965	1,965	1,967	1,965	1,967	6,612	0,655
	12:32:00	1,956	1,953	1,951	1,950	1,949	1,952	6,561	0,707
	13:40:00	1,948	1,947	1,948	1,947	1,948	1,948	6,547	0,721
	14:35:00	1,943	1,941	1,938	1,938	1,935	1,939	6,518	0,750
15/02/2018	9:12:00	1,902	1,899	1,899	1,899	1,897	1,899	6,384	0,883
	12:40:00	1,882	1,883	1,882	1,882	1,878	1,881	6,324	0,943
	15:35:00	1,879	1,877	1,877	1,876	1,873	1,876	6,307	0,960
16/02/2018	9:26:00	1,845	1,845	1,844	1,842	1,841	1,843	6,196	1,071
	12:35:00	1,838	1,839	1,835	1,836	1,835	1,837	6,173	1,094
	15:35:00	1,828	1,828	1,828	1,827	1,827	1,828	6,143	1,124
19/02/2018	9:05:00	1,764	1,764	1,762	1,762	1,761	1,763	5,925	1,343
	12:05:00	1,758	1,758	1,758	1,758	1,758	1,758	5,909	1,358
	16:30:00	1,754	1,753	1,751	1,753	1,753	1,753	5,892	1,375
20/02/2018	11:50:00	1,735	1,733	1,735	1,737	1,734	1,735	5,831	1,436
	15:01:00	1,736	1,736	1,736	1,737	1,735	1,736	5,835	1,432
21/02/2018	13:03:00	1,719	1,720	1,720	1,720	1,721	1,720	5,782	1,486
22/02/2018	11:30:00	1,707	1,706	1,707	1,706	1,706	1,706	5,736	1,531
26/02/2018	10:30:00	1,678	1,677	1,678	1,677	1,676	1,677	5,638	1,630
27/02/2018	9:00:00	1,670	1,670	1,668	1,668	1,669	1,669	5,610	1,657
28/02/2018	9:22:00	1,661	1,658	1,656	1,658	1,654	1,657	5,571	1,696

01/03/2018	15:37:26	1,650	1,649	1,649	1,649	1,651	1,650	5,545	1,722
02/03/2018	13:39:00	1,641	1,643	1,643	1,642	1,642	1,642	5,520	1,747
05/03/2018	9:34:00	1,635	1,635	1,633	1,632	1,632	1,633	5,490	1,777
06/03/2018	9:21:07	1,628	1,629	1,629	1,629	1,629	1,629	5,475	1,792
07/03/2018	9:39:00	1,628	1,627	1,627	1,627	1,627	1,627	5,470	1,798
08/03/2018	12:26:00	1,626	1,624	1,624	1,623	1,624	1,624	5,459	1,808
12/03/2018	9:42:00	1,621	1,621	1,621	1,621	1,621	1,621	5,449	1,818

Table 16.26. LVDT data for PE FRM bars.

Ref PE	**Time**	**Measures**					Average	**Microstrain**	
Date		**1**	**2**	**3**	**4**	**5**	mm	µm/mm	
15/02/2018	10:05:00	1,948	1,940	1,931	1,930	1,930	1,936	6,507	0,000
	11:05:00	1,931	1,931	1,927	1,925	1,926	1,928	6,481	0,026
	12:30:00	1,918	1,916	1,917	1,915	1,916	1,916	6,442	0,065
	13:10:00	1,912	1,912	1,909	1,911	1,910	1,911	6,423	0,084
	13:40:00	1,910	1,908	1,908	1,907	1,907	1,908	6,413	0,093
	14:40:00	1,895	1,987	1,894	1,894	1,892	1,912	6,428	0,079
	15:35:00	1,891	1,890	1,890	1,890	1,890	1,890	6,354	0,153
16/02/2018	9:23:00	1,819	1,819	1,818	1,818	1,818	1,818	6,112	0,395
	10:17:00	1,814	1,814	1,813	1,813	1,812	1,813	6,095	0,412
	11:20:00	1,809	1,809	1,808	1,808	1,808	1,808	6,079	0,428
	12:35:00	1,802	1,801	1,801	1,801	1,802	1,801	6,055	0,452
	13:30:00	1,797	1,798	1,798	1,797	1,795	1,797	6,040	0,467
	14:30:00	1,792	1,791	1,791	1,792	1,790	1,791	6,021	0,486
	15:30:00	1,789	1,789	1,788	1,788	1,785	1,788	6,009	0,497
19/02/2018	9:03:00	1,661	1,661	1,661	1,661	1,661	1,661	5,583	0,924
	12:02:00	1,657	1,657	1,657	1,657	1,657	1,657	5,570	0,937
	16:30:00	1,651	1,652	1,653	1,651	1,651	1,652	5,552	0,955
20/02/2018	9:48:00	1,628	1,628	1,628	1,628	1,628	1,628	5,472	1,035
	11:49:00	1,627	1,625	1,626	1,627	1,626	1,626	5,466	1,041
	14:49:00	1,628	1,628	1,629	1,628	1,628	1,628	5,473	1,034
21/02/2018	13:01:00	1,606	1,605	1,605	1,605	1,605	1,605	5,396	1,111
	15:40:00	1,603	1,603	1,603	1,603	1,603	1,603	5,388	1,119
22/02/2018	9:21:00	1,590	1,590	1,590	1,590	1,589	1,590	5,344	1,163
	11:30:00	1,587	1,587	1,586	1,587	1,587	1,587	5,334	1,173
	14:15:00	1,586	1,586	1,585	1,585	1,585	1,585	5,329	1,178
26/02/2018	10:27:00	1,541	1,541	1,541	1,541	1,541	1,541	5,180	1,327
27/02/2018	8:57:00	1,533	1,533	1,534	1,534	1,534	1,534	5,155	1,352
28/02/2018	9:16:00	1,523	1,525	1,524	1,524	1,524	1,524	5,123	1,384
01/03/2018	9:20:00	1,516	1,517	1,516	1,517	1,516	1,516	5,097	1,410
02/03/2018	13:40:00	1,509	1,509	1,509	1,509	1,509	1,509	5,072	1,435

05/03/2018	9:35:00	1,497	1,497	1,497	1,497	1,497	1,497	5,032	1,475
06/03/2018	9:31:00	1,493	1,493	1,493	1,493	1,493	1,493	5,018	1,488
07/03/2018	9:36:00	1,492	1,492	1,492	1,492	1,492	1,492	5,015	1,492
08/03/2018	12:25:00	1,489	1,489	1,489	1,489	1,489	1,489	5,005	1,502
12/03/2018	9:45:00	1,484	1,484	1,485	1,484	1,484	1,484	4,989	1,518
13/03/2018	9:30:00	1,483	1,484	1,484	1,483	1,483	1,483	4,986	1,521
14/03/2018	10:00:00	1,481	1,481	1,481	1,481	1,481	1,481	4,978	1,529

Table 16.27. LVDT data for PE2 FRM bars.

Date	**Time**	**Measures**					**Average**	**Microstrain**	
		1	**2**	**3**	**4**	**5**	mm	um/mm	
20/02/2018	9:46:00	-0,268	-0,275	-0,276	-0,283	-0,285	-0,2774	-0,932	0,000
	10:46:00	-0,287	-0,291	-0,295	-0,296	-0,296	-0,2930	-0,985	0,052
	11:46:00	-0,302	-0,304	-0,304	-0,306	-0,307	-0,3046	-1,024	0,091
	12:46:00	-0,311	-0,312	-0,312	-0,313	-0,312	-0,3120	-1,049	0,116
	14:11:00	-0,318	-0,315	-0,317	-0,315	-0,318	-0,3166	-1,064	0,132
	15:03:00	-0,320	-0,320	-0,321	-0,322	-0,326	-0,3218	-1,082	0,149
21/21/18	12:55:00	-0,405	-0,405	-0,406	-0,406	-0,405	-0,4054	-1,363	0,430
	14:02:00	-0,411	-0,410	-0,411	-0,411	-0,411	-0,4108	-1,381	0,448
	15:02:00	-0,417	-0,418	-0,417	-0,418	-0,417	-0,4174	-1,403	0,471
	16:00:00	-0,420	-0,420	-0,421	-0,421	-0,422	-0,4208	-1,414	0,482
22/02/2018	9:14:00	-0,467	-0,467	-0,467	-0,468	-0,470	-0,4678	-1,572	0,640
	10:30:00	-0,473	-0,472	-0,472	-0,473	-0,472	-0,4724	-1,588	0,655
	11:28:00	-0,478	-0,478	-0,478	-0,479	-0,479	-0,4784	-1,608	0,676
	14:15:00	-0,486	-0,486	-0,485	-0,485	-0,486	-0,4856	-1,632	0,700
26/02/2018	10:30:00	-0,598	-0,598	-0,598	-0,598	-0,597	-0,5978	-2,009	1,077
	13:34:00	-0,602	-0,602	-0,601	-0,602	-0,602	-0,6018	-2,023	1,090
27/02/2018	9:02:00	-0,616	-0,615	-0,616	-0,616	-0,616	-0,6158	-2,070	1,137
28/02/2018	9:25:00	-0,634	-0,635	-0,634	-0,633	-0,633	-0,6338	-2,130	1,198
	11:20:00	-0,635	-0,635	-0,636	-0,636	-0,636	-0,6356	-2,136	1,204
01/03/2018	9:25:00	-0,647	-0,647	-0,648	-0,647	-0,647	-0,6472	-2,175	1,243
02/03/2018	9:45:00	-0,660	-0,660	-0,659	-0,659	-0,659	-0,6594	-2,216	1,284
05/03/2018	9:40:00	-0,681	-0,680	-0,681	-0,680	-0,681	-0,6806	-2,288	1,355
06/03/2018	9:35:00	-0,687	-0,688	-0,688	-0,688	-0,688	-0,6878	-2,312	1,379
07/03/2018	9:40:00	-0,691	-0,689	-0,691	-0,691	-0,692	-0,6908	-2,322	1,390
08/03/2018	12:27:00	-0,697	-0,695	-0,697	-0,698	-0,698	-0,6970	-2,343	1,410
12/03/2018	9:50:00	-0,708	-0,708	-0,708	-0,708	-0,709	-0,7082	-2,381	1,448
13/03/2018	9:32:00	-0,709	-0,710	-0,710	-0,709	-0,710	-0,7096	-2,385	1,453
14/03/2018	10:05:00	-0,712	-0,713	-0,713	-0,712	-0,713	-0,7126	-2,395	1,463
15/03/2018	9:10:00	-0,718	-0,716	-0,718	-0,717	-0,718	-0,7174	-2,411	1,479
16/03/2018	9:15:00	-0,720	-0,721	-0,720	-0,721	-0,721	-0,7206	-2,422	1,490

19/03/2018	9:10:00	-0,725	-0,726	-0,726	-0,726	-0,725	-0,7256	-2,439	1,507

The tables below presented the data obtained in the repetition of the LVDT tests for reference bars and PP FRM bars to check the controversial results obtained in the previous test.

Table 16.28. LVDT data from the repetition of reference bars.

Ref - Rep		**Measures**					**Average**	**Microstrain**	
Date	**Time**	**1**	**2**	**3**	**4**	**5**	mm	µm/mm	
05/04/2018	16:30	-1,651	-1,645	1,658	-1,649	-1,651	-1,652	-5,553	0,000
06/04/2018	9:30	-1,737	-1,743	-1,746	-1,748	-1,751	-1,745	-5,866	0,313
10/04/2018	15:30	-1,912	-1,924	-1,926	-1,928	-1,928	-1,924	-6,466	0,913
13/04/2018	12:25	-1,979	-1,979	-1,981	-1,983	-1,984	-1,981	-6,659	1,107
16/04/2018	9:40	-1,994	-1,994	-1,994	-1,994	-1,994	-1,994	-6,703	1,150
17/04/2018	9:40	-1,995	-1,995	-1,995	-1,995	-1,995	-1,995	-6,706	1,153
18/04/2018	10:00	-1,996	-1,996	-1,996	-1,996	-1,996	-1,996	-6,709	1,156
19/04/2018	11:50	-1,996	-1,996	-1,996	-1,996	-1,996	-1,996	-6,709	1,156
23/04/2018	16:30	-1,996	-1,996	-1,996	-1,996	-1,996	-1,996	-6,709	1,156
03/05/2018	2:35	-1,996	-1,996	-1,996	-1,996	-1,996	-1,996	-6,709	1,156

Table 16.29. LVDT data from the repetition of PP FRM bars.

Ref PP Rep		**Measures**					**Average**	**Microstrain**	
Date	**Time**	1	2	3	4	5	mm	µm/mm	
17/04/2018	9:40	-0,554	-0,559	-0,565	-0,570	-0,571	-0,564	-1,895	0,000
18/04/2018	10:00	-0,650	-0,644	-0,646	-0,648	-0,648	-0,647	-2,175	0,280
19/04/2018	11:50	-0,705	-0,706	-0,706	-0,708	-0,708	-0,707	-2,375	0,480
23/04/2018	16:30	-0,796	-0,796	-0,797	-0,793	-0,799	-0,796	-2,676	0,781
26/04/2018	14:35	-0,816	-0,817	-0,817	-0,818	-0,820	-0,818	-2,748	0,853
27/04/2018	15:00	-0,820	-0,820	-0,823	-0,821	-0,823	-0,821	-2,761	0,866
02/05/2018	15:50	-0,857	-0,856	-0,857	-0,857	-0,856	-0,857	-2,879	0,984
03/05/2018	14:40	-0,863	-0,865	-0,861	-0,866	-0,866	-0,864	-2,905	1,010
09/05/2018	13:30	-0,891	-0,889	-0,890	-0,892	-0,892	-0,891	-2,994	1,099
11/05/2018	12:00	-0,898	-0,899	-0,899	-0,899	-0,899	-0,899	-3,021	1,126